C01

Hepatocyte-specific deletion of HIF2α is associated with basal dysfunction, but protection against Western diet induced sympathetic dominance in the mouse heart

Lorenz Holzner[1], Youguo Niu[1], Paula Darwin[1], Dino Giussani[1], Andrew Murray[1]

[1]*Department of Physiology, Development and Neuroscience, University of Cambridge, Cambridge, United Kingdom*

Introduction: Non-alcoholic fatty liver disease (NAFLD) is an independent risk factor for heart disease (1). Hepatic HIF2α deletion, is protective against NAFLD in some rodent models (2), but the effects on basal or stimulated cardiac function are unknown.

Objective: To determine cardiac function *ex vivo* in Western diet-induced NAFLD and the impact of hepatocyte-specific HIF2α deletion in mice.

Methods: HIF2α was deleted in hepatocytes using Cre-recombinase under control of the albumin promoter in male HIF2α$^{fl/fl}$ mice. These mice (hHIF2α$^{-/-}$), and related male, Cre-negative (WT) mice were fed a high fat, fructose and cholesterol Western diet (WD, Research Diets D09100310), or chow for 28 weeks (n = 4-5 per group). Cardiac basal systolic and diastolic function, and responsiveness to the acetylcholine receptor agonist carbachol (range: 10^{-8}-10^{-6} M) and the β-adrenergic receptor agonist isoprenaline (range: 10^{-9}-10^{-7} M) were assessed in isolated, Langendorff-perfused hearts. Sympathetic dominance was calculated as the ratio of left ventricular (LV) developed pressure (LVDP) responses to maximum doses of isoprenaline and carbachol. Data were analysed by two-way ANOVA with Tukey's *post hoc* test for significant genotype:diet interactions, and presented as mean ± standard deviation.

Animal procedures were approved by the University of Cambridge Animal Welfare and Ethical Research Board and conducted according to UK Home Office regulations under the Animals in Scientific Procedures Act (1986).

Results: Three indices of basal cardiac dysfunction occurred in hHIF2α$^{-/-}$ mice relative to WT mice. The minimum first derivative of LV pressure (dP/dt_{min}), a measure of diastolic function, was 34% lower in hHIF2α$^{-/-}$ mice than WT mice ($p = 0.0007$; 1006 ± 93 mmHg.s^{-1} in chow-fed WT mice, 720 ± 228 mmHg.s^{-1} in WD-fed WT mice, 552 ± 126 mmHg.s^{-1} in chow-fed hHIF2α$^{-/-}$ mice, 561 ± 63 mmHg.s^{-1} in WD-fed hHIF2α$^{-/-}$ mice) (Fig. 1A). Similarly, the maximum first derivative of LV pressure (dP/dt_{max}), a measure of systolic function, was 32% lower in hHIF2α$^{-/-}$ mice ($p = 0.0035$; 1338 ± 172 mmHg.s^{-1} in chow-fed WT mice, 1097 ± 381 mmHg.s^{-1} in WD-fed WT mice, 830 ± 151 mmHg.s^{-1} in chow-fed hHIF2α$^{-/-}$ mice, 808 ± 119 mmHg.s^{-1} in WD-fed hHIF2α$^{-/-}$ mice) (Fig. 1B). LVDP, another measure of systolic function, was 25% lower in WD-fed mice ($p = 0.0278$) and 24% lower in hHIF2α$^{-/-}$ mice ($p = 0.0384$; 48 ± 9 mmHg in chow-fed WT mice, 32 ± 8 mmHg in WD-fed WT mice, 33 ± 13 in chow-fed hHIF2α$^{-/-}$ mice, 27 ± 8 mmHg in WD-fed hHIF2α$^{-/-}$ mice) (Fig. 1C). In contrast, relative to chow-fed WT mice (ratio = 1.0 ± 0.3), the sympathetic dominance ratio, a measure of cardiac stimulated function, was 5.3-fold higher (5.3 ± 2.4) in WD-fed WT mice but normalised in WD-fed hHIF2α$^{-/-}$ mice (Fig. 2).

Conclusion: The data provide novel insight into liver-heart crosstalk. Hepatocyte-specific deletion of HIF2α was associated with basal cardiac dysfunction, but protection against cardiac sympathetic dominance in the mouse heart. Since cardiac sympathetic dominance has been linked to cardiac arrhythmia and heart failure (3), further investigation of hepatic HIF2α deletion may suggest strategies for cardiac therapy in NAFLD.

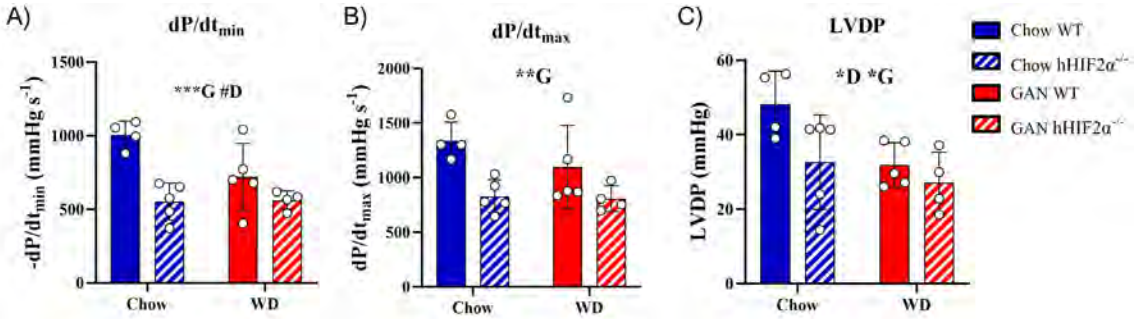

Figure 1: Diastolic and systolic function in chow and WD-fed WT and hHIF2α$^{-/-}$ mice. A) The minimal first derivate of left ventricular pressure dP/dt_{min}, a measure of diastolic function. B) The maximal first derivative of left ventricular pressure dP/dt_{max}, a measure of systolic function. C) Left ventricular developed pressure (LVDP). D = diet effect, G = genotype effect in two-way ANOVA. # $p < 0.1$, * $p < 0.05$, ** $p < 0.01$, *** $p < 0.0001$. Data are presented as mean ± standard deviation, n = 4-5 per group.

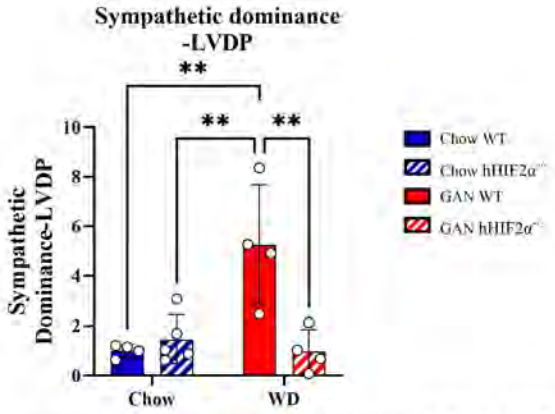

Figure 2: Cardiac sympathetic dominance in chow and WD-fed WT and hHIF2α$^{-/-}$ mice. The left ventricular developed pressure (LVDP) response to the maximal isoprenaline dose was divided by the response to the maximal carbachol dose to calculate the sympathetic dominance ratio. Due to a significant genotype:diet effect in two-way ANOVAm results of Tukey's *post hoc* test are shown. ** $p < 0.01$. Data are presented as mean ± standard deviation, n = 4-5 per group.

1. Anstee QM, Mantovani A, Tilg H, Targher G: Risk of cardiomyopathy and cardiac arrhythmias in patients with nonalcoholic fatty liver disease. Nat Rev Gastroenterol Hepatol.(2018);15. p. 425-39. doi: 10.1038/s41575-018-0010-0. 2. Morello E, Sutti S, Foglia B, Novo E, Cannito S, Bocca C, et al.: Hypoxia-inducible factor 2alpha drives nonalcoholic fatty liver progression by triggering hepatocyte release of histidine-rich glycoprotein. Hepatology.(2018);67. p. 2196-214. doi: 10.1002/hep.29754. 3. Shen MJ, Zipes DP: Role of the autonomic nervous system in modulating cardiac arrhythmias. Circ Res.(2014);114. p. 1004-21. doi: 10.1161/CIRCRESAHA.113.302549.

C02

Thrombocytes constitutes an efficient clearance system for uropathogenic Escherichia coli in a murine urosepsis model

Nanna Johnsen[1], Emil Lambertsen[1], Mette Christensen[1], Thomas Corydon[1], Helle Praetorius[1]

[1]Aarhus University, Department of Biomedicine, Aarhus, Denmark

Sepsis is a life-threatening host reaction to circulating pathogens associated with reduced microperfusion and tissue hypoxaemia. Thrombocytopenia, one of the central diagnostic criteria for sepsis, is a distinct negative prognostic marker for survival (1, 2). Thrombocytes capability has transcended, solely within the coagulation system, to encompass a modulatory role in the immune response and a direct mediator of pathogen killing. Studies has shown a binding capability among others to monocytes, neutrophils and pathogens (3-5). Interestingly, our preliminary data in a murine model of sepsis reveal that the thrombocyte number falls prior to intravascular coagulation. Here we investigate the fate of circulating thrombocytes during sepsis.

All experiments were carried out in male Balb/cJRj mice (8-10 weeks, 24.8 ± 0.2 g). Mice were anaesthetised for the entire experiment with ketamine/xylazine (100/10 mg kg^{-1}) sc. A bolus of $330 \cdot 10^6$ *E. coli* (O6:K13:H1) with or without eGFP-pBAD plasmid was administered through the tail vein. The number of circulating thrombocytes ($CD42^+$), neutrophils ($Ly6G^+$) and monocytes ($Ly6C^+$/$CD11b^+$) were determined by flow cytometry. Bacterial load was quantified as CFU on LB-agar plates or by flow cytometry (EGFP). The results are given as mean±S.E.M., and statistical significance was tested by two-way ANOVA in GraphPad Prism v10.2.1 Experiments were approved by the National Animal Experiment Expectorate, Denmark (2020-15-0201-00422).

In this model, sepsis-induced thrombocytopenia develops in a biphasic manner. We detected an early reduction of about 38.6%, already 30 min after *E. coli* injection ($48.9 \cdot 10^7 \pm 97.8 \cdot 10^6$ thrombocytes/ml, n=6) compared to mice receiving vehicle ($77.4 \cdot 10^7 \pm 48.2 \cdot 10^6$ thrombocytes/ml, n=6 $p<0.06$). Thrombocytes are known to form complexes with neutrophils or monocytes. However, the number of thrombocytes in complex with neutrophils or monocytes remained constant during the early fall in thrombocyte number and, thus, cannot explain the early drop in circulating thrombocytes. Interestingly, we found that the number of bacteria in the blood fell in parallel with the thrombocytes from $1.0 \cdot 10^7 \pm 0 \cdot 10^7$CFU (n=4) immediately after injection to $5.1 \cdot 10^5 \pm 0.9 \cdot 10^5$ CFU (n=7) 30 minutes after injection. By image-enhanced flow cytometry, we were able to show that the EGFP-expressing uropathogenic *E. coli* instantly and primarily is scavenged by circulating thrombocytes and that these complexes are acutely removed from the circulation. Preliminary *in vitro* data support the theory of thrombocytes acting primary as a scavenger system during sepsis. Data indicates that thrombocytes possess the ability to induce bacterial death, albeit gradually, but not sufficiently pronounced to achieve a 94.9% reduction in bacterial load within 30 min.

The data strongly suggest that circulating thrombocytes constitute the most important cell type for fast scavenging and clearance of invading bacteria during urosepsis.

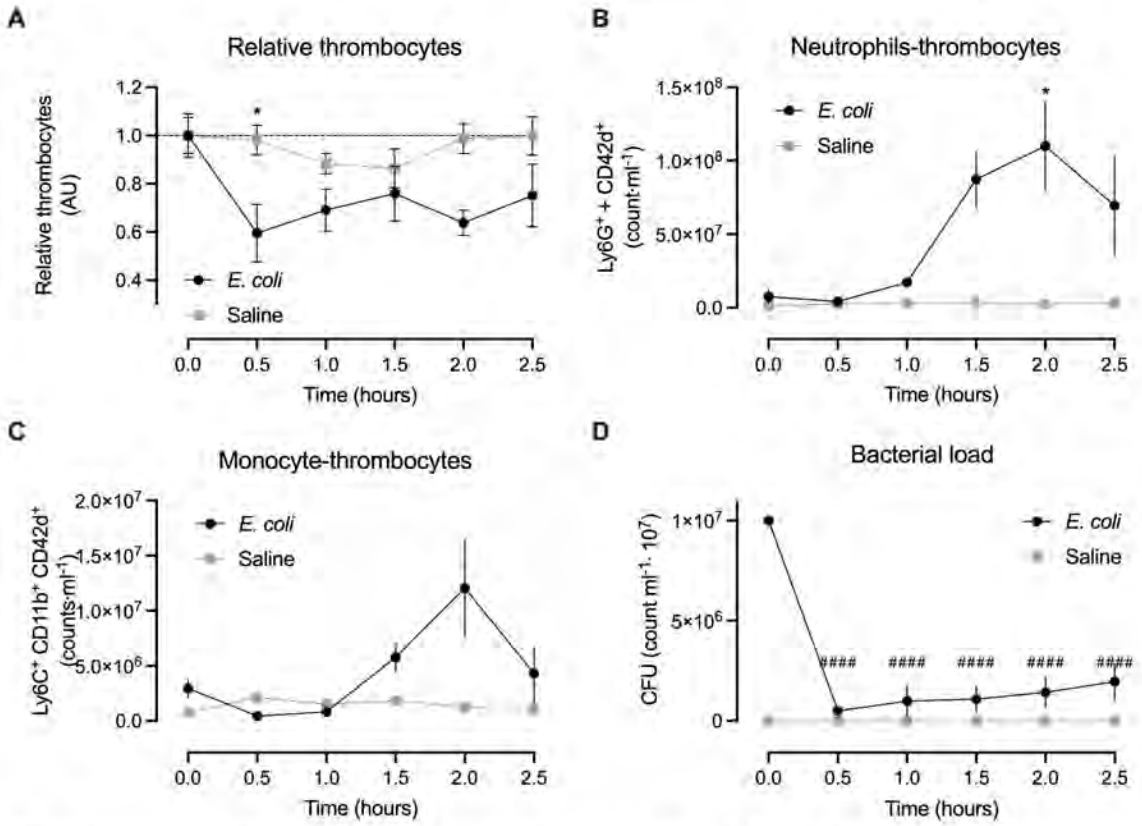

Sepsis induces a parallel rapid and persistent drop in thrombocytes and *E. coli* (**A**) Relative number of circulating thrombocytes at different time points after injection with either saline (150 µl) or 3.3 10^8 *E. coli*. (n=4-7) (**B**) Counts of neutrophils in complex with thrombocytes whole blood from mice at different timepoints with or without sepsis (n=4-7) (**C**) Counts of monocytes in complex with thrombocytes in whole blood at different timepoints after induction of sepsis or saline (n=4-7) (**D**) Colony forming units (CFU) in blood from mice with or without sepsis (n=4-7). Data were tested for normal distribution. Normally distributed data were tested by two-way ANOVA Šídák's multiple comparisons test, and data, which were not normally distributed, were analysed with Mann-Whitney test to compare sepsis and non-sepsis (indicated with asterisk). CFU was only tested with a two-way ANOVA within the sepsis-group (indicated with hashtags). Data are shown as mean ± SEM. * indicates $p<0.05$, ####indicates $p<0.001$.

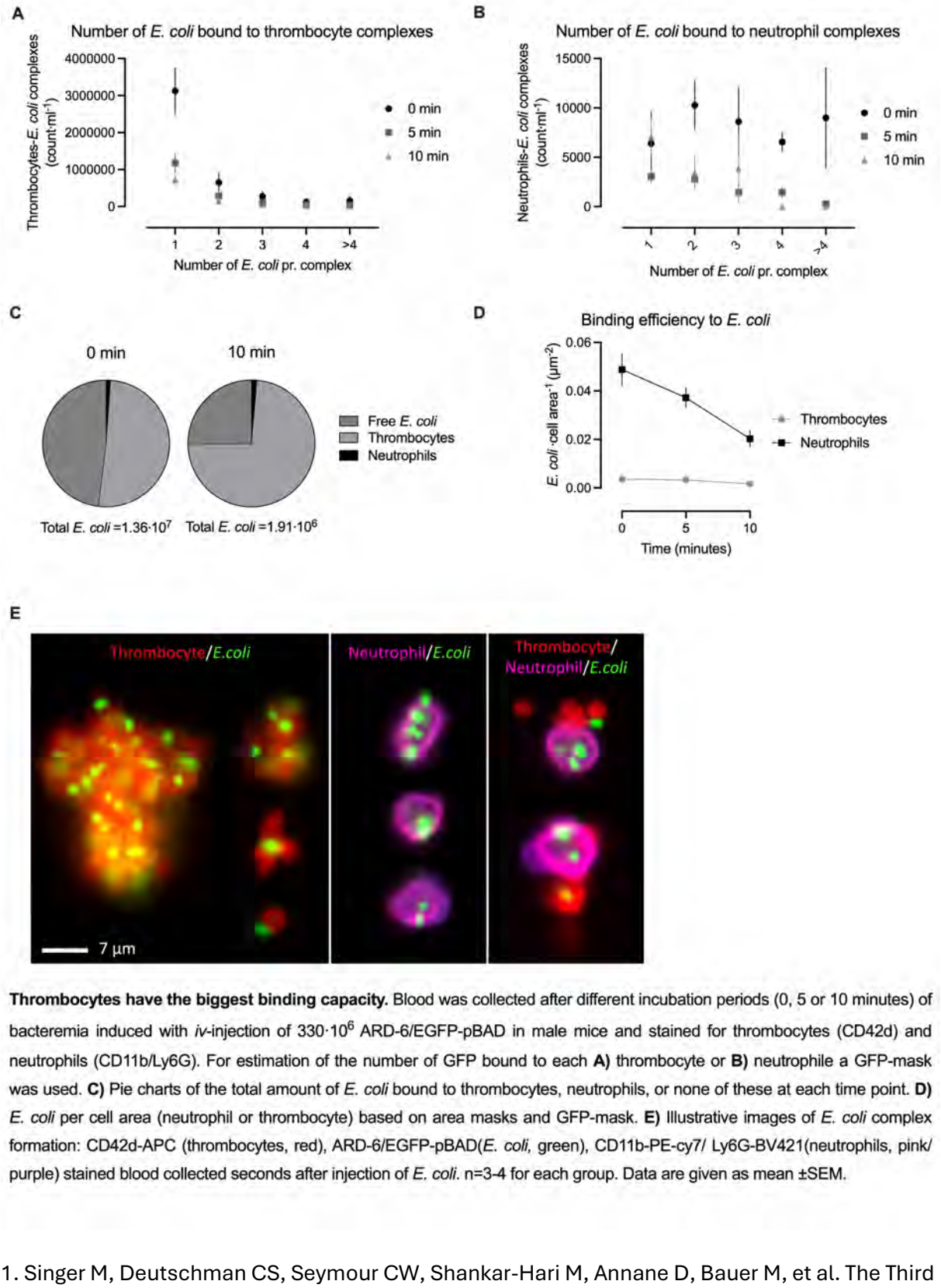

Thrombocytes have the biggest binding capacity. Blood was collected after different incubation periods (0, 5 or 10 minutes) of bacteremia induced with *iv*-injection of $330 \cdot 10^6$ ARD-6/EGFP-pBAD in male mice and stained for thrombocytes (CD42d) and neutrophils (CD11b/Ly6G). For estimation of the number of GFP bound to each **A)** thrombocyte or **B)** neutrophile a GFP-mask was used. **C)** Pie charts of the total amount of *E. coli* bound to thrombocytes, neutrophils, or none of these at each time point. **D)** *E. coli* per cell area (neutrophil or thrombocyte) based on area masks and GFP-mask. **E)** Illustrative images of *E. coli* complex formation: CD42d-APC (thrombocytes, red), ARD-6/EGFP-pBAD(*E. coli*, green), CD11b-PE-cy7/ Ly6G-BV421(neutrophils, pink/ purple) stained blood collected seconds after injection of *E. coli*. n=3-4 for each group. Data are given as mean ±SEM.

1. Singer M, Deutschman CS, Seymour CW, Shankar-Hari M, Annane D, Bauer M, et al. The Third International Consensus Definitions for Sepsis and Septic Shock (Sepsis-3). Jama.

2016;315(8):801-10. 2. Wang D, Wang S, Wu H, Gao J, Huang K, Xu D, et al. Association Between Platelet Levels and 28-Day Mortality in Patients With Sepsis: A Retrospective Analysis of a Large Clinical Database MIMIC-IV. Frontiers in Medicine. 2022;9. 3. Hurley SM, Lutay N, Holmqvist B, Shannon O. The Dynamics of Platelet Activation during the Progression of Streptococcal Sepsis. PLOS ONE. 2016;11(9):e0163531-e. 4. Gawaz M, Fateh-Moghadam S, Pilz G, Gurland HJ, Werdan K. Platelet activation and interaction with leucocytes in patients with sepsis or multiple organ failure. European Journal of Clinical Investigation1995. p. 843-51. 5. Palankar R, Kohler TP, Krauel K, Wesche J, Hammerschmidt S, Greinacher A. Platelets kill bacteria by bridging innate and adaptive immunity via platelet factor 4 and FcγRIIA. Journal of Thrombosis and Haemostasis. 2018;16(6):1187-97.

C03

High-fat diet blunts the carotid body mediated-ventilatory effects of TNF-α

Gonçalo M. Melo[1], Joana F. Sacramento[1], Kryspin Andrzejewski[2], Adriana M. Capucho[1], Katarzyna Kaczyńska[2], Sílvia V. Conde[1]

[1]NOVA Medical School|Faculdade de Ciências Médicas, Universidade NOVA de Lisboa, Lisboa, Portugal, [2]Departament of Respiration Physiology, Mossakowski Medical Research Center, Polish Academy of Sciences, Pawińskiego, Poland

Metabolic diseases pose a significant global health challenge, with profound impact on mortality and morbidity rates. The carotid bodies (CBs), traditionally recognized as an oxygen-sensitive organ, is a metabolic sensor implicated in these diseases [1-3]. In dysmetabolic states the CB is dysfunctional and the abolishment of its activity improves metabolic function [1-3]. Contributing to CB dysfunction is hyperinsulinemia and hyperleptinemia and probably inflammatory cytokines [4], whose presence, along with their receptors, has been evidenced within the CB [1,5]. By exploring the effects of TNF-α in the cardioventilatory responses and on CB inflammation this study aims to investigate the contribution of TNF-α to CB dysfunction in metabolic diseases. Moreover, the sexual dimorphism on TNF-α action was also explored.

Methods: Two groups of Wistar rats (male and female) were used - a control group (CTL) submitted to a standard diet and a group fed with high-fat diet (HF, 60% energy from fat) for 3 weeks. Animals were anesthetized with pentobarbital (60 mg/kg i.p.), and ventilation, blood pressure, and autonomic activity (heart rate variability) were assessed before and after the administration of TNF-α (0.5 and 5 ng/ml) in CTL and HF groups with and without resection of the carotid sinus nerve (CSN). Blood levels of TNF-α and the levels of TNF-α and its receptors in the CBs of CTL and HF animals were evaluated. For statistical analysis, ANOVA with Dunnett's comparison test and t-Student test were used. Ethical approval was obtained from the Animal Welfare Committee, from the NMS Ethics Committee and from The Portuguese Authorities (DGAV).

Results: In male CTL rats, TNF-α increased minute ventilation (MV) by 26.5% and 52.0% ($p<0.001$) in response to 0.5 and 5 ng/ml TNF-α, respectively. Resection of the CSN attenuated MV response to TNF-α. In male HF animals, ventilatory response to TNF-α was blunted, increasing only 8%. In male CTL rats 0.5 and 5 ng/ml TNF-α reduced mean arterial pressure by 8.0% and 13.7% ($p<0.01$), an effect not altered by CSN resection. CTL and HF females exhibit lower basal ventilation parameters, but similar responses to TNF-α. The CBs of HF rats showed a 46% increase in TNF-α compared to CTLs ($p<0.01$).

Conclusion: TNF-α increases ventilation, and effect that is mediated by the CB and blunted in high-fat animals. It seems that there is no sexual dimorphism in TNF-α ventilatory responses mediated by the CB. The effect of TNF-α in the CB might contribute to its dysfunction in dysmetabolic states.

References: [1] Conde SV et al. J. Physiol. 2017; 595: 31-41; [2] Sacramento JF et al. Diabetologia. 2018; 61: 700-710; [3] Ribeiro MJ et al. Diabetes. 2013; 62: 2905-2916; [4] Sacramento JF et al. Int.

J. Mol. Sci. 2020; 21(15): 1-22; [5] Conde and Monteiro 2004, J Neurochem. 89:1148-56; [6] de Toda et al. Mechanisms of Ageing and Development. 2023; 211(1).

C04

The effects of water temperature and immersion depth on shear stress, arterial dilation, and Flow-Mediated Dilation following heating

Campbell Menzies[2], Charles Steward[2], Neil Clarke[3], Doug Thake[2], Chris Pugh[1], Tom Cullen[2]

[1]Cardiff Metropolitan University, Cardiff, United Kingdom, [2]Coventry University, Coventry, United Kingdom, [3]Birmingham City University, Birmingham, United Kingdom

Repeated exposure to hot water immersion improves arterial function [1,2]. However, there is a lack of evidence supporting specific protocol selection. Acute elevations in shear rate and flow-mediated dilation (FMD) positively correlate to subsequent chronic adaptations with exercise [3] and therefore may provide evidence with hot water immersion to support a particular immersion protocol. Core and skin temperature have distinct contributions to acute vascular responses [4 meaning, different immersion protocols may lead to divergent responses. Accordingly, this study aimed to compare the effects of (i) immersion depth, (ii) water temperature, and (iii) rectal temperature on acute changes in brachial artery diameter, shear rate, and subsequent FMD. It was hypothesised that shear stress and arterial diameter would differ between conditions and that greater increases in diameter post-heating would result in larger reductions in FMD.

Twenty-two healthy young adults completed three thirty-minute bouts of hot water immersion in a randomised order consisting of (i) Shoulder-deep immersion in 40 °C water (40-Shoulder), (ii) Waist-deep immersion in 40 °C water (40-Waist), and (iii) Waist-deep immersion in 42 °C water (42-Waist). Rectal temperature and vascular responses in the brachial artery (arterial diameter, blood flow, shear rate, FMD) were measured. Data were analysed using two-way repeated-measures ANOVAs, with the exception of FMD, which was allometrically scaled according to baseline diameter [5] and analysed using a generalised estimation equation. Significance was accepted at $p < 0.05$. Ethical approval was provided by the Coventry University (P146084) and conformed to the Declaration of Helsinki.

Rectal temperature increased less in the 40-Waist (Δ0.5 ± 0.1 °C) condition than either the 40-Shoulder (Δ0.9 ± 0.3 °C. $p < 0.001$), or 42-Waist condition (Δ0.9 ± 0.3 °C. $p < 0.001$), which were similar ($p = 1.0$). Shear rate differed between all conditions ($p < 0.001$. 40-Shoulder: Δ225 ± 131 1/s. 42-Waist: Δ105 ± 117 1/s 40-Waist: Δ-22 ± 66 1/s), whilst a greater increase in diameter was observed in the 40-Shoulder condition (Δ0.43 ± 0.22 mm), than either the 42-Waist (Δ0.11 ± 0.33 mm $p < 0.001$) or 40-Waist (Δ-0.02 ± 0.33 mm. $p < 0.001$) condition, which were similar ($p = 0.14$). Similarly, the 40-Shoulder condition demonstrated a larger decrease in FMD (Δ-3.9 ± 3.8%) than either the 42-Waist (Δ-1.7 ± 6.2%. $p = 0.01$) or 40-Waist (Δ0.2 ± 5.4%. $p < 0.001$) condition, which were similar ($p = 0.14$).

This study demonstrates that in response to a 30-minute hot water immersion bout, immersion depth has a larger influence than water temperature, or rectal temperature on arterial dilation, shear rate, and subsequent FMD. These findings provide novel evidence for the importance of heating larger body surface areas, over increases in rectal temperature, in the prescription of heating stimuli to elicit larger vasoactive and haemodynamic responses. In line with the stated hypothesis, larger reductions in FMD were observed in conditions that elicited greater brachial

vasodilation. Future work is required to examine the physiological meaningfulness of this in terms of changes to endothelial function and potential inference for effects on subsequent adaptation.

[1] Brunt et al. (2016). J Physiol, 594(18), 5329-5342. [2] Bailey et al. (2016). Int J Sports Med, 757-765. [3] Dawson et al. (2018). Eur J Appl Physiol, 118, 523-530. [4] Coombs et al. (2021). J Appl Physiol, 130(1), 149-159. [5] Atkinson et al. (2013). J Hypertens, 31(2), 287-291.

C05

Cerebral pulsatility index in a mouse model of acute ischemic stroke

Christina Shen-Zhuang Nielsen[1], Dmitry Postnov[2], Christian Aalkjaer[1], Vladimir Matchkov[1]

[1]Department of Biomedicine, Faculty of Health, Aarhus University, Aarhus, Denmark, [2]Center of Functionally Integrative Neuroscience, Department of Clinical Medicine, Faculty of Health, Aarhus University, Aarhus, Denmark

Background: Cerebral pulsatility index (PI) is used as a proxy for downstream vascular resistance in acute ischemic stroke in clinical studies, with PI measurements from the contralateral hemisphere serving as reference value[1]. We hypothesize that PI and cerebral blood flow changes occur in both hemispheres during acute ischemic stroke and aim to investigate these changes in a mouse model of transient acute ischemic stroke.

Methodology: Cerebral blood flow and PI before, during and after stroke-induction were measured using laser speckle contrast imaging in both brain hemispheres through bilateral cranial windows in five C57BL/6JRj male mice (age: 15-16 weeks). All animals received 10-13 training sessions for both handling[2,3] and for head fixation to allow for cerebral blood flow imaging in awake mice, as anaesthesia with isoflurane affects cerebral arteries[4]. All surgeries were performed under inhalation of isoflurane (induction: 4 %, 100% O_2, flow: 0.6 L/min; maintenance: 1,5%, 100% O_2, flow: 0.4 L/min).

The middle cerebral artery (MCA) was accessed through a 2-3 mm craniotomy in the right temporal bone, and the MCA was gently compressed for 1 hour with two micropipettes[5]. Decrease in MCA blood flow was assessed in real-time to validate MCA-occlusion (MCA-O). Cerebral blood flow and PI were measured repeatedly at baseline (awake and anaesthetized mouse), during MCA-O and immediately after pipette retraction (anaesthetized mouse), and on daily follow-ups for seven days (awake mouse).

Data are presented as mean ± SD, and changes between the two MCA were analysed with paired t-test. Longitudinal changes in PI and cerebral blood flow were analysed with two-way repeated measures ANOVA and corrected for multiple comparisons with post-hoc Bonferroni test. Significant effects are defined as $p< 0.05$.

Results: There were no differences in PI between both MCA at baseline, during MCA-O and follow-up. There were no significant changes in PI for both MCAs over time during MCA-O. Changes in PI for the right MCA were observed during follow-up at 48h (0.15 ± 0.04 vs 0.21 ± 0.03, p=0.0004) and 96h (0.16 ± 0.03 vs 0.21 ± 0.03, p=0.0125) as compared to baseline.

Changes in PI for the left MCA were identified during follow-up at 48h (0.15 ± 0.02 vs 0.22 ± 0.01, p<0.0001) and 96h (0.17 ± 0.03 vs 0.22 ± 0.01, p=0.0053) as compared to baseline.

Blood flow index did not change between both MCA at baseline and during follow-up. There were no changes in blood flow index over time at baseline and follow-up (awake). Blood flow index between the right and left MCA (107.4 ± 45.6 vs 455.2 ± 215.3, p <0.003) was significantly different

during MCA-O. Significant changes in blood flow index over time were observed in the right MCA between baseline (anaesthetized) and during MCA-O (360 ± 148.9 vs 107.4 ± 45.6, $p<0.0007$).

Conclusion: There were no differences between PI in both MCA before, during and after MCA-O. PI from both MCA were reduced during follow-up, as compared to baseline. Blood flow index did not differ between the two MCAs at baseline and during follow-up, except during MCA-O.

1. Ng, F. C. et al. Stroke 49, 2512-2515, doi:10.1161/STROKEAHA.118.021631 (2018). 2 Hurst, J. L. & West, R. S. Nat Methods 7, 825-826, doi:10.1038/nmeth.1500 (2010). 3 Marcotte, M. et al. J Vis Exp, doi:10.3791/62593 (2021). 4 Sullender, C. T et al. J Neurosci Methods 366, 109434, doi:10.1016/j.jneumeth.2021.109434 (2022). 5 Erdener, Ş. E. et al. Journal of Cerebral Blood Flow & Metabolism 41, 236-252, doi:10.1177/0271678X20914179 (2020).

C06

Novel Dbh+ Catecholaminergic Cardiomyocytes Contributing to the Structure and Function of the Cardiac Conduction System in Murine Heart

Tianyi Sun[1], Alexander Grassam-Rowe[2], Weinian Shou[3], Nicola Smart[4], Xiaoqiu Tan[5], Ming Lei[1]

[1]Department of Pharmacology, University of Oxford, Oxford, United Kingdom, [2]Department of Pharmacology, University of Oxford, Oxford, United Kingdom, [3]Herman B Wells Centre for Pediatric Research, Department of Pediatrics, Indiana University School of Medicine, Indianapolis, United States, [4]Department of Physiology, Anatomy & Genetics, University of Oxford, Oxford, United Kingdom, [5]Department of Cardiology, the Affiliated Hospital of Southwest Medical University, Luzhou, China

Research rationale

The heterogeneity of functional cardiomyocytes arises during heart development, which is essential to the complex and highly coordinated cardiac physiological function[1]. Yet the biological and physiological identities and the origin of the specialized cardiomyocyte populations have not been fully clarified.

Methodology

Single-cell RNA-seq and spatial transcriptomic technologies are applied to investigate cardiogenesis and the genetic profile of the cells of interest. The genetic mouse model DbhCre/Td-ChR2 was generated for lineage tracing and cell fate mapping. Transmission electron microscopy was applied for structural and functional study.

Results

Using single-cell RNA sequencing (scRNA-Seq), we mapped the transcriptional landscape of CCS (Cardiac Conduction System) formation and maturation in the murine heart. This led to the identification of an unreported cardiomyocyte population expressing *Dbh gene* encoding Dopamine-beta-hydroxylase which is key enzyme for biosynthesis of neurotransmitter Noradrenaline. We determined how these myocytes are distributed across the heart by utilising advanced single-cell and spatial transcriptomic analyses, genetic fate mapping and molecular imaging with computational reconstruction. From E14.5 to adulthood, Dbh+ CMs were abundant in the CCS regions where sympathetic innervation is enriched, as detected by immunostaining with anti-Th antibody, particularly in the adult heart, revealing their close relationship with sympathetic innervation. Immuno-Electron Microscopy further unveiled the presence of high electron-density vesicles in adult Dbh+ cardiomyocytes, which strongly indicates the secretory function of Dbh+ cardiomyocytes.

Conclusions

We discovered a uniquely distributed group of unreported catecholaminergic cardiomyocytes with key regulatory roles in cardiac excitation conduction, providing new insights into neuron-endocrine

function of cardiomyocytes. The physiological and pathophysiological implications of such function need to be further explored in the future.

We discovered a uniquely distributed group of unreported catecholaminergic cardiomyocytes with key regulatory roles in cardiac excitation conduction. We also revealed their close relationship with sympathetic innervation during cardiac conduction system (CCS) formation.

Our study thus provides new insights into the development and heterogeneity of the mammalian cardiac conduction system by revealing a new cardiomyocyte population with potential catecholaminergic endocrine function.

Ethics declarations

Competing interests: The chip, procedure, and application of Stereo-seq are covered in pending patents. The remaining authors declare no other competing interests.

Animals and ethical approval

All animal experiments were performed on mice neonatal or adult mice (both genders) in accordance with the United Kingdom Animals (Scientific Procedures) Act 1986 and were approved by the University of Oxford Pharmacology ethical committee (approval ref. PPL: PP8557407) or Animal Care and Use Committee of the Southwest Medical University, Sichuan (China) (No: 20160930) in conformity with the national guidelines under which the institution operates.

Statistics

For the spatial transcriptomics, we had at least $n = 3$ sections for hearts from *Dbh*^{Cre}/Rosa26-tdTomato mice at E12.5, E14.5, P3, and P56, respectively.

Whole embryos (E8.5, E9.5, E10.5, E12.5, E14.5, $n = 5$ embryos per stage) or isolated hearts (E12.5, E13.5, E14.5, E16.5, P3, P56, $n = 5$ hearts per stage) were analyzed by using multiplex nucleic acid in situ hybridization (RNAscope), immunohistological staining, confocal microscopic imaging and EM.

Reference 1. Lescroart, F. et al. Defining the earliest step of cardiovascular lineage segregation by single-cell RNA-seq. https://www.science.org.

C07

P2X3 antagonists as a novel anti-arrhythmic

Carol T Bussey[1], Rexson Tse[2], Martin K Stiles[3], David J Paterson[4], Julian FR Paton[5]

[1]Manaaki Manawa Centre for Heart Research, Department of Physiology, Faculty of Medical & Health Sciences, University of Auckland, Auckland, New Zealand, [2]Gold Coast Hospital and Health Service, Queensland Health, Gold Coast, Australia, [3]Waikato Clinical School, Faculty of Medical & Health Sciences, University of Auckland, Hamilton, New Zealand, [4]Burdon Sanderson Cardiac Science Centre, Department of Physiology, Anatomy and Genetics, Medical Sciences Division, University of Oxford, Oxford, United Kingdom, [5]Manaaki Manawa Centre for Heart Research, Department of Physiology, Faculty of Medical & Health Sciences, University of Auckland, Auckland, New Zealand

Introduction: Cardiovascular diseases are characterised by elevated sympathetic nerve activity, which contributes to end-organ damage, morbidity and mortality. Surgical removal of the stellate ganglion to short-circuit sympathetic nerve overactivity can eradicate arrhythmias, however this is a highly invasive approach with significant side-effects, necessitating discovery of novel non-invasive druggable targets. Recent transcriptomic data shows upregulation of P2X3 purinergic receptors in the stellate ganglia of Spontaneously Hypertensive (SHR) compared to Wistar rats (Bardsley EN *et al*. 2018. Sci Rep 8, 8633). We hypothesise that these purinergic receptors within cardiac stellate ganglia contribute to sympathetic overactivity and the development of cardiovascular diseases such as hypertension and arrhythmias.

Objectives: Confirm expression of P2X3 receptor in stellate ganglia, investigate cardiac responses to stellate ganglia P2X3 receptor stimulation/inhibition, and examine effect of P2X3 receptor antagonism on cardiac arrhythmias.

Methods: Stellate ganglia from Wistar and SH rats (n=6) and humans (n=2) were immunofluorescently stained for P2X3 receptor and tyrosine hydroxylase, and P2X3 receptor expression in rat stellate ganglia was quantified using qPCR. Cardiac responses to stellate ganglion P2X3 receptors were investigated in the decerebrated working heart-brainstem preparation of Wistar and SH rats (4-5 week old), following anaesthesia with 5% isoflurane in oxygen. Arrhythmias were triggered in SHR, which exhibit increased arrhythmogenicity, with a combination of atropine (30μM) and caffeine (100μM) delivered in the perfusate, followed by electrical stimulation of the stellate ganglion.

Results: We have confirmed in both rat and human stellate ganglia that P2X3 receptors are co-localised with tyrosine hydroxylase-expressing sympathetic cells. P2X3 receptor expression is upregulated in SHR stellate ganglia (Wistar 1.03±0.10, SHR 3.77±0.78 fold, mean±SEM, n=7-8, $p<0.01$ students t-test). Microinjection of stable ATP analogue αβmethylene-ATP (100μg) directly into the stellate ganglion causes tachycardia (Wistar 45.6±8.3; SHR 62.5±14.1 Δbpm, n=7), which is attenuated by P2X3 inhibition with AF353 (Wistar 25.0±7.5; SHR 19.5±7.5 Δbpm; n=4-5, $p<0.05$ mixed effects model). Arrhythmias were triggered in the ECG of 61% of experiments (n=13), particularly AV block (n=3), and fragmented QRS complexes (n=4), with bundle block and

bradyarrhythmia also observed. Of these arrhythmias, 70% were attenuated or abolished following blockade of P2X3 receptors (n=9).

Conclusions: Stellate ganglion P2X3 purinergic receptors regulate cardiac function, and P2X3 overexpression likely contributes to sympathetic overactivity in cardiovascular disease. P2X3 inhibition rapidly and profoundly recovers arrhythmic heart rhythms, and reverses electrical instability.

C08

The Na,K-ATPase-dependent Ca2+-sensitization by cSrc kinase in murine middle cerebral arteries is partially independent of the Rho kinase pathway

Ask Carit Andersen[1], Christian Staehr[1], Vladimir Matchkov[1]

[1]Aarhus University, Aarhus, Denmark

Aims: In the vascular wall of cerebral arteries, micromolar ouabain inhibits the α2 Na,K-ATPase and activates cSrc kinase, which was shown to increase Ca^{2+}-sensitivity of the smooth muscle cell contractile machinery. It has been proposed, that this cSrc-dependent Ca^{2+}-sensitization depends on the phosphorylation of myosin phosphatase target subunit 1 (MYPT1) by Rho kinase signaling, as the conventional pathway for Ca^{2+}-sensitization of vascular smooth muscle cells. However, this Src-Rho-MYPT1 signaling remains to be shown and validated in cerebral arteries. Familial hemiplegic migraine type 2 is associated with mutations in the α2 Na,K-ATPase, including the G301R missense mutation, associated with reduced abundancy of the Na,K-ATPase in cerebrovascular smooth muscle cells, resulting in increased cSrc activation. We aimed to test whether cSrc potentiates Ca^{2+}-sensitivity via Rho-kinase-dependent MYPT1 phosphorylation in middle cerebral arteries and to compare this signaling in mice bearing the G301R mutation ($ATP1A2^{+/G301R}$) and wild types.

Methods: Middle cerebral artery contractility to thromboxane A_2 analog, U46619, was assessed ex-vivo in isometric myograph. The effects of pre-incubation with Rho kinase inhibitor, Y27632 ($3 \cdot 10^{-6}$M) and ouabain (10^{-5}M) were studied. Arteries from $ATP1A2^{+/G301R}$ and wild type mice were compared.
To assess cSrc and MYPT1 phosphorylation and its dependence on Rho kinase, U46619-stimualted middle cerebral arteries from wild type and $ATP1A2^{+/G301R}$ mice were studied with Western blot upon pre-incubation with Y27632, ouabain or both.

Results: Ouabain potentiated the U46619-induced contraction of middle cerebral arteries from wild type mice (n=5), while Y27632 inhibited it (n=4). In the presence of Y27632, ouabain still potentiated the contraction of wild type arteries (n=5). In contrast, ouabain did not significantly affect the contraction of $ATP1A2^{+/G301R}$ mice (n=5), neither under control conditions nor after Rho kinase inhibition, while Y27632 still suppressed the contraction (n=3). Western blot data indicates a positive correlation between cSrc kinase and MYPT1 phosphorylation, which is only partially prevented by Rho kinase inhibition (24 mice divided into 6 groups exposed to 4 different interventions).

Conclusion: We suggest, that cSrc kinase increases Ca^{2+}-sensitivity in vascular smooth muscle cells via MYPT1 phosphorylation. Our results suggest that this arterial tonus regulating pathway is partially independent of Rho kinase signaling.

Staehr, C., et al., Smooth muscle Ca2+ sensitization causes hypercontractility of middle cerebral arteries in mice bearing the familial hemiplegic migraine type 2 associated mutation. Journal of Cerebral Blood Flow & Metabolism, 2018. 39(8): p. 1570-1587.

C09

The differential pro-contractile effect of ouabain depends on agonist and smooth muscle activation state.

Anna Giné Martínez[1,2], Daniel Løgstrup Nielsen[2], Josef Khalid[2], Elizaveta Melnikova[2], Vladimir Matchkov[2]

[1]Facultat de Medicina i Ciències de la Salut, Universitat Internacional de Catalunya, Barcelona, Spain, [2]Department of Biomedicine, Health, Aarhus University, Aarhus, Denmark

The Na,K-ATPase modulates arterial tone by means of ionic gradients, and via the Na,K-ATPase-dependent signal transduction, including the Src kinase signaling pathway. Inhibition of the Na,K-ATPase leads to accumulation of intracellular Na^+, which modifies the Na,Ca-exchanger activity leading to elevation of intracellular Ca^{2+} and smooth muscle contraction. Src kinase activates upon interaction with the Na,K-ATPase inhibitor, i.e., cardiotonic steroid ouabain, which leads to sensitization of smooth muscle cell contractile machinery and potentiation of arterial contraction. It has been proposed that both Na,K-ATPase-dependent mechanisms potentiate the contraction in response to different pro-contractile stimuli, however, their contribution depends on contractile agonist.

This study aims to analyze the agonist-dependence (methoxamine, U46619, and noradrenaline) of the pro-contractile action of ouabain, and its effect at different activation states in the vascular wall.

Male Wistar Hannover rats were obtained from Janvier-Labs (France) and sacrificed with CO_2 inhalation. Mesenteric arteries (2^{nd} – 3^{rd} order branches) were dissected and used in isometric myography, where the contraction was induced by either U46619 (thromboxane A_2 mimetic), methoxamine (alpha1-adrenergic receptor agonist), or noradrenaline (unspecific adrenoreceptor agonist). The arterial segments were compared under control conditions and in the presence of either ouabain, or iberiotoxin (IbTX), the inhibitor of big conductance Ca^{2+}-activated potassium channels, or in the combination of these drugs. Intracellular Ca^{2+} was measured with Ca^{2+}-sensitive dye, FURA-2/AM simultaneously with contractile responses in myograph. Western blot with arterial segment lysates was performed to assess the phosphorylation of Src kinase and MYPT protein responsible for Ca^{2+} sensitization. The comparison of concentration-response curves was done with two-way ANOVA. Data presented as mean±standard deviation.

Ouabain (10 μM) significantly potentiated the contraction in response to U46619 (pEC50 changes from 6.2±0.5 to 6.8±0.7, n=7, P=0.016). IbTX also potentiated the U46619-induced contraction in comparison with the control (pEC50: 7.5±3, n=7, P<0.0001). Pro-contractile effects of IbTX and ouabain were not additive (pEC50: 7.1±0.7, n=5, P=0.0003). In contrast, ouabain showed no clear potentiation of methoxamine-induced constriction (pEC50: 5.2±0.7 and 5.5±0.3, n=7, P=0.92). However, the pro-contractile effect of IbTX was still seen (pEC50: 5.8±0.3, n=7, P=0.03) but this was not affected by a combination of IbTX and ouabain (pEC50: 5.7±0.2, n=7, P=0.13). Finally, no potentiation of vessel contractility by ouabain was observed in the stimulation with noradrenaline (pEC50: 5.9±0.2 and 6.0±0.1, n=6, P=0.20), neither with IbTX (pEC50: 6.1±0.2, n=6, P=0.28), but this effect was strengthened in the presence of both IbTX and ouabain (pEC50: 6.2±0.2, n=6, P=0.03).

Further analyses demonstrated that a major part of ouabain pro-contractile action is not associated with elevation of intracellular Ca^{2+} but with Ca^{2+} sensitization. In contrast, IbTX strongly elevates intracellular Ca^{2+} in smooth muscle cells.

This study demonstrates the agonist-dependent character of the pro-contractile action of ouabain, where agonists whose action is primarily mediated by Ca^{2+}-sensitization are most sensitive to inhibition of the Na,K-ATPase. Importantly, this ouabain action can further be potentiated by the elevation of intracellular Ca^{2+} with IbTX. This study suggests that caution should be taken when comparing the pro-contractile ouabain action for different agonists and at different activation states of the vascular wall.

Staehr, C., Aalkjaer, C., & Matchkov, V. V. (2023). The vascular Na,K-ATPase: clinical implications in stroke, migraine, and hypertension. Clinical science (London, England : 1979), 137(20), 1595–1618. Blaustein, M. P., & Hamlyn, J. M. (2024). Sensational site: the sodium pump ouabain-binding site and its ligands. American journal of physiology. Cell physiology, 326(4), C1120–C1177. Hangaard, L., Jessen, P. B., Kamaev, D., Aalkjaer, C., & Matchkov, V. V. (2015). Extracellular Calcium-Dependent Modulation of Endothelium Relaxation in Rat Mesenteric Small Artery: The Role of Potassium Signaling. BioMed research international, 2015, 758346. Zhang, L., Aalkjaer, C., & Matchkov, V. V. (2018). The Na,K-ATPase-Dependent Src Kinase Signaling Changes with Mesenteric Artery Diameter. International journal of molecular sciences, 19(9), 2489. Bouzinova, E. V., Hangaard, L., Staehr, C., Mazur, A., Ferreira, A., Chibalin, A. V., Sandow, S. L., Xie, Z., Aalkjaer, C., & Matchkov, V. V. (2018). The α2 isoform Na,K-ATPase modulates contraction of rat mesenteric small artery via cSrc-dependent Ca2+ sensitization. Acta physiologica (Oxford, England), 224(1), e13059.

C10

Evaluating the impact of succinate on cardiac electrical integrity in the mouse

Sean Benson[1,2], Andrew Coney[1,2], Andrew Holmes[1,2]

[1]School of Biomedical Sciences, Institute of Clinical Sciences, University of Birmingham, Birmingham, United Kingdom, [2]Institute of Cardiovascular Sciences, University of Birmingham, Birmingham, United Kingdom, [3]School of Biomedical Sciences, Institute of Clinical Sciences, University of Birmingham, Birmingham, United Kingdom

Introduction. During cardiac ischaemia-reperfusion, high levels of succinate accumulation and metabolism promote reactive oxygen species mediated cell death and dysfunction [1]. There is also a high risk of both atrial and ventricular arrhythmias following exposure to ischaemia/reperfusion. However, the impact of succinate on cardiac electrical function remains largely uncharacterised and it is unclear if elevated succinate metabolism may have a role in promoting cardiac arrhythmia.

Aims/Objectives. This study analysed the effects of succinate on murine ECGs to identify potential proarrhythmic electrical changes in the atria and ventricles.

Methods. ECGs were recorded from male and female adult FVB mice (n=15) under alfaxalone anaesthesia (Alfaxan®; Vetoquinol UK Ltd), at 20-25 mg kg^{-1} h^{-1}, i.v., with 0.02 ml boluses as necessary. The left jugular vein was cannulated to allow for infusion of diethyl succinate (DESucc) a cell permeable form of succinate [2]. ECG recordings were measured at baseline (Pre-infusion), throughout 15-20 minutes infusion of Vehicle (n=3) or low dose DESucc (8 mg kg^{-1} min^{-1} (n=3)) or high dose DESucc (80 mg kg^{-1} min^{-1} (n=9)), and again 10 minutes post-infusion. Analysis was performed in ECG and HRV modules in LabChart v8 (AD Instruments, Oxford, UK). Signal averaged ECGs were used for waveform analysis. The arrhythmia index (number of premature or delayed R-waves per minute) was recorded across the whole experiment. Following the experiment, animals were killed by a schedule 1 method. Values are expressed as mean±SEM. Statistical analysis was performed using a one-way repeated measures Analysis of Variance with Bonferroni post hoc analysis (Prism9, GraphPad, Cal, USA). Significance was taken as $P<0.05$.

Results. High dose DESucc infusion did not significantly modify heart rate (Pre-infusion: 476±9; high DESucc: 494±25; Post-infusion: 517±41 beats per minute, n=9). However, high dose DEsucc infusion produced an elevation in irregularly spaced R-R intervals and delayed beats as evidenced by an increase in arrhythmia index (Pre-infusion: 0.8±0.3; high DESucc: 4.1±0.9; Post-infusion: 1.9±0.8 abnormal beats per minute, n=9, $P<0.05$). Similarly, high dose DESucc infusion increased the standard deviation of the R-R interval (SDRR) (Pre-infusion: 5.7±0.5; high DESucc: 20±3; Post-infusion: 7±3 ms, n=9, $P<0.05$). Analysis of ECG waveforms showed that high dose DESucc significantly prolonged the P-R interval, the QRS duration and the Q-T interval. However, the most striking effect was to cause irreversible prolongation the P-wave duration (Pre-infusion: 9±0.4; high DESucc: 13±1; Post-infusion: 13±1 ms, n=9, $P<0.05$). Arrhythmia index, SDRR, P-wave duration, P-R interval, QRS duration and Q-T interval were not significantly modified by Vehicle (n=3) or low dose DESucc (n=3) infusion.

Conclusion. High dose DESucc infusion causes acute cardiac arrhythmia and changes in ECG waveforms which are consistent with major conduction disturbances in both the atria and ventricles. More work is required to determine if these actions are dependent on direct modifications in ion channel function, such as $Na_v1.5$, which may be preventable by targeted treatment.

1. Chouchani ET, Pell VR, Gaude E, Aksentijević D, Sundier SY, Robb EL, Logan A, Nadtochiy SM, Ord ENJ, Smith AC, Eyassu F, Shirley R, Hu CH, Dare AJ, James AM, Rogatti S, Hartley RC, Eaton S, Costa ASH, Brookes PS, Davidson SM, Duchen MR, Saeb-Parsy K, Shattock MJ, Robinson AJ, Work LM, Frezza C, Krieg T, Murphy MP. Ischaemic accumulation of succinate controls reperfusion injury through mitochondrial ROS. Nature 515:431-435. 2. Swiderska A, Coney AM, Alzahrani AA, Aldossary HS, Batis N, Ray CJ, Kumar P & Holmes AP. (2021). Mitochondrial Succinate Metabolism and Reactive Oxygen Species Are Important but Not Essential for Eliciting Carotid Body and Ventilatory Responses to Hypoxia in the Rat. Antioxidants 10(6):840.

C11

The effect of interrupting prolonged sitting with light movement on central and peripheral haemodynamics in Long COVID

Nicholas Hudson[1], Scott Hannah[1], Simon Fryer[2], Mark Rickenbach[3], Margaret Husted[1], Helen Ryan Stewart[4], James Faulkner[1]

[1]University of Winchester, Winchester, United Kingdom, [2]University of Gloucestershire, Gloucester, United Kingdom, [3]Park and St Francis Surgery, Eastleigh, United Kingdom, [4]Eastern Institute of Technology, Napier, New Zealand

Long COVID-19 is defined as signs, symptoms and conditions that develop after initial SARS-CoV-2 infection and persist for over four weeks. Nearly 2 million people in the UK are currently experiencing self-reported long COVID, of which 61% of these people have been living with symptoms for more than a year. (*Office for National Statistics*, 2023).

Long COVID presents with over fifty different symptoms, which can vary significantly from person to person. People with long COVID demonstrate significantly greater levels of sedentary behaviour (Delbressine *et al.*, 2021), partially explained by fatigue being one of the most common symptoms. Sedentary time is known to have an adverse effect on vascular function and can increase the risk of cardiovascular disease. Acute sitting periods as short as one hour can worsen vascular function (Taylor *et al.*, 2022), however, interrupting these periods with short bouts of movement has been shown to mitigate the negative effect on vascular health (Paterson *et al.*, 2020). Arterial stiffness is a measure of vascular dysfunction through changes in the structure and function of blood vessels. Carotid-femoral pulse wave velocity (cfPWV) is the gold standard tool to non-invasively measure arterial stiffness.

This study aimed to investigate whether prolonged sitting for 2 hours induces a vascular response in people with long COVID and if interrupting sitting periods has a beneficial effect on arterial stiffness. Participants were tasked with sitting still for two hours. Interruption includes three bouts of five sit-to-stands, five calf raises, and three minutes of self-paced walking to mimic activities of daily living. Measures of central and peripheral blood pressure, arterial stiffness (SphygmCor XCEL), executive function (TrailMaking Tasks), and cerebral oxygenation (Near Infrared Spectroscopy) were recorded at baseline and following two hours of interrupted or uninterrupted sitting. Ethical approval was obtained by Health and Care Research Wales (IRAS: 309606 22/SC/0120).

Thirty participants (52.84 $\pm$ 13.19 years, symptoms lasting >12 months) completed both experimental visits and were used in the analysis. Repeated measures ANOVA demonstrated a significant increase in central systolic blood pressure (cSBP) ($P=0.005$, $\eta_p^2 = 0.258$), central diastolic blood pressure (cDBP) ($P<0.001$, $\eta_p^2 = 0.519$), brachial systolic blood pressure (SBP) ($P<0.001$, $\eta_p^2 = 0.348$) and mean arterial pressure (MAP) ($P<0.001$, $\eta_p^2 = 0.391$) following prolonged sitting regardless of interruptions. There was no significant change in cfPWV ($P=0.541$). Mental fatigue significantly increased in both conditions ($P=0.019$, $\eta_p^2 = 0.194$).

This research demonstrates that sitting for 2 hours instigates changes in central and peripheral blood pressure, which is thought to be driven by blood pooling in the lower limbs resulting in a decrease in venous return and cardiac output causing compensations through the sympathetic nervous system including increased peripheral vascular resistance (Adams *et al.*, 2023). Although interrupting sitting did not affect cfPWV, it is unclear whether the intensity of interruption or the duration of sitting time was sufficient to induce changes in arterial stiffness. Additionally, understanding the effect of chronic periods of sedentary behaviour through prolonged sitting on arterial stiffness is important to understand the clinical relevance of increased sedentary behaviour in long COVID.

Adams, N. et al. (2023) 'The Effect of Sitting Duration on Peripheral Blood Pressure Responses to Prolonged Sitting, With and Without Interruption: A Systematic Review and Meta-Analysis', Sports Medicine, 54. Available at: https://doi.org/10.1007/s40279-023-01915-z. Delbressine, J.M. et al. (2021) 'The Impact of Post-COVID-19 Syndrome on Self-Reported Physical Activity', International Journal of Environmental Research and Public Health, 18(11), p. 6017. Available at: https://doi.org/10.3390/ijerph18116017. Paterson, C. et al. (2020) 'The Effects of Acute Exposure to Prolonged Sitting, With and Without Interruption, on Vascular Function Among Adults: A Meta-analysis', Sports Medicine, 50(11), pp. 1929–1942. Available at: https://doi.org/10.1007/s40279-020-01325-5. Prevalence of ongoing symptoms following coronavirus (COVID-19) infection in the UK - Office for National Statistics (no date). Available at: https://www.ons.gov.uk/peoplepopulationandcommunity/healthandsocialcare/conditionsanddiseases/bulletins/prevalenceofongoingsymptomsfollowingcoronaviruscovid19infectionintheuk/2february2023 (Accessed: 17 March 2023). Taylor, F.C. et al. (2022) 'The Acute Effects of Prolonged Uninterrupted Sitting on Vascular Function: A Systematic Review and Meta-analysis', Medicine & Science in Sports & Exercise, 54(1), p. 67. Available at: https://doi.org/10.1249/MSS.0000000000002763.

C12

Raising the Bar on Health: Can one year of endurance exercise training enhance vascular function in healthy individuals?

Marcos Paulo Rocha Alves[1], Casper Sejersen[1], Mads Fischer[1], Andrea Tamirezz-Ellemann[1], Lasse Gliemann[1]

[1]The August Krogh Section for Human Physiology, Department of Nutrition, Exercise and Sports, University of Copenhagen, Copenhagen, Denmark., Copenhagen, Denmark

Introduction: Endurance exercise training improves aerobic capacity and endothelial function in people with an elevated risk of cardiovascular disease by augmenting nitric oxide synthesis through the shear stress mechanism. However, whether long-term endurance exercise enhances vascular function concomitant with aerobic capacity in healthy individuals is unclear. We hypothesized that long-term endurance exercise training improves aerobic capacity and enhances global vascular function in healthy individuals. **Aim:** To determine the impact of one year of supervised endurance exercise training on healthy individuals' vascular function and aerobic capacity. **Materials and Methods:** Over one year, seven health subjects (4 males and 3 females; 25 ± 5.2 yrs, 74.8 ± 14.6 kg) engaged in regular supervised cycling training three times per week, 60 minutes for each section. Aerobic capacity ($\dot{V}O_2$max) was assessed at entry (Baseline) and after 1, 2, 6, and 12 months; forearm vascular function was assessed at Baseline, 1, 4, 6, and 12 months. Catheters (20-gauge arterial cannula; BD) were placed in the brachial artery to measure arterial pressure and for drug infusion. Endothelium-dependent and -independent vasodilation were estimated by a cumulative increase in infusion rates of acetylcholine (10, 25, and 100 µg/L/min) and sodium nitroprusside (1.5, 3, and 6 µg/L/min). Mean arterial pressure (MAP), brachial artery diameter (BA), and blood velocity (BV) were simultaneously quantified (Doppler ultrasound) at the last 30 sec of each infusion rate. Blood flow (BF) was calculated as $BV \bullet \pi \bullet (BA/2)^2 \bullet 60$. **Statistical analysis:** Data were analyzed using one-way repeated measures ANOVA. The area under the curve (AUC) was used to calculate the total BF response for each drug infusion. The AUC was calculated as the sum of the three infusion rates over the last 30-second period above the baseline values representing the total BF (100/ml.min^{-1}). Data are expressed as mean±SD, with statistical significance accepted at $p < 0.05$. **Ethical:** The local institutional review board approved the study, and the subjects gave written informed consent. **Results:** Six months after the commencement of cycling training, a significant improvement in aerobic capacity was evident, with an increase in $\dot{V}$O2max from 40.1 ml.min^{-1}.kg^{-1} to 50.8 ml.min^{-1}.kg^{-1}; $p = 0.02$. This enhancement continued over a year, resulting in an increase in $\dot{V}O_2$max by 28 % (Baseline 40.1 ml.min^{-1}.kg^{-1} vs. 12 months, 51.3 ml.min^{-1}.kg^{-1}; $p = 0.04$). The MAP remained stable during pharmacological challenges at all infusion rates and visits. The BF response curve (AUC) to acetylcholine and sodium nitroprusside across different visits was not different from baseline at any timepoint ($p > 0.05$). **Conclusion:** The preliminary results confirm that a year-long supervised endurance exercise training significantly increases aerobic capacity in healthy individuals. Contrary to our hypothesis, increased aerobic capacity was not followed by increased vascular function, suggesting that vascular health is already at its optimum in those who are untrained yet healthy subjects.

1. Hellsten Y, Nyberg M, Jensen LG, Mortensen SP. Vasodilator interactions in skeletal muscle blood flow regulation. J Physiol 590: 6297–6305, 2012. PMID: 22988140 2. Green DJ. Exercise

training as vascular medicine: direct impacts on the vasculature in humans. Exerc Sport Sci Rev. 2009 Oct;37(4):196-202 PMID: 19955869. 3. Maiorana A, O'Driscoll G, Dembo L, Goodman C, Taylor R, Green D. Exercise training, vascular function, and functional capacity in middle-aged subjects. Med Sci Sports Exerc. 2001 Dec;33(12):2022-8PMID: 11740294. 4. Møller S, Hansen CC, Ehlers TS, Tamariz-Ellemann A, Tolborg SÁR, Kurell ME, Pérez-Gómez J, Patrzalek SS, Maulitz C, Hellsten Y, Gliemann L. Exercise Training Lowers Arterial Blood Pressure Independently of Pannexin 1 in Men with Essential Hypertension. Med Sci Sports Exerc. 2022 Sep 1;54(9):1417-1427. Epub 2022 Apr 12. PMID: 35420578. 5. Padilla J, Simmons GH, Vianna LC, Davis MJ, Laughlin MH, Fadel PJ. Brachial artery vasodilatation during prolonged lower limb exercise: role of shear rate. Exp Physiol. 2011 Oct;96(10):1019-27. Epub 2011 Jul 22. PMID: 21784788;

C13

Teamwork, proposal writing, and application-style assignments prepare undergraduates for research and science-related careers.

Michelle French[1], Helen Miliotis[1], Stavroula Andreopoulos[4], Rebecca Laposa[4], Christina Zakala[5], Michelle Arnot[3]

[1]Department of Physiology, University of Toronto, Toronto, Canada, [2]Department of Physiology, Toronto, Canada, [3]Department of Pharmacology and Toxicology, University of Toronto, Toronto, Canada, [4]Department of Pharmacology and Toxicology, University of Toronto, Toronto, Canada, [5]University of Toronto, Toronto, Canada

Undergraduate education serves to both broaden and deepen knowledge of a specific discipline while also aiming to develop transferrable skills. In terms of physiology majors, published transferable skills encompass four broad areas: critical thinking, communication, professional behaviours, and laboratory proficiency[1,2]. While these skills are often developed through laboratory and independent research project courses, opportunities can be limited due to funding and space constraints. In addition, the size and need to cover content limits opportunities in lecture-based courses. More broadly, we observed that undergraduates were under-prepared for independent research courses and were unaware of the diverse range of science-related careers. To address this gap and help build transferrable skills, we created *Research Readiness and Advancing Biomedical Discoveries*, a third-year course for life science students. Central to the course is a scaffolded research proposal assignment aimed at solving real-world problems. Online pre-class modules and in-class group work cover topics such as project management and good laboratory practice (see https://experientialmodules.utoronto.ca/research-readiness/). To assess the usefulness of the course in the long term, we surveyed former students one to four years post course completion (Univ. Toronto REB#18345). Survey questions included statements rated on a five-point Likert scale and open-ended prompts. For the latter, two research assistants independently identified and grouped the responses into themes. Of the 63 former students who completed the survey (a 29% response rate), the majority (n = 52) had taken the course three or four years before. Almost two thirds were pursuing advanced degrees: the most common being in research-based graduate programs (41%). Most of the remainder were employed in science-related positions. Responses to the quantitative questions were favourable with students agreeing or strongly agreeing that the course improved their skill set to achieve future goals (4.14 +/- 0.10, mean +/- SEM, 4 = agree, 5 = strongly agree); consider flexible career paths (4.16 +/- 0.10) and in helping them prepare for research opportunities (4.00 +/- 0.12). The most common themes that emerged from the open-ended prompt: "*What aspects of the course helped with your current career pursuits*" were: working in teams (68% of respondents), developing and writing an original research proposal (68% of respondents) and applying your knowledge (59% of respondents). While this study was for a single course, we believe that our results are broadly applicable and encourage educators to incorporate teamwork, proposal writing, and assignments requiring the application of knowledge into the curriculum. Our results also illustrate the value of surveying former students to learn the aspects of a course that are most useful for graduates.

1. French MB et al. (2020) Adv Physiol Educ 44, 653-657. 2. Zubek J et al. (2023) Adv Physiol Educ 47, 117-123.

C14

Cheating or Not Cheating? A workflow for including critical appraisal when writing paragraphs using a large language model.

Matthew Hardy[1]

[1]*University of Bradford, Bradford, United Kingdom*

Since OpenAI made ChatGPT publicly available in November 2022, the use of large language models (LLMs) within academia and higher education has been widely scrutinised. Some points of view are critical of their use: using LLMs to generate written work has been considered akin to plagiarism, while software that can be used to identify work written using generative artificial intelligence (AI) is fallible. This suggests that the impact of LLM use may include restructuring of assessments and, in some cases, reverting to pen and paper-based submissions (Milano *et al.,* 2023). Alternatively, the accessibility and widespread use of LLMs suggests that they are tools that will become common in many future careers and thus there is a responsibility of academics to teach students how to use them ethically and effectively (Hardy, 2023). Indeed, Russel Group Universities have released a statement to this effect (Russel Group, 2023).

In response to this dilemma, this project aimed to develop a workflow utilising an LLM to include critical appraisal in paragraphs suitable for written academic work. This was to be done in a manner that would facilitate writing production, without reducing the need for understanding of the scientific content.

ChatGPT 4 was provided with a sequence of prompts that utilised a combination of Generate Knowledge Prompting (Liu *et al.,* 2021) and Prompt Chaining (Anthropic, 2024). The LLM was instructed that it would be provided with knowledge and it should then write a paragraph according to the following structure: Claim, Justification, Evidence, Conclusion. Constraints were provided that defined content and a range for the number of sentences for each part of the paragraph. Knowledge was provided that included appraisal from two journal articles, as well as providing a hierarchy regarding the importance of details. The resultant paragraph was refined by providing additional prompts for ease of reading, academic format, and to remove statements that could not be confirmed with the knowledge that had been provided. While ChatGPT 4 successfully produced a comprehensible paragraph, the text produced was identified as being generated by AI using the Turnitin AI-checker.

This workflow demonstrates that using LLMs can be a valid approach to producing written work and can be done without encouraging cognitive dissonance from the scientific content incorporated. Furthermore, using LLMs may provide more inclusive writing practices for authors who may have barriers to producing written content, for example, those for whom English is a second language. However, using such approaches provides content that will be identified as being generated by AI, which will impact future approaches to identifying and defining academic misconduct within written work.

Anthropic. https://docs.anthropic.com/claude/docs/chain-prompts /accessed 03 April 2024 Hardy M.E. (2023) The Impact of Artificial Intelligence on Teaching Writing Skills to Life Science Students.

Physiology News. 132, pp. 38-9. Liu, J., Liu, A., Lu, X., Welleck, S., West, P., Bras, R.L., Choi, Y. and Hajishirzi, H. (2021) Generated knowledge prompting for commonsense reasoning. arXiv preprint arXiv:2110.08387. Milano, S., McGrane, J.A. and Leonelli, S. (2023) Large language models challenge the future of higher education. Nature Machine Intelligence, 5(4), pp.333-334. Russel Group. (2023) New principles on use of AI in education. https://russellgroup.ac.uk/news/new-principles-on-use-of-ai-in-education/ accessed 13 October 2023

C15

Ten Years of Worms: Development of an 'Earthworm Action Potentials' Practical Class

Matthew Mason[1]

[1]*University of Cambridge, Department of Physiology, Development & Neuroscience, Cambridge, United Kingdom*

Michael Foster, who introduced experimental physiology to Cambridge, used a frog sciatic nerve-muscle preparation in his practical classes. A very similar preparation was used to teach generations of medical, veterinary and natural science students over a period of around 140 years. However, obtaining frogs became increasingly difficult, and there was a desire to reduce the use of vertebrates in our classes. As a result, in 2014 we moved to the use of earthworms (*Lumbricus terrestris*) instead. We report here on the 'Earthworm Action Potentials' practical class which we have developed and refined over the last ten years, with a view to inspiring the development of similar introductory neurobiology classes in other physiology departments.

Worms, readily obtained from a fishing-bait supplier, are anaesthetized by immersion in a 15% ethanol solution for 7 minutes, and are then decapitated. Standard dressmakers' pins are inserted at different positions along the length of the worm. Stimulating and recording electrodes attached to AD Instruments' PowerLab system are connected to these pins and can be used to initiate action potentials in the worm's median and lateral giant fibres. Because these are essentially single-fibre action potentials, the all-or-none law can be easily demonstrated. Experiments that students then perform within our three-hour class include measuring conduction velocity, refractory period, bidirectionality and effects of temperature. Following dissection to expose the nerve cord, students also investigate the effects of reducing sodium levels in the worm's extracellular fluid. Unexpected findings from this class have led to final-year honours research projects using the same preparation, described separately in a cognate submission (Knight & Fraser).

A small minority of first-year students are uncomfortable with the use of worms in a practical class, and so we have developed an interactive, online tutorial for those who do not wish to participate. However, responses from students have generally been positive and the class has been welcomed by our neurobiology staff members, who see it as an excellent introduction to their field. This very simple preparation helps to meet many of the same learning objectives that were covered in the traditional frog sciatic nerve preparation, plus some new ones, but with minimal consumable cost and a much higher level of reliability.

[*This submission forms one of a pair of submissions together with the abstract of Knight and Fraser. We are hoping that, if accepted, they could please be allocated adjacent slots within a teaching-focused podium session*]

C16

Investigating action potential conduction velocity supernormality in Earthworm giant fibres as a student project.

James Fraser[1], Rosie Knight[1]

[1]*University of Cambridge, Cambridge, United Kingdom*

Introduction

In the 'Earthworm Action Potentials' practical class described in the companion abstract (Mason), it was clear that the simple preparation provides a stable platform with which to investigate some fundamental questions of nerve conduction. In comparison to amphibian and mammalian nerve preparations, benefits of the earthworm median fibre include single fibre recording, long length and relatively slow conduction, which together permit accurate measurement of conduction velocity. In particular, visual inspection of student recordings showed that the preparation demonstrated strong conduction velocity supernormality, a phenomenon whereby when one action potential immediately follows another, the second shows faster conduction.

Aims

The aetiology of conduction velocity supernormality has received considerable attention over the years but there is no unifying hypothesis that fully describes it. The earthworm nerve preparation offered an opportunity to further investigate the supernormality phenomenon as a final-years Honours research project.

Methods

Earthworms were prepared as described by Mason. They were placed within a chamber and each end was passed through holes in opposite sides that were then sealed with adhesive putty. This allowed the long central length of the worm to be exposed to worm Ringer at different temperatures, while keeping short end lengths of the worm sufficiently dry in the regions of the extracellular stimulation and recording electrodes.

Results

Figure 1A shows an example of two stimuli delivered with a 7 ms interval and the resultant extracellular action potential traces. The measurements of latency from each stimulus to each action potential peak is shown (marked L1 and L2). Pairs of stimuli were delivered with stimulus intervals ranging from less than the refractory period to the point where the first action potential had no influence on the latency of the second. *Figure 1B* shows the influence of stimulus interval on the latency of the first and second action potentials in each pair. As has been described previously in a range of different preparations, the second action potential of each pair shows a reduction in latency, representing an increase in conduction velocity, over a range of stimulus intervals. Note that even very small changes in latency (<<5%) are consistently detectable in this simple preparation. Exposure of the earthworm median giant fibre allowed an investigation into the

effects of changes in temperature and extracellular ion concentrations on the supernormality phenomenon.

Conclusions

The earthworm nerve preparation is quick and easy for a student to set up without the need for continuous academic supervision. As an invertebrate model, research students are able to conduct original experiments on live nerve fibres without any requirement for a Home Office licence. As a robust single-fibre preparation, it lends itself to experiments investigating the effects of extracellular ion concentrations, pH, temperature, osmolality or pharmacological agents for both teaching and research purposes.

Note This submission forms one of a pair of submissions together with the abstract of M. Mason. We are hoping that, if accepted, they could be allocated adjacent slots within a teaching-focused podium session.

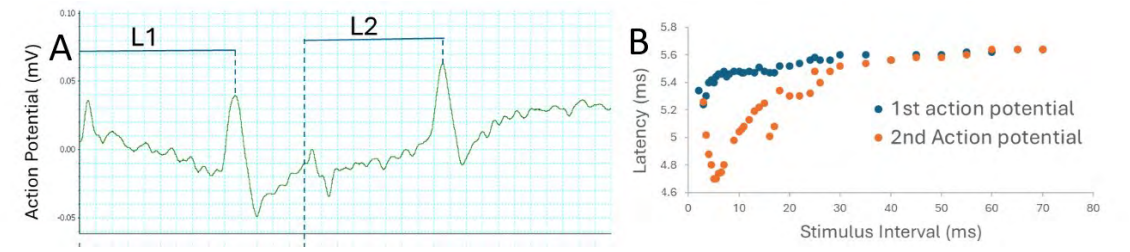

C17

Decolonising the curriculum: healthcare inequalities faced by Gypsy, Traveller, Roma, Showmen and Boater Communities

Emílie Puttová[1], Iain Rowe[1], Marie Bowers[1]

[1]*University of Aberdeen, Aberdeen, United Kingdom*

Decolonising the curriculum is an ongoing process in our Universities as we identify areas where we can challenge the bias that has meant that marginalised communities are excluded from our traditional teaching approaches (1). To support this we need our students to be partners and agents of change, helping to improve and invigorate our physiology and medical science teaching. In this case study a final year Honours project focuses on contextualising healthcare inequalities faced by Gypsy, Traveller, Roma, Showmen and Boaters (GTRSB) communities to collate relevant information and consider how it could be best utilised in future teaching and outreach events.

A narrative review of Ovid and PubMed databases revealed a lack of peer-reviewed research publications, therefore a grey literature search of governmental, parliamentary and charity publications was performed to fill knowledge gaps (2,3). This produced 12 peer-reviewed papers and 28 grey literature sources which were synthesised to describe: who GTRSB communities are; moments of their history which may impact on current healthcare inequalities with a focus on the Tinker Experiments in Scotland and forced sterilisations of Roma women in the Czech Republic; present-day disparities in healthcare outcomes of GTRSB communities compared to mainstream society; proposed drivers of current healthcare inequalities; and proposed routes for improvement through education. Examples of the inequalities include: 6-7x higher suicide rates; reduced life expectancy by 10-15 years; 20x higher premature death of an offspring; 2-4x times higher risk of death/hospitalisation following COVID-19 diagnosis; all data compared to the wider population. A poster session within the Honours project timeline allowed some of the data to be presented to staff and students within Medical Sciences at the University of Aberdeen. This revealed a significant lack of knowledge of the GTRSB communities, their history, and current healthcare inequalities.

This work offers a unique Scottish and Central/Eastern European perspective on the topics of health inequalities and GTRSB communities. It has revealed that decolonising our curriculum can highlight bias and racism in our current approaches to communities that are often unseen in medical science teaching. Based on the lack of awareness of these issues within our own University community, and the scale of the healthcare inequalities identified, the next steps will focus on working with the diverse GTRSB communities to create inclusive teaching resources. We will use a community-informed activist-based model to improve our teaching and outreach.

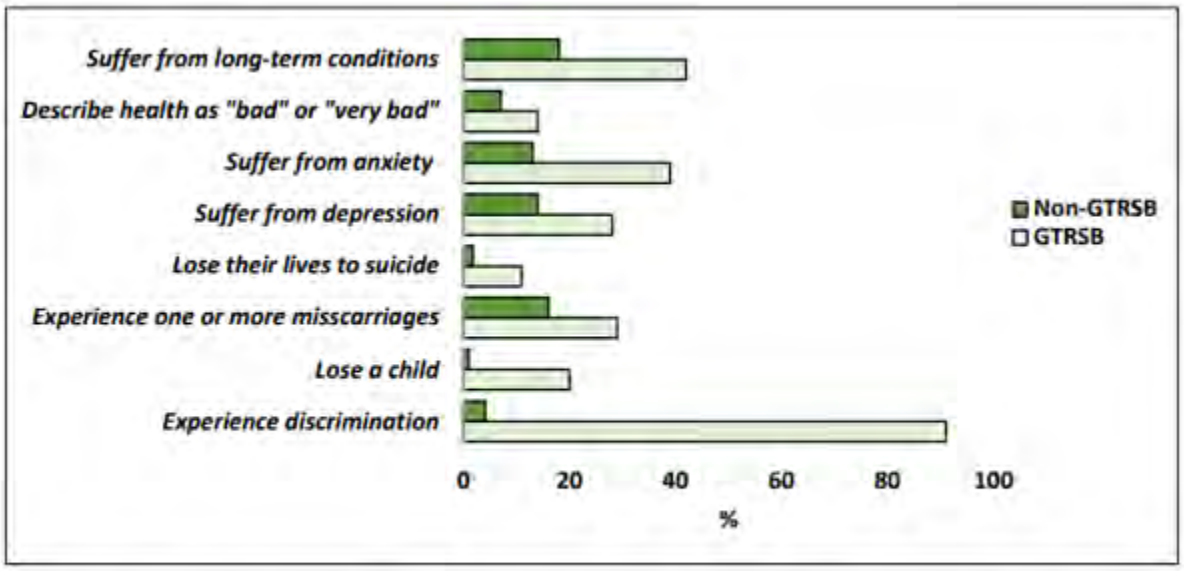

Figure 1. Health outcomes of GTRSB communities compared to non-GTRSB, where the x-axis shows the percentage of population affected and y-axis shows the health outcome in question.

(1) Lu et al. (2023) A framework for decolonising and diversifying biomedical sciences curricula: rediscovery, representation and readiness. bioRxiv. (2) All Ireland Traveller Health Study Team (2010). All Ireland Traveller Health Study: Summary of Findings. University College Dublin, pp.91–95. (3) Women and Equalities Committee (2019). Tackling inequalities faced by Gypsy, Roma and Traveller communities - Women and Equalities Committee Parliament. U.K

C18

The Importance of Re-establishing group work in post-Covid Physiology Laboratory Team Activities.

Elizabeth Sheader[1], Michelle Keown[2]

[1]Faculty of Biology, Medicine and Health. The University of Manchester., Manchester, United Kingdom, [2]Faculty of Biology, Medicine and Health. The University of Manchester., Manchester, United Kingdom, Manchester, United Kingdom

Society and learning approaches have changed over the last 5 years, particularly due to the Covid-19 pandemic with a notable shift towards independent and online learning approaches being observed. We have noticed an increased reluctance of some students to volunteer for roles within group settings and to engage with teamwork, as well as a decline in student confidence when working in teams. We feel laboratory practicals remain key in fostering interpersonal skills, promoting collaboration, improving self-esteem and reconnecting students by encouraging team-work opportunities.

This small study aims to evaluate student perceptions of in person face to-face team-based activity post pandemic in our 2nd year human volunteer exercise physiology projects.

Comprising two teams of 15, students were tasked with designing and implementing their projects, organising tasks, designing protocols and allocating roles to all team members.

The effectiveness of this approach was evaluated by questionnaire (n=26). 88% of students reported that the pandemic affected their experiences with group work. Initial data shows a positive experience with the face-to-face project format. 100% of students enjoyed the team format and the same number confirmed that the format motivated them to actively participate in the project. Furthermore, 23 out of the 26 students reported that the practical environment was inclusive and conducive to collaboration. When asked to rank factors that most positively influenced team-work and collaboration, the highest ranking factor was “face to face interaction” (Mode of 1) All students ranked “The pandemic has no effect on my experience of teamwork and collaboration” as the lowest factor.

Qualitative feedback, given in free text comments, supported the numerical values reported above, students repeatedly reported: (1) making friends more easily, (2) getting to know people better and (3) being more engaging than online interactions as important outcomes from this project format.

The initial findings of this study highlights, the pivotal role and benefit of teamwork in our physiology practical sessions and the importance of allowing students face-to-face activities to support their interpersonal skills development and overall learning. It suggests that face-to -face interaction can help to rebuild the social bonds that were weakened during the pandemic. By working in teams in the physiology laboratory, students may regain their confidence in their abilities to contribute effectively to a group setting. Group work allows students to learn from each other, benefit from diverse perspectives and appreciate the value of collaborative effort. It is also vital

preparation for professional opportunities as face- to-face group work in the curriculum could better prepare students for future employment.

C20

A students as partners approach to developing online interactive physiology content

Israth Miskin Sahibu[1], Sowda Dhaqane[1], Iain Rowe[1], Catriona Jane Cunningham[1]

[1]School of Medicine, Medical Sciences & Nutrition, University of Aberdeen, Aberdeen, United Kingdom

Physiology is widely considered to be a challenging subject by students on medicine and medical science degrees [1,2]. To increase student engagement and understanding of complex content, many educators have adopted active learning approaches. While active learning has been shown to be effective in improving exam performance across STEM subjects [3] there are challenges. This includes negative perceptions among students and lack of guidance for educators [4]. Personally, we have found active learning approaches can be more difficult to integrate with large class sizes.

Here, we share our experiences of student-led online interactive content creation. Our two resources were targeted at year 2 undergraduate medical sciences students (n=220) and year 1 undergraduate medical students (n=330) to supplement respective cardiovascular physiology teaching. Content was created using H5P (HTML5 Package) and hosted on a WordPress website.

The first resource developed was “Escape the Pharoh’s Tomb” digital escape room. This consisted of a series of 6 interactive puzzles including a cipher and crossword. Correctly solving each puzzle revealed a code to “unlock” the door and allow the participant to progress to the next room. To simulate the physical escape room experience, a countdown timer which carried across pages was integrated into the design. Secondly, we developed a clinical case study about a patient presenting to his GP with atrial fibrillation and hypertension. The interactive elements included multiple choice questions, fill in the blanks and labelling a diagram.

The resources were shared with both cohorts of students via email and a QR code displayed during an in-person lecture. Anonymous feedback was collected using surveys (Microsoft Forms), including both Likert scales and free text questions. To assess interaction with the content, the H5PxAPIkatchu plugin was used to collect data including puzzle scores. Google Analytics was used to quantify number of page views and average time spent on each page.

The feedback for both resources was overwhelmingly positive. Over 90% of respondents (n=14) strongly agreed that the escape room was enjoyable and helped them apply their cardiovascular physiology knowledge. In the free-text comments, most students (n=7) found it engaging but some (n=3) reported difficulties with the ECG puzzle and found the clues confusing. This was reflected in

the analytics data which showed students spent more than twice as long on this puzzle than any other (557 vs. ≤224 s). All respondents (n=14) reported the case study was clear and 92.3% strongly agreed it was a good supplement to their lectures. Several positively commented that the case study covered a range of lecture content and it was useful for revision (n=5).

In conclusion, involving students as co-designers is a successful approach for developing new online interactive physiology content.

1. Bordes SJ, Manyevitch R, Huntley JD, Li Y, Murray IVJ. Medical student misconceptions in cardiovascular physiology. Advances in Physiology Education. 2021 Jun 1;45(2):241–9. 2. Michael J. What makes physiology hard for students to learn? Results of a faculty survey. Advances in Physiology Education. 2007 Jan;31(1):34–40. 3. Freeman S, Eddy SL, McDonough M, Smith MK, Okoroafor N, Jordt H, et al. Active learning increases student performance in science, engineering, and mathematics. Proceedings of the National Academy of Sciences. 2014 May 12;111(23):8410–5. 4. Rhodes A. Lowering barriers to active learning: a novel approach for online instructional environments. Advances in Physiology Education. 2021 Sep 1;45(3):547–53.

C21

Evaluating the implementation of online exam proctoring on physiology module attainment and student experience

Matthew Jones[1], Pika Miklavc[2]

[1]Biomedical Research Centre, School of Science, Engineering and Environment, University of Salford, Salford, United Kingdom, [2]Biomedical Research Centre, School of Science, Engineering and Environment, University of Salford, Salford, United Kingdom

Introduction

Online examination is a widely utilised strategy for higher education assessment due to its numerous benefits for universities, academic staff, and students. Exemplar benefits of online assessment include increased student flexibility to complete the exam and automated marking, decreasing academic workload (Huber et al., 2024). However, within the wider sector, online examinations have been shown to inflate grades due to students completing exams in groups or as open-book exams, meaning knowledge acquisition is inadequately tested (Newton & Essex, 2023). A phenomenon which became prominent during the rapid shift to online assessment during the COVID-19 pandemic.

To mitigate this, invigilation of online assessments using approaches known as proctoring has been suggested. Proctoring software utilises recording or artificial intelligence-based approaches to monitor student information associated with potential academic misconduct, thus ensuring online examinations are conducted under comparable conditions to in-person examinations (Nigam et al., 2021). With knowledge acquisition one of the key intended learning outcomes of physiology-based modules, developing a detailed understanding of proctored online examinations may benefit students and staff. This study aims to evaluate the impact of implementing online examination proctoring on student academic attainment, experience, and wellbeing.

Methods

Physiology-aligned module grade analysis was conducted using exam board data from 2022/23 (Unproctored) and 2023/24 (Proctored) academic years following ratification by internal and external moderation. The student experience was evaluated by the completion of an anonymous survey following the completion of proctored examinations. All questions used a 5-point Likert scale containing negative, neutral, and positive options. Survey questions related to student experience, academic integrity, and wellbeing. This study was approved by the University of Salford's ethical review board (Ethics ID: 11889).

Results

Evaluation of student attainment following proctoring implementation revealed a leftward shift in grade distributions following the addition of proctoring to online exams. This resulted from average exam grades significantly decreasing from 65.8±12.4% (n=307) to 57.8±15.9% (n=274) following the addition of proctoring (P<0.0001). When compared to students' coursework grades achieved in the

same academic year, the disparity in attainment between assessment styles significantly increased from 7.7±14.5 % to 12.4±18.2 % following the implementation of exam proctoring (n=273-300; *P*=0.0006). Irrespective of proctoring status, there was a positive correlation between coursework attainment and exam attainment (Unproctored: R=0.33, *P*<0.0001, n=300; Proctored: R=0.32, *P*<0.0001, n=270).

A total of 36 students completed the student experience and wellbeing survey following proctored exams. Students stated that they believed proctoring negatively impacted their attainment (41.7% of respondents) but decreased academic misconduct (55.6%) and ensured exam conditions (72.2%). Only a third of respondents had positive experiences using proctoring with 38.9% stating they had a negative experience. Students revealed they were more nervous before proctored exams compared to unproctored ones (77.8%). The majority of students surveyed (72.2%) found proctoring easier and less stressful in subsequent proctored exams.

Conclusion

These data show that exam proctoring is an effective tool to combat grade inflation whilst simultaneously ensuring academic conduct and rigour in online examinations. However, its implementation may adversely impact student experience, which should be accounted for before its implementation.

Huber, E., Harris, L., Wright, S., White, A., Raduescu, C., Zeivots, S., Cram, A., & Brodzeli, A. (2024). Towards a framework for designing and evaluating online assessments in business education. Assessment & Evaluation in Higher Education, 49(1), 102-116. Newton, P. M., & Essex, K. (2023). How Common is Cheating in Online Exams and did it Increase During the COVID-19 Pandemic? A Systematic Review. Journal of Academic Ethics. https://doi.org/10.1007/s10805-023-09485-5 Nigam, A., Pasricha, R., Singh, T., & Churi, P. (2021). A systematic review on AI-based proctoring systems: Past, present and future. Education and Information Technologies, 26(5), 6421-6445.

C22

The use of 'hospital ward' clinical simulations and escape games to enhance career development for physiology students studying Life Sciences courses

Sara Namvar[1]

[1]*University of Salford, Salford, United Kingdom*

Sara Namvar, Komal Amar, Matthew Jones, Nathan Connell, Danielle Mayo, Lee Forde and Niroshini Nirmalan

Introduction

There is an increasing focus in higher education on graduate employment outcomes, but we know that success is not only shaped by the quality of traditional classroom and laboratory-based teaching. Extensive evidence suggests that prior learning experiences, socioeconomic status, and the multiple forms of 'graduate capital' shape sense of belonging and confidence to reach one's full potential. Physiology educators are under increasing pressure to think more creatively about how university experiences prepare all students, irrespective of prior learning or privileges for the world of work. The use of clinical scenarios is popular in healthcare programmes, but there is little training in this area for students undertaking Life Sciences courses, despite many such students intending to pursue postgraduate clinical careers.

Aim

The University of Salford runs a highly popular and successful mentorship programme for Life Sciences students hoping to pursue postgraduate clinical careers. We set out to introduce the use of clinical simulations and escape game-based learning that could provide students with insight into clinical decision making and enhance the existing preparation we offer for clinical interviews.

Methods

We designed four clinical scenarios that were then played out in the University of Salford cutting-edge hospital ward simulations facilities. Scenarios included a patient requiring cancer investigations, safeguarding issues surrounding a domestic violence case, ethical dilemmas around liver transplants and clinical observations under pressure in an immersive escape game. Each case unfolded in a separate' hospital room' appropriately dressed to bring realism and excitement to the scenario, with academic actors as well as 'talking' and moving mannequins. Students rotated between each room every 15min, followed by a debriefing session at the end.

Results

A total of 65 students from several programmes took part in this extracurricular opportunity, many from BAME backgrounds and low participation neighbourhoods. Most students indicated a strong interest in pursuing a postgraduate Medicine or Physician Associate career, with 100% reporting they enjoyed the experience and would like to see such experiences embedded into programmes.

Over 90% of students felt the experience helped develop their confidence and communication skills, whilst 87% felt it improved their employability. Examples of feedback included '*It was such a wonderful experience and I hope there will be more sessions like this*...' and '*I enjoyed having alumni back ... along with the simulations which enabled us to have a real understanding of what to expect*".

Conclusion

Collectively we present evidence of the value that clinical simulations and escape games add to the development of transferable employability skills in a fun and engaging manner for Life Sciences students. Co-creating such experiences with alumni and working across Schools is an important approach to developing Life Sciences graduates that are better prepared for the world of work.

C23

Comparison of undergraduate science student evaluation of skills confidence before and after Objective Structured Practical Examinations (OSPEs)

Alison Jenkinson[1], Derek Scott[1]

[1]*University of Aberdeen, Aberdeen, United Kingdom*

Introduction: Increasing student numbers and diversity of academic backgrounds, combined with the need to effectively evidence practical and employability skills has challenged traditional delivery of core practical skills (Lakshmipathy, 2015; Hultgren et al., 2023). We have been pioneering the use of Objective Structured Practical Examinations (OSPEs) in medical science teaching and have reported successful delivery of theoretical, practical and problem-solving skills at multiple stations to formally examine a wide range of communication and science laboratory practical skills (Scott et al., 2018). Feedback from students has indicated that they find this assessment approach challenging but, overall, a positive experience. However, we lack information regarding student perceptions of their skills and whether they felt the OSPE experience helped them improve these.

Aims: We aimed to assess students' evaluations of their own confidence in practical and transferable skills before and after the OSPE.

Methods: Prior to attending a practice session, students were encouraged to consider their level of confidence in the skills assessed during the OSPE - general laboratory skills, time management (both organising time and dealing with time pressures), communication skills, and awareness of both ethics and laboratory health and safety. An audit of questionnaire data collected during this process demonstrated that 83% of final year undergraduate students from anatomy, physiology, pharmacology and sport science degrees completed the pre-OSPE skills evaluation questionnaire (n = 76) and 48% (n= 44) the post-OSPE questionnaire. Students also considered whether the OSPE would improve awareness of skill levels and the post-OSPE questionnaire issued after the assessment session encouraged exploration of skill strengths and weaknesses.

Results: Pre-OSPE students were least confident in general laboratory skills and aspects of time management. After the OSPE assessment levels of confidence were generally improved in all areas with the proportion of students expressing good or high levels of confidence increasing in several areas e.g. Extreme and Somewhat Confidence in Lab skills pre-and post-OSPE increased from 63.2% to 90.9% (P=0.0009, Z score test), Lab Health & Safety 84.2% to 97.8% (P=0.02). There was no significant difference in communication skills (Pre 85.6%, Post 84.1%). The OSPE was considered to be helpful with identifying strengths and weaknesses and improving awareness of skill levels.

Conclusions: These results suggest that confidence in and awareness of both practical laboratory and key employability skills may be positively influenced by practical assessment approaches. The OSPE may encourage students to consider their strengths and weaknesses. However, although confidence in these skills generally improved following preparation, practice and delivery of the assessment, some aspects (e.g. one to one communication skills and managing time under

pressure) were particularly highlighted as areas where students recognised that further skill development was required. This has given staff a better awareness of skills gaps and the inclusion of this assessment at the beginning of the Honours year allows students time to develop skills they felt needed enhancement. Our hope is that this approach will help students enhance their employability.

Lakshmipathy, K (2015) MBBS student perceptions about physiology subject teaching and objective structured practical examination based formative assessment for improving competencies. Adv Physiol Educ 39(3), 198-204 https://doi.org/10.1152/advan.00073.2014 Hultgren C, Lindkvist A, Curbo S, Heverin M (2023) Students' performance of and perspective on an objective structured practical examination for the assessment of preclinical and practical skills in biomedical laboratory science students in Sweden: a 5-year longitudinal study. J Educ Eval Health Prof (20), 13 DOI: https://doi.org/10.3352/jeehp.2023.20.13 Scott DA, Kirkman J, Malcolm CJ, Jenkinson AM (2018) Use of student-created video resources to enhance practical training in Objective Structured Practical Examinations (OSPE's). Proc Physiol Soc 41, PCB083

C24

Rubric-based assessment of Flipped Classroom Presentations – A Marker's Perspective

Marta Woloszynowska-Fraser[1], Ella Maysami[1], Simon Trent[1]

[1]Keele University, Newcastle-under-Lyme, United Kingdom

This study explores the use of rubric in the flipped classroom presentations assessment in the final year neuroscience module Behavioural Neuroscience at Keele University (from 2020 to current 2024 cohort). Students are tasked with delivering presentations in a flipped classroom format, where they take ownership of their learning by preparing and delivering content. Staff employ a predefined rubric to evaluate student performance across various four domains including verbal skills, visual aids, content, organisation, and teamwork, with a total of 17 specific criteria (adapted from Peeters et al., 2010). Presentations, each lasting 45 minutes, are recorded for assessment, with one marker present during the presentation and a second marker assessing the presentation from the recording. By engaging students in active learning through presentation preparation, the flipped classroom model promotes deeper comprehension and retention of course material. Meanwhile, the use of a rubric for assessment ensures clarity and consistency in grading, guiding markers in evaluating presentations based on predefined criteria. Additionally, the rubric is explained during a tutorial and readily available afterwards, thereby providing students with clear expectations, enabling them to focus on key aspects of their presentations and align their efforts with assessment criteria. Moreover, the integration of rubric-based assessment enhances the comprehensiveness of evaluation in the final year module. By encompassing various dimensions of presentation quality, including verbal communication, visual aids, content coherence, organisation, and collaborative skills, the rubric offers a holistic assessment of student performance. This comprehensive evaluation approach provides valuable insights into students' abilities beyond mere content knowledge, such as their communication proficiency and teamwork skills, which are essential for success in academia and beyond. Nevertheless, there are some challenges with this approach, such as ensuring consistency in the application of the rubric across different markers and presentations requires clear guidelines. Additionally, technical issues related to recording quality and accessibility may arise, impacting the reliability of assessment data. In conclusion, the integration of rubric-based assessment into flipped classroom presentations offers a promising avenue for enhancing final year module evaluation. By combining the active learning benefits of flipped classroom pedagogy with the clarity and comprehensiveness of rubric-based assessment, educators can foster student engagement and provide meaningful feedback on presentation skills. However, addressing logistical challenges and ensuring robust assessment procedures are essential for the successful implementation of this approach.

Peeters, M. J., Sahloff, E. G., & Stone, G. E. (2010). A Standardized Rubric to Evaluate Student Presentations. American Journal of Pharmaceutical Education, 74(9), 171. https://doi.org/10.5688/aj7409171

C25

Regulation of the NaCl cotransporter NCC and blood pressure by the ubiquitin E3 ligase CHIP

Mariavittoria D'Acierno[1], Robert Little[1], Jonathan C Schisler[2], Vladimir Matchkov[1], Robert A Fenton[1]

[1]Department of Biomedicine, Aarhus University, Aarhus, Denmark, [2]Department of Pharmacology, University of North Carolina, Chapel Hill, United States

The activity of the thiazide-sensitive sodium-chloride cotransporter NCC within the kidney distal convoluted tubule (DCT) is crucial for modulating blood pressure (BP). Emerging evidence also suggests that alterations in NCC activity play a pivotal role in the effects of dietary potassium (K^+) on BP. Greater dietary K^+ intake lowers NCC abundance and activity, which is often associated with reduced BP. Our previous studies have demonstrated that during high K^+ intake there is greater ubiquitin-dependent NCC degradation, a process that involves an interaction between heat shock protein 70 (Hsp70) and NCC, and is potentially orchestrated by the ubiquitin E3 ligase CHIP (carboxy-terminus of Hsc70-interacting protein) (1). To validate this mechanism, we investigated the role of CHIP in modulating NCC activity *in vivo* and its implications for BP control.

Methods: CHIP knockout (KO) and wildtype (WT) control mice were fed diets with variable K^+ content; low (0% K^+), normal (1%), or high (5%) for 5 days. BP measurements on the various diets or after treatment with the NCC inhibitor hydrochlorothiazide (HCTZ) (37.5 mg/kg BW) or the epithelial sodium channel (ENaC) inhibitor amiloride (5 mg/kg BW) were obtained using telemetry (24 h readings) or tail cuff plethysmography (early evening). To examine NCC half-life, e*x vivo* kidney tubule suspensions from KO and control mice were incubated in control media (4.0 mM K^+) containing cycloheximide and actinomycin for various time points and NCC expression was evaluated by immunoblotting.

Results: On a normal K^+ diet, CHIP KO mice had elevated NCC protein levels (n = 5/ group; $p<0.0001$), but NCC mRNA levels were not significantly different between the genotypes. CHIP KO mice had higher BP compared to WT controls (n = 8/group; $p<0.001$) on a normal diet. Inhibition of NCC activity using hydrochlorothiazide normalized BP in the CHIP KO mice to similar levels as WT mice (n = 4-5/group; $p<0.001$), emphasizing NCC's predominant role in the observed higher BP phenotype. Inhibition of ENaC activity with amiloride had a similar effect to lower BP in WT and CHIP KO mice (n = 4-5/group; $p<0.05$). The ability of a high K^+ diet to reduce NCC abundance was attenuated in CHIP KO mice (n = 4-5/group; $p<0.0001$). In *ex vivo* tubule suspensions from CHIP KO mice, NCC half-life was prolonged compared to WT controls (n = 3/group with 3 technical replicates; $p <0.05$), suggesting a role for CHIP in NCC degradation.

Conclusions: Our findings highlight the critical involvement of CHIP-mediated NCC ubiquitylation for regulating NCC abundance and BP. Preliminary studies also suggest a role for CHIP in mediating the effects of higher dietary potassium intake on NCC. Understanding the molecular mechanisms governing NCC regulation may offer valuable insights into hypertension pathophysiology and facilitate the development of targeted therapeutic interventions.

(1) Kortenoeven, MLA. et al., J Biol Chem 297, (2):100915 (2021)

C26

Interstitial cell of Cajal-like cells (ICC-LC) exhibit dynamic spontaneous activity but are not functionally innervated in mouse urethra

Neha Gupta[1], Salah Baker[2], Kenton Sanders[2], Caoimhin Griffin[1], Mark Hollywood[1], Gerard Sergeant[1], Bernard Drumm[1]

[1]Dundalk Institute of Technology, Dundalk, Ireland, [2]University of Nevada, Reno School of Medicine, Reno, United States

Urethral smooth muscle cells (USMC) sustain tonic contractions to occlude the internal urethral sphincter during bladder filling. Interstitial cells also exist in urethral tissues and are hypothesized to influence USMC behaviours and neural responses. These cells are similar to Kit^+ interstitial cells of Cajal (ICC), gastrointestinal pacemakers and neuroeffectors. Isolated cell studies of urethral ICC-like cells (ICC-LC) exhibit spontaneous intracellular Ca^{2+} signalling behaviours linked to proposed roles as USMC pacemakers and neuromodulators similar to ICC in the gut, although observation and direct stimulation of ICC-LC within intact urethral tissues is lacking. Using a mouse line with cell-specific expression of the Ca^{2+} indicator GCaMP6f, driven off the Kit promoter (Kit-GCaMP6f mice), we unequivocally identified ICC-LC within *in situ* urethra preparations and characterized their activity. Across 54 cells imaged from 13 animals, ICC-LC fired spontaneous Ca^{2+} waves that propagated on average 40.1 ± 0.7 mm, with varying amplitudes (0.08 - 1.96 DF/F_0), which originated from multiple firing sites per cell (average 3.1 ± 0.2). ICC-LC imaged from Kit-GCaMP6f urethra did not form interconnected networks. ICC-LC activity was uncoordinated across multiple cells with no obvious entrainment of ICC-LC. ICC-LC Ca^{2+} event frequency was unaffected by the L-type Ca^{2+} channel inhibitor nifedipine (P=0.25, n=5) but was abolished by cyclopiazonic acid (P=0.0005, n=6) and decreased by an inhibitor of store-operated Orai Ca^{2+} channels (GSK-7975A, P<0.0001, n=6). While the a-adrenoceptor agonist phenylephrine increased Ca^{2+} wave frequency (P=0.0007), amplitude (P=0.04) and spread (P=0.14) (n=6), the nitric oxide (NO) donor DEA-NONate had no effect (n=7). Electrical field stimulation (EFS, 10 Hz) of intrinsic nerves under excitatory (n=6) or inhibitory conditions (n=7) failed to elicit responses in ICC-LC. In contrast, EFS of ICC from Kit-GCaMP6f colon yielded consistent excitatory (cholinergic, n=3) and inhibitory (nitrergic, n=5) postjunctional responses. We conclude urethral ICC-LC are spontaneously active but are not functionally innervated.

C27

Maternal, paternal and combined parental obesity impact fetal growth via parent-specific and combined effects on placental morphology and transport function.

Sachi Gwalani[1], Jonas Zaugg[2], Edina Gulacsi[1], Jorge Lopez-Tello[1], Amanda Sferruzzi-Perri[1]

[1]Centre for Trophoblast Research, Department of Physiology, Development and Neuroscience, University of Cambridge, UK, Cambridge, United Kingdom, [2]Centre for Trophoblast Research, Department of Physiology, Development and Neuroscience, University of Cambridge, UK, Cambridge, United Kingdom

Introduction

Concerningly, 20% of women and 14% of men are estimated to be obese by 2030[1]. The reproductive effects of maternal and paternal obesity have been investigated independently and include subfertility, fetal growth abnormalities, gestational disorders and adverse offspring health[2,3,4]. We hypothesise that two obese parents have divergent and compounded effects on male and female fetal growth associated with unique effects on placental morphology, transport and imprinted gene expression.

Aim

To assess the individual and combined role of parental obesity on fetal development, placental morphology and transport.

Methods

Female and male mice were fed a chow diet (11% fat, 7% sugar) or obesity-inducing high-fat/high-sugar diet (38% fat, 33% sugar). They were time-mated 5 weeks later, creating 4 pregnancy groups and females continued on the diet they consumed prior to mating. Stereological analyses on placentas (embryonic day 18.5; 4-6 fetuses/group) of gross morphology (point counting), interhaemal membrane thickness (length measurements), surface area for exchange (SA; cycloid arc intersections) and glycogen deposition (ImageJ analysis) were conducted following Haematoxylin and Eosin staining, Periodic acid-Schiff staining and double-label immunohistochemistry (4-6 replicates/group)[5], respectively. Relative mRNA expression of imprinted genes and nutrient transporters was measured by RT-qPCR (6-8 fetuses/group; 1-2 fetuses/litter). To assess *in vivo* transplacental transport (>11 fetuses/group; 1-2 fetuses/litter), anaesthesia was induced in dams on embryonic day 18 by 90.9mg/kg Ketamine + 4.55mg/kg Xylazine via intraperitoneal injection (0.01mL/g body weight), followed by injection of radiolabelled glucose/amino acid analogues into the jugular vein.

Results (data quoted as mean±SEM)

Male and female fetuses: Combined parental obesity reduced fetal weight relative to controls (734.0±8.202mg vs 777.8±10.54mg; p=0.0459; one-way ANOVA). Paternal obesity increased trophoblast volume (14.16±0.7277mm^3 vs 9.274±1.126mm^3; p=0.0031; one-way ANOVA) and

maternal obesity increased interhaemal membrane thickness (5.177±0.06273μm vs 4.378±0.1919μm; p=0.0230; Kruskal-Wallis test) relative to controls. Combined parental obesity increased glycogen deposition relative to controls (2.731±0.6736% vs 0.8152±0.2813%; p=0.0242; one-way ANOVA) and reduced theoretical diffusion capacity relative to paternal obesity ($0.008240±0.0003738cm^2.min^{-1}.kPa^{-1}$ vs $0.01047±0.0003094cm^2.min^{-1}.kPa^{-1}$; p=0.0452; Kruskal-Wallis test).

Male fetuses: Combined parental obesity reduced fetal weight (744.0±10.40mg vs 800.7±9.069mg; p=0.0225; one-way ANOVA), increased relative brain weight (0.07795±0.001488 vs 0.06748±0.003793; p=0.0214; Kruskal-Wallis test) compared to controls and decreased relative liver weight compared to paternal obesity (0.04370±0.0005922 vs 0.04917±0.001412; p=0.0470; one-way ANOVA), indicating asymmetric growth restriction. Maternal blood space SA was reduced in combined parental obesity ($15.20±0.5187cm^2$ vs $23.95±1.668cm^2$; p=0.0282; one-way ANOVA) relative to paternal obesity. Combined parental obesity reduced relative *H19* (-0.7055±0.1045 vs 0; p=0.0002; one-way ANOVA), *Igf2* (-0.2911±0.06285 vs 0; p=0.0373; one-way ANOVA) and *Slc2a1/GLUT1* (-0.2771±0.04968 vs 0; p=0.0158; one-way ANOVA) expression compared to controls. Reductions in glucose and amino acid placental transfer in maternal and combined parental obesity, respectively, were normalised by average SA.

Female fetuses: Fetal and placental weight/morphology were unaltered by parental obesity. *H19* expression was reduced in combined parental obesity relative to maternal obesity (-0.4861±0.1163 vs 0.1954±0.2225; p=0.0089; one-way ANOVA).

Conclusion

Singular and combined parental obesity compromise fetal growth via sex-specific, parent-specific and combined effects on placental morphology, nutrient transporter and imprinted gene expression. Such changes would disturb transplacental transfer and highlight the reproductive ramifications of obesity/calorie-dense diets in both parents.

References 1 One billion people globally estimated to be living with obesity by 2030 (no date) World Obesity Federation. Available at: https://www.worldobesity.org/news/one-billion-people-globally-estimated-to-be-living-with-obesity-by-2030 (Accessed: 19 February 2024). 2 Lean, S.C. et al. (2022) 'Obesogenic diet in mice compromises maternal metabolic physiology and lactation ability leading to reductions in neonatal viability', Acta Physiologica, 236(2), p. e13861. Available at: https://doi.org/10.1111/apha.13861 (Accessed: 2 January 2024). 3 Lin, J., Gu, W. and Huang, H. (2022) 'Effects of Paternal Obesity on Fetal Development and Pregnancy Complications: A Prospective Clinical Cohort Study', Frontiers in Endocrinology, 13. Available at: https://www.frontiersin.org/articles/10.3389/fendo.2022.826665 (Accessed: 3 January 2024). 4 McPherson, N.O. et al. (2015) 'When two obese parents are worse than one! Impacts on embryo and fetal development', American Journal of Physiology-Endocrinology and Metabolism, 309(6), pp. E568–E581. Available at: https://doi.org/10.1152/ajpendo.00230.2015 (Accessed: 6 January 2024). 5 De Clercq, K. et al. (2020) 'Double-label immunohistochemistry to assess labyrinth structure of the mouse placenta with stereology', Placenta, 94, pp. 44–47. Available at: https://doi.org/10.1016/j.placenta.2020.03.014 (Accessed: 17 October 2023).

C28

E. coli Nissle improves short-chain fatty acid absorption, microbial composition, and gut barrier function in the inflamed cecum of slc26a3−/− mice

Zhenghao Ye[1], Qinghai Tan[1,2], Sabrina Woltemate[1], Xinjie Tan[1,3], Dorothee Römermann[1], Guntram Grassl[1], Marius Vital[1], Ursula Seidler[1], Archana Kini[1]

[1]Hannover Medical School, Hannover, Germany, [2]Tongji Medical School, Wuhan, China, [3]Zhejiang University Medical School, Hangzhou, China

Background

Defects in *SLC26A3*, the major colonic Cl^-/HCO_3^- exchanger, result in chloride-rich diarrhea, a reduction in short-chain fatty acids (SCFA) producing bacteria, and a high incidence of inflammatory bowel disease (IBD) in humans and in mice. *Slc26a3*$^{-/-}$ mice are therefore an interesting animal model for spontaneous but mild colonic inflammation, and for testing strategies to reverse or prevent the inflammation. This study investigates the effect of *E. coli* Nissle (EcN) application on the microbiome, SCFA production, barrier integrity and mucosal inflammation in *slc26a3*$^{-/-}$ mice.

Methods

In vivo fluid absorption and bicarbonate secretion were assessed in the gut of *slc26a3*$^{+/+}$ and *slc26a3*$^{-/-}$ mice before and during luminal perfusion with 100mM sodium acetate. Age-matched *slc26a3*$^{+/+}$ and *slc26a3*$^{-/-}$ mice (13 wt and 12 ko) were intragastrically gavaged twice daily with 2×10^8 CFU/100µL of EcN for 21 days. Body weight and stool water content were assessed daily, stool and tissues were collected for further analysis. The data was analysed using Graphpad Prism Version 8.0.2. The unpaired Student´s was used for parametric data with normal distribution or non-parametric Mann-Whitney U test for the comparisons within genotypes and/or between control and EcN-treated groups. For the microbial 16s rRNA gene analysis, the analysis, alpha-diversities, and non-metric multidimensional scaling (NMDS) based on relative abundance data were conducted using the phyloseq package (McMurdie & Holmes, PlosOne 2013).

Results

Luminal addition of sodium acetate significantly increased both fluid absorption and luminal alkalinization in the *slc26a3*$^{-/-}$ mice. Gavage with EcN resulted in significantly improving overall SCFA levels and the expression of its transporters primarily in the *slc26a3*$^{-/-}$ cecum, the predominant habitat of EcN in mice (n=12-13, $p<0.05$). This was accompanied by an increase in mucus producing goblet cells, a decrease in the expression of inflammatory markers as well as of host defense anti-microbial peptides. EcN did not improve the overall diversity of the luminal microbiome, but resulted in a significant increase in SCFA producers *Lachnospiraceae* and *Ruminococcaceae* in the *slc26a3*$^{-/-}$ feces (n=7 for *slc26a3*$^{+/+}$ and *slc26a3*$^{-/-}$ w/o EcN: n=12 for slc26a3$^{+/+}$ and n=13 for *slc26a3*$^{-/-}$, $p<0.05$.

Conclusions: These findings suggest that EcN is able to proliferate in the inflamed cecum of the *slc26a3*$^{-/-}$ mice, resulting in increased microbial SCFA production, decreased inflammation, and improved gut barrier properties. In sufficient dosage, probiotics may thus be an effective anti-inflammatory strategy in the diseased gut.

C29

The antimicrobial peptide cathelicidin gates the bacterial survival in urine from newly renal transplanted recipients

Laura Vang Sparsø[2], Aimi Danielle Klostergaard Hamilton[2], Lene Ugilt Pagter Ludvigsen[1,3], Bente Jespersen[1,3], Mathias Skov[2], Helle Prætorius[2]

[1]Department of Clinical Medicine, Aarhus University, Aarhus, Denmark, [2]Department of Biomedicine, Aarhus University, Aarhus, Denmark, [3]Department of Renal Medicine, Aarhus University Hospital, Aarhus, Denmark

Introduction:

Urinary tract infections (UTIs) are one of the most common types of infections in humans. Renal transplant recipients are known to be especially prone to these infections, which can lead to renal damage and graft dysfunction. Normally, the urinary tract is sterile, and antimicrobial peptides (AMPs) play an important role in this as part of the innate immune system. AMPs are generally released into the urine in response to inflammation[1]. Here, we hypothesise that urine concentration of cathelicidin determines the survival of uropathogenic *E. coli* in the urinary tract of newly renal transplanted recipients.

Methods:

Urine was collected on day 4 after renal transplantation at Aarhus University Hospital (n=50) and from healthy gender and age-matched controls (n=50). Growth and damage (propidium iodide (PI) assay) of uropathogenic *E. coli* strain RAR0001 (resistant to sulfamethoxazole and trimethoprim) in the human urine samples was determined by flowcytometry. Urine concentrations of cathelicidin (LL-37), Human b-defensin 1 (HBD-1), lipocalin-2 and uromodulin were determined by ELISA. Direct effect of purified cathelicidin on bacterial damage and lysis was addressed by adding increasing concentrations of cathelicidin measuring damage with a PI-assay and by Green Fluorescence Protein (GFP) release from GFP-producing *E. coli*.

Results:

The current study represents preliminary data from 14-36 transplant patients and matched controls, depending on the assay. Urine from renal transplant recipients had a statistically significantly higher mean concentration of the AMPs cathelicidin, HBD-1 and Lipocalin-2 compared to controls (table 1), even though the urine was more dilute as indicated by a lower osmolality and creatinine concentration compared to controls (table 1). Notably, urine uromodulin concentrations were reduced markedly more in renal transplant recipients compared to controls than what could

be explained by dilution. Corresponding to the high urinary AMP levels, RAR0001 had a mean of 19.9 ±2.2 % PI-positive bacteria after one hour of incubation in urine from renal transplanted patients (n=33). In contrast, there were only 7.4 ±0.95% PI-positive RAR0001 in urine from controls (n=33) after one hour of incubation (Figure 1, $p<0.0001$, Mann-Whitney test). Moreover, we confirm that cathelicidin is bactericidal in the used *E. coli*, since cathelicidin concentration-dependently (0-10 µM) increased the lysis of GFP-producing *E. coli* (n=3), and cathelicidin (10 µM for four hours) caused 91.5 ±1.2% RAR0001 E. coli to become PI positive (n=3).

Conclusion:

Recently renal transplanted recipients have significantly higher levels of the antimicrobial peptides cathelicidin, HBD-1 and Lipocalin-2, and our *in vitro* studies confirm bactericidal properties of cathelicidin in uropathogenic *E. coli*. *E. coli* is markedly more damaged in urine from these patients compared to urine from healthy controls. We speculate this to be caused by inflammation-induced cathelicidin secretion to the pre-urine caused by the transplantation and propose that higher levels of antimicrobial peptides in the urine can be protective against UTIs in the acute phase after transplantation.

	Renal transplant patients (Mean ± SEM)	**Controls (Mean ± SEM)**	**P-value (Mann-Whitney test)**
Cathelicidin (ng/ml), n=23	16.7 ± 2.8	2.7 ± 0.3	**P<0.0001**
HBD-1 (ng/ml), n=27	3.9 ± 0.3	2.1 ± 0.3	**P<0.0001**
Lipocalin-2 (ng/ml), n=27	14.8 ± 4.2	1.5 ± 0.3	**P<0.0001**
Uromodulin (ng/ml), n=14	1906 ± 333	10978 ± 1934	**P<0.0001**
Creatinine (mM), n=36	7.4 ± 0.6	11.0 ± 0.9	**P=0.0032**
Osmolality (mOsmol/kg), n= 33	409 ± 19.5	633 ± 43.9	**P=0.0004**

Table 1. Concentration of the AMPs Cathelicidin, HBD-1, Lipocalin-2 and Uromodulin and osmolality and creatinine concentration of urine samples from recently renal transplanted patients and healthy age and gender-matched controls. Data are presented as mean ± SEM. Statistical analysis was performed with a Mann-Whitney test.

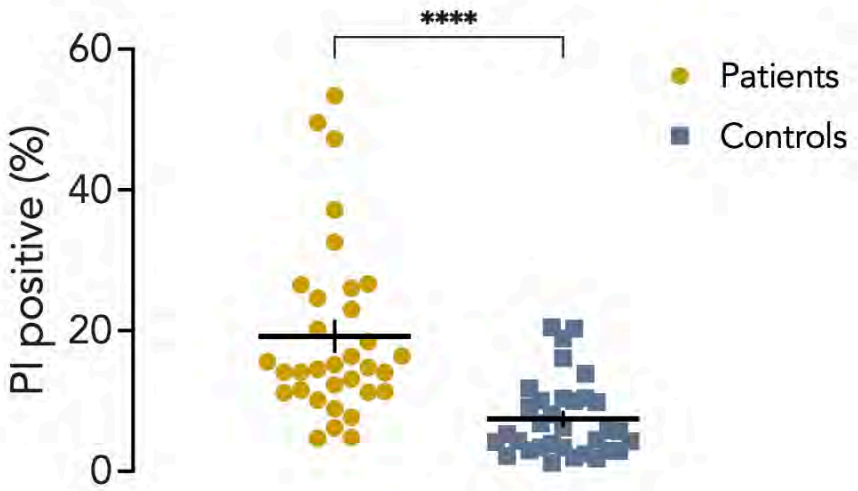

Figure 1. Propidium iodide (PI) positive percentage after one hour of incubation in urine from recently renal transplanted patients and healthy age and gender-matched controls (n=33). Data are presented as mean ± SEM. Statistical analysis was performed with a Mann-Whitney test. P<0.0001.

1. Lindblad A, Wu R, Persson K, et al. The Role of NLRP3 in Regulation of Antimicrobial Peptides and Estrogen Signaling in UPEC-Infected Bladder Epithelial Cells. Cells 2023;12(18) doi: 10.3390/cells12182298 [published Online First: 20230918]

C30

The role of Aquaporin-2 in cyst progression in Autosomal Dominant Polycystic Kidney Disease

Vishalini Venkatesan[1], Robert A. Fenton[2], Emma Tina Bisgaard Olesen[1]

[1]Department of Biomedical Sciences, University of Copenhagen, Copenhagen N, Denmark,
[2]Department of Biomedicine, Aarhus University, Aarhus C, Denmark

Introduction: Cystogenesis in Autosomal Dominant Polycystic Kidney Disease (ADPKD) is caused by a mutation in the genes encoding polycystin-1 or 2 (Pkd1/Pkd2), and involves dysregulated fluid transport in the kidney tubules. ADPKD patients present with a urinary concentrating defect, even prior to decreased glomerular filtration rate despite higher plasma vasopressin levels. Hence, we investigated whether vasopressin-mediated aquaporin-2 (AQP2) trafficking and water balance are dysregulated in ADPKD and lead to cyst expansion.

Methods: Doxycycline-inducible, kidney-tubule-specific Pkd1 knock-out (KO) mice (Pax8; tetO-Cre; Pkd1$^{flox/flox}$) and control littermates (Pax8; tetO-Cre; Pkd1$^{wt/wt}$) were treated with doxycycline on postnatal (PN) day 10, 11 and 12. On PN day 21, dDAVP (0.1 µg/kg), a synthetic analog of vasopressin, was administered as a single intraperitoneal (IP) injection and mice were euthanized after 6 hours (acute studies). For long term studies, dDAVP (0.1µg/kg) was administered IP for 5 days (PN day 17 to 21). Urine samples were collected for osmolality measurements, and kidneys were harvested for western blotting and immunohistochemistry (IHC). A novel polycystin-1 deficient mouse cortical collecting duct cell line (mpkCCD-Pkd1$^{-/-}$) was developed using the CRISPR/Cas9 technique, and validated through PCR, western blotting, 3D cell morphogenesis, and cAMP assays.

Results: At 3 weeks of age, KO mice (n=3) had lower urine osmolality at baseline compared with control mice (n=5) (481.7 versus 1874 mOsm/Kg; p≤ 0.01). Urine osmolality increased with dDAVP administration in the control mice (p≤ 0.001), whereas no response was noted in the KO mice. In long-term studies, AQP2 expression increased and was apically targeted with dDAVP treatment in the renal cortex and inner medulla of both control (n=4) and KO mice (n=4). However, AQP2 expression was lower in the inner medulla of both saline (p<0.01) and dDAVP-treated (p<0.01) KO mice compared to controls. IHC indicated that NKCC2 and NHE3 protein expression were reduced in the whole kidneys of KO mice. Large cysts were observed in the cortex of KO mice. When grown in a basement membrane matrix (cultrex), mpkCCD-Pkd1$^{-/-}$ cells grew as cysts while the control-transduced mpkCCD cells grew as tubules, providing a phenotypical confirmation of the cell lines. mpkCCD-Pkd1$^{-/-}$ cells exhibited significantly lower dDAVP-induced AQP2 protein expression (n=3, p≤ 0.05) when compared to control cells, although both mpkCCD-Pkd1$^{-/-}$ and control cells displayed dDAVP-induced cAMP production.

Conclusion: ADPKD mice have a urine concentrating defect, which may be explained by the downregulation of AQP2 in the inner renal medulla, and sodium transporters important for countercurrent multiplication such as NKCC2 and NHE3. In mpkCCD-Pkd1$^{-/-}$ cells, AQP2 is downregulated despite dDAVP-induced cAMP elevation, suggesting AQP2 dysregulation. Further investigations are required to understand AQP2 trafficking in these models.

Ethical approval: All protocols of the animal studies were approved by the Animal Experiments Inspectorate of the Ministry of Food, Agriculture and Fisheries in Denmark.

C31

Adenine-Induced Kidney Disease: An Animal Model to Study Uremic Toxins

Søren Elsborg[3], Jasmine Atay[3], Johan Palmfeldt[3,4], Henricus Mutsaers[3], Rikke Nørregaard[3,5]

[1]Aarhus University, Aarhus, Denmark, [2]Aarhus University, Aarhus, Denmark, [3]Department of Clinical Medicine, Aarhus University, Aarhus, Denmark, [4]Research Unit for Molecular Medicine, Aarhus University, Aarhus, Denmark, [5]Department of Renal Medicine, Aarhus University Hospital, Aarhus, Denmark

Chronic kidney disease (CKD) increases the risk of cardiovascular disease (CVD) development. However, conventional treatments for CVD shows limited efficacy in patients with concurrent CKD, suggesting a different CVD mechanism. To better treat these patients, an improved understanding of how uremic toxins accumulate in the plasma during CKD is needed. Therefore, we aimed to characterise the plasma and urinary metabolic profiles of adenine-treated mice, with a focus on key renal drug transports, across various stages of renal injury to evaulate the fidelity of this model to study uremic toxicity.

8-week-old C57BL/6J male mice were exposed to a diet supplemented with 0.2% adenine to induce renal injury and divided into five groups: 1) control group (n=11), 2) two weeks of adenine diet (n=8), 3) four weeks of adenine diet (n=8), 4) four weeks of adenine diet and one week without (n=8), and 5) four weeks of adenine diet and two weeks without (n=7). The latter two groups allowed us to study recovery of the kidney disease. 24-h urine samples were collected the day before termination and blood and kidneys were harvested at termination. At termination, mice were anesthesised with 4% sevoflurane and the kidneys were harvested and a blood sample was collected from the heart. The mice were euthanasised using cervial dislocation. LC-MS/MS was employed for urinary and plasma metabolic profiling. Compound identification was performed using the mzLogic Data Analysis Algortihm (Compound Discover, Thermo Fischer), and untargeted data analysis was conducted using MetaboAnalyst 5.0. Gene expression of renal transporters in cortical kidney tissue was determined by qPCR.

Targeted metabolomics revealed a signifcant increased in mean plasma levels of the uremic toxins indoxyl sulfate, hippuric acid, and kynurenic acid after 2 and 4 weeks of adenine-feeding, which normalized after the 2-week washout period ($p<0.05$). This was accompanied by significantly reduced levels of urinary kynurenic acid, hippuric acid and indole-3-acetic. Importantly, these levels normalized after the washout period. Untargeted metabolomics demonstrated elevated plasma and reduced urinary levels of specifically uremic toxins after 2 weeks of adenine treatment. After 4 weeks, nucleic acids became the predominant metabolites in both plasma and urine. Notably, we found two previously unidentified metabolites among the top 20 upregulated metabolites in adenine-fed mice. mRNA expression analysis revealed a significant decreased of the proximal tubule influx transporters *Slc22a6*, *Slc22a8*, *Slco4c1*, *Slc22a2* after 2 weeks, while only *Slc22a6* and *Slc22a2* was significantly reduced after 4 weeks. On the contrary, the proximal tubule efflux transporter *Slc47a1* was significantly increased after 2 weeks, while the *Abcg2* levels were decreased after both 2 and 4 weeks. This dysregulation of the proximal tubule drug transporters suggested proximal tubular stress.

In summary, adenine-feeding in mice induced a state of uremia characterised by increased levels of plasma uremic toxins and reduced levels in the urine probably due to proximal tubule transporter dysregulation. After 2 weeks of washout, renal transporter levels fully recovered, partially restoring the uremic state. We show that the adenine-model in mice is fit to investigate uremic toxicity.

C32

Species differences in renal response to the bile acid lithocholic acid

Sandra M. Hansen[1], Rianne V. Dekken[1], Rikke Nørregaard[1], Henricus A.M. Mutsaers[1]

[1]*Department of Clinical Medicine, Aarhus University, Aarhus, Denmark*

Background: Hydrophobic bile acids (BA) have long been known to be cytotoxic. Because of this, growing attention has centered on their role in the development of renal injury. So far research has predominantly relied on mouse models to study BA toxicity. This is despite the fact that humans and mice have substantially different BA pool compositions, with hydrophobic BAs being much more predominant in humans than in mice. To address this disparity, this study utilizes Precision-Cut Kidney Slices (PCKS) to conduct a comparative analysis of the impact of Lithocholic acid (LCA), the most hydrophobic BA, on human and mouse kidney tissue.

Methods: Using an Alabama R&D Tissue Slicer (formerly Krumdieck Tissue Slicer), human PCKS (hPCKS) (n=3) were prepared from macroscopically healthy kidney tissue obtained from tumor nephrectomies. Mice PCKS (mPCKS) (n=5) were prepared from kidneys harvested from C57BL/6 mice. Mice were anesthetized with 5% sevoflurane and sacrificed by cervical dislocation. Both hPCKS and mPCKS were cultured for 24H, 48H, and 72H with and without 100 µM LCA. The inflammatory and fibrotic responses in the PCKS were characterized by qPCR of the inflammatory genes IL-6 and IL-1β and the fibrotic genes fibronectin and collagen 1A1. Gene expression levels were compared with two-tailed unpaired T-test. The use of human tissue for the hPCKS was approved by the Central Denmark Region Committees on Biomedical Research Ethics and the Danish Data Protection Agency.

Results: Exposure to LCA for 24H induced a strong inflammatory response in the mPCKS, seen by a large increase in *Il6* (p: 0.0034) and in *Il1b* (p: 0.0088). This was accompanied by an increase in the fibrotic genes *Fn*(p: 0.0430) and *Col1a1* (p: 0.0170). Only the increase in *Fn* persisted after 48H of exposure (p: 0.0263), and this was likewise no longer evident after 72H of exposure. However, mPCKS exposed to LCA for 48H and 72H exhibited markedly low RNA concentrations, which might indicate low viability. Further viability measures will be done.

hPCKS exhibited no alteration in *IL6* and *IL1B* levels after 24H, 48H, and 72H of LCA exposure. The non-exposed hPCKS exhibited culture-induced fibrosis at 48H and 72H compared to the 24H ($p<0.041$), a response normally seen in PCKS. This phenomenon was absent in LCA-exposed hPCKS, where *FN* and *COL1A1* levels remained stable throughout all time points.

Conclusion: This study demonstrated that mouse and human kidney tissue differ in their response to LCA. As anticipated, LCA had harmful effects on mPCKS, evidenced by heightened expression of inflammatory and fibrotic genes. Surprisingly the opposite was observed in hPCKS, where LCA protected against culture-induced fibrosis. This species difference in response to BAs emphasizes the importance of incorporating human models in research on the nephrotoxicity of BAs.

C33

Acute thrombocyte-dependent clearance of Escherichia coli requires D-mannose-sites for bacterial adherence

Emil Herrig Lambertsen[1], Nanna Johnsen[1], Thomas Corydon[1], Helle Praetorius[1]

[1]*Department of Biomedicine, Aarhus University, Aarhus C, Denmark*

EH Lambertsen, N. Johnsen, T. Corydon, H. Prætorius[1]

Aarhus University, Department of Biomedicine, 8000 Aarhus, Denmark

Background:

Uropathogenic *E. coli* (UPEC) is the leading cause of urinary tract infections (UTIs). UPEC causing severe disease express various virulence factors that allow the UPEC to colonise the bladder, ascend to the kidney and disseminate to urosepsis[1,2]. Our preliminary data show that thrombocytes are important for acute clearing of UPEC from the blood in a murine model of urosepsis. UPEC are known to adhere to epithelia via type 1 fimbriae, recognising D-mannose-rich structures[3,4]. Here, we investigate if thrombocyte/*E. coli* complexes are prevented by pre-incubating UPEC with DM or preincubating thrombocytes with concanavalin A, a soluble lectin that binds D-mannose.

Methods:

Here, we use an *in vitro* assay of GFP-expressing UPEC ($165{\cdot}10^6$ ml^{-1}) added to whole blood samples or isolated thrombocytes from humane healthy volunteers (Danish Research Ethics Committees: 1-10-72-202-17). Complex formation between UPEC and thrombocytes (using CD42b as a thrombocyte marker) was determined at various time points by flow cytometry (Accuri 6plus, BD Biosciences). Data are analysed using one-way ANOVA and given as mean±SEM.

Results:

In our assay, we could easily confirm the instant formation of UPEC-thrombocyte complexes similar to what we observe in a mouse model of urosepsis. The complexes also readily form after thrombocytes have been fixed with 0.4% paraformaldehyde. Although thrombocytes have previously been suggested to be able to adhere *E. coli* via surface lipopolysaccharide (LPS) binding to thrombocyte TLR4, we could not prevent complex formation by either preincubation with TLR4 antagonists, TLR4 antibodies or pre-incubating thrombocytes with LPS. Moreover, we have not been able to prevent complex formation with antibodies directed against FcγRII or CD41/CD61.

Both D-mannose and concanavalin A cause a concentration-dependent reduction in UPEC/thrombocyte complexes. D-mannose reduced UPEC-thrombocyte complex formation from $6.71 \cdot 10^6 \pm 0.78 \cdot 10^6$ counts/ml to $2.69 \cdot 10^6 \pm 0.56 \cdot 10^6$ counts/ml equal to a ~60% decrease (n=8, p=0.023). Concanavalin A reduced complex formation from $3.21 \cdot 10^5 \pm 0.34 \cdot 10^5$ counts/ml to $1.57 \cdot 10^5 \pm 0.91 \cdot 10^5$ counts/ml equal to a ~51% decrease (n=7, p=0.004).

Conclusions:

We show that pre-treatment of UPEC with DM, and pre-treatment of thrombocytes with Concanavalin A reduced complex formation *in vitro*. These data suggest that type 1 fimbriae and not LPS are important for E. coli-thrombocyte interaction, and currently, we are gaining further evidence for this notion. Once confirmed, the relevant mannose-bearing interaction partners on thrombocytes will be determined by proteomics.

1) Medina M, Castillo-Pino E. An introduction to the epidemiology and burden of urinary tract infections. Ther Adv Urol, 2019 May 2:11:1756287219832172. 2) Whelan S, Lucey, B, Finn K. Uropathogenic Escherichia coli (UPEC)-Associated Urinary Tract Infections: The Molecular Basis for Challenges to Effective Treatment. Microorganisms, 2023 Aug 28;11(9):2169 3) Lane MC, Mobley, HLT. Role of P-fimbrial-mediated adherence in pyelonephritis and persistence of uropathogenic Escherichia coli (UPEC) in the mammalian kidney. Kidney Int, 2007 Jul;72(1):19-25 4) Sheikh A, Rashu R, Begum YA, Kuhlman FM, Ciorba MA, Hultgren SJ, Qadri F, Fleckenstein JM. Highly conserved type 1 pili promote enterotoxigenic E. coli pathogen-host interactions PLoS Negl Trop Dis, 2017 May 22;11(5):e0005586

C34

The SGLT-2 inhibitor empagliflozin reduces intrarenal complement activation in patients with diabetes and chronic kidney disease

Mia Jensen[1], Steffen Flindt Nielsen[2,3], Steffen Thiel[4], Søren W.K. Hansen[5], Yaseelan Palarasah[5], Per Svenningsen[1], Jesper N. Bech[2,3], Frank H. Mose[2,3], Boye L. Jensen[1]

[1]Unit of Cardiovascular and Renal Research, Department of Molecular Medicine, University of Southern Denmark, Odense, Denmark, [2]University Clinic in Nephrology and Hypertension, Gødstrup Hospital, Herning, Denmark, [3]Department of Clinical Medicine, Aarhus University, Aarhus, Denmark, [4]Department of Biomedicine, Aarhus University, Aarhus, Denmark, [5]Unit of Cancer and Inflammation Research, Department of Molecular Medicine, University of Southern Denmark, Odense, Denmark

Background and hypothesis: Sodium-glucose cotransporter 2 (SGLT-2) inhibitors (SGLT2i) improve kidney and cardiovascular outcomes in patients with diabetes and chronic kidney disease (CKD). Since complement system precursors are aberrantly filtered and activated in conditions with albuminuria, it was hypothesized that SGLT2i lower plasma collectins and attenuate intratubular complement activation and deposition in patients with CKD.

Methods: Patient plasma and urine samples were analyzed from three randomized, blinded, cross-over intervention studies where patients with type 2 diabetes mellitus (DM) and CKD (DM-CKD, n=17), DM without CKD (DM, n=16), and CKD without DM (CKD, n=16) were given empagliflozin (10 mg/day) and placebo for four weeks with a washout of at least two weeks in-between. ELISA was used to determine concentrations of collectin kidney 1 (CL-K1), collectin liver 1 (CL-L1), mannose-binding lectin (MBL), MBL-associated serine protease (MASP-2), anaphylatoxins C3a and C5a, stable C3 split product C3dg and the membrane attack complex (sC5b-9) in urine and plasma. Apical deposition of membrane-bound C5b-9 was determined in isolated extracellular vesicles (EVs) from urine by western blotting (n=5). A paired two-tailed t-test was used to determine statistical significance between the treatments in each group. Non-normal distributed values were reported as median [interquartile range]. The studies were approved by the Ethical Committee of the Central Jutland Region and the Danish Health and Medicine Authority. The collection of samples was performed in accordance with the Helsinki Declaration, the EU Directive on Good Clinical Practice (GCP), and International Conference of Harmonization (ICH-GCP) guidelines and all participants gave written informed consent before inclusions.

Results: Empagliflozin induced no change in plasma levels of CL-K1, CL-L1, MBL, MASP-2, C3a, C5a, and C5b-9 while C3dg levels increased (18%, 114.1 [91-139] vs. 131.9 [98-157] units/mL, p=0.03) in DM-CKD. Collectins were not detectable in protease-inhibited spot urine or in *ex vivo* up-concentrated urine. Empagliflozin decreased urine C3a/creatinine ratio in the DM (32.5%, 5.7 [2.6-15] vs. 4.1 [1.8-6.4] ng/µmol, p=0.01) and DM-CKD groups (58.3%, 5.1 [3.6-238] vs. 4.7 [2.0-105] units/µmol, p=0.012), whereas urine C5a- and C3dg/creatinine ratio did not change. Urine sC5b-9/creatinine decreased significantly (45%, 0.9 [0.1-17] vs. 0.4 [0.1-12] units/µmol, p=0.02) after empagliflozin but only in the DM-CKD group. This was recapitulated in urine EVs by immunoblotting for C5b-9. Empagliflozin reduced the urine albumin/creatinine ratio in the DM-CKD group (24.5%, 201 [62-1130] vs. 164 [44-719] mg/g, p=0.02).

Conclusion: While SGLT2i do not lower plasma concentrations of collectins and complement activation products, they significantly reduce indices of intrarenal complement activation and membrane deposition in patients with DM and DM-CKD. Thus, SGLT2 inhibitors may protect kidneys in diabetic patients with CKD by reducing complement-induced tubular injury.

C35

The Secondary Bile acid, Lithocholic Acid, Exerts Anti-secretory Actions in Colonic Epithelial Cells in Vitro

Caitriona Curley[1], Magdalena Mroz[1], Stephen Keely[1]

[1]*Royal College of Surgeons in Ireland, Dublin, Ireland*

Introduction: Bile acids, classically known for their roles in facilitating lipid digestion, are now also appreciated as a family of enterocrine hormones that modulate many aspects of intestinal and metabolic function. We have previously shown lithocholic acid (LCA), a secondary bile acid formed in the colon, to be protective against colonic inflammation. Here, we sought to investigate if LCA might also regulate colonic epithelial fluid and electrolyte transport.

Methods: T_{84} cell monolayers were mounted in Ussing chambers for measurements of Cl^- secretion, the primary driving force for colonic fluid secretion. qRT-PCR and Western blotting were used to analyze mRNA and protein expression. To assess the effects of LCA on CFTR promoter activity, we used a luciferase promoter/reporter system in HEK293. Results were expressed as mean ± SEM and data were analyzed by one way ANOVA and Tukey's post hoc test or by mixed-effects analysis and Dunnett's post hoc test.

Results: Pretreatment of T_{84} cell monolayers with LCA inhibited subsequent Cl^- secretory responses to the cAMP-dependent agonist, forskolin (FSK; 10 mM), in a concentration (1 – 10 μM) and time-dependent (3 - 24 hrs) manner. Maximal effects of LCA were observed at a concentration of 10 μM after treatment for 24 hrs, when responses to FSK were reduced to 50.9 ± 8.5% of those in controls ($n = 6$; $p < 0.01$). LCA (10 μM; 24 hrs) also inhibited responses to the Ca^{2+}-dependent secretagogues, thapsigargin (2 μM) and histamine (100 μM), by 59.4 ± 2.4% ($n = 4$; $p < 0.001$) and 52.2 ± 1.9% ($n = 5$; $p < 0.001$), respectively. In further experiments, using nystatin-permeabilized T_{84} monolayers to isolate apical Cl^- conductances, LCA (10 μM; 24 hrs) reduced FSK-stimulated responses to 72.7 ± 6.6% ($n = 17$; $p < 0.001$) of those in control cells. Analysis of CFTR expression, the primary exit pathway for Cl^- in colonic epithelial cells, revealed that LCA treatment reduced mRNA and protein expression of the channel to 0.65 ± 0.05 ($n = 7$; $p < 0.01$) and 0.43 ± 0.06 ($n = 6$; $p < 0.001$) fold of controls, respectively. In CFTR promoter assays, LCA (10 μM) reduced CFTR promoter activity to 0.7 ± 0.02 fold of that in control cells ($n = 5$; $p < 0.01$), with expression of FXR being required for this effect to be observed. Finally, while LCA activated both FXR and the vitamin D receptor (VDR) in T_{84} cells, its effects in downregulating CFTR expression and Cl^- conductances were mimicked by the FXR agonist, GW4064, but not by the VDR agonist, calcitriol.

Conclusion: LCA, at physiologically-relevant concentrations, inhibits Cl^- secretion across colonic epithelial cells, likely through a mechanism involving FXR activation and inhibition of CFTR expression. These data add to the growing pool of knowledge regarding regulatory actions of LCA in the colon and its potential role as a target for the treatment of intestinal disorders.

C36

Induction of ATF4-Regulated Atrogenes Is Uncoupled from Muscle Atrophy during Disuse in Halofuginone-Treated Mice and in Hibernating Brown Bears

Lydie Combaret[1], Laura Cussonneau[2], Cécile Coudy-Gandilhon[3], Guillemette Gauquelin-Koch[4], Fabrice Bertile[5], Etienne Lefai[1], Pierre Fafournoux[1], Anne-Catherine Maurin[1]

[1]Université Clermont Auvergne, INRAE, Unité de Nutrition Humaine, UMR 1019, Clermont-Ferrand, France, [2]Université Clermont Auvergne, INRAE, Unité de Nutrition Humaine, UMR 1019, Clermont-Ferrand, France, [3]Université Clermont Auvergne, INRAE, Unité de Nutrition Humaine, UMR 1019, Clermont-Ferrand, France, [4]Centre National d'Etudes Spatiales, CNES, Paris, France, [5]Université de Strasbourg, CNRS, IPHC UMR 7178, Strasbourg, France

Introduction: Muscle atrophy observed in several physio-pathological situations has harmful consequences for the patients and results from an imbalance between protein synthesis and proteolysis. With no proven treatment of muscle atrophy, there is still a need to develop efficient strategies. Activation of the transcription factor 4 (ATF4) is involved in muscle atrophy through the overexpression of some atrogenes, i.e. genes whose mRNA levels are regulated during muscle atrophy. However, ATF4 also controls the transcription of genes involved in muscle homeostasis maintenance (1), and a controlled activation of the eIF2alpha/ATF4 pathway before a stressful event preserved organ function (2).

Aim: Here, we explored whether such a controlled activation of ATF4 before induction of atrophy may preserve muscle function.

Method: For that purpose, mice were treated with the pharmacological molecule halofuginone (0.25mg/kg, 3 times a week) for 3 weeks, before inducing muscle atrophy by hindlimb suspension for 3 or 7 days. Data were analyzed by ANOVA and were considered statistically different between groups for p-values below 0.05.

Results: Firstly, we reported that periodic activation of ATF4-regulated atrogenes (Gadd45a, Cdkn1a, and Eif4ebp1) by halofuginone was not associated with muscle atrophy in untreated and treated healthy mice (6 mice/group). Secondly, the atrophy induced by hindlimb suspension was reduced in halofuginone-treated mice compared to untreated ones, although the induction of the ATF4 pathway by hindlimb suspension was identical in halofuginone treated and untreated mice (8-19 mice/group). We further showed that transforming growth factor-β (TGF-β) signaling was inhibited, while bone morphogenetic protein (BMP) signaling was promoted in halofuginone-treated healthy mice compared to untreated ones (5-8 mice/group). In addition, halofuginone treatment also slightly preserved protein synthesis during hindlimb suspension (5-8 mice/group). Finally, ATF4-regulated atrogenes were also induced in the atrophy-resistant muscles of hibernating compared to active brown bears (6 bears/group), in which we previously also reported concurrent TGF-β inhibition and BMP maintenance during hibernation (3).

Conclusions: Overall, we show that ATF4-induced atrogenes can be uncoupled from muscle atrophy. Our data also indicate that halofuginone can control the TGF-β/BMP balance toward muscle mass maintenance. Whether halofuginone-induced BMP signaling can counteract

the effect of ATF4-induced atrogenes needs to be further investigated and may open a new avenue to fight muscle atrophy. Finally, our study opens the way for further studies to identify well-tolerated chemical compounds in humans that enable fine-tuning of the TGF-β/BMP balance and could be used to preserve muscle mass during catabolic situations.

(1) Kasai et al. Role of the ISR-ATF4 Pathway and Its Cross Talk with Nrf2 in Mitochondrial Quality Control. J. Clin. Biochem. Nutr. 2019;64:1–12. doi: 10.3164/jcbn.18-37. (2) Peng et al. Surgical Stress Resistance Induced by Single Amino Acid Deprivation Requires Gcn2 in Mice. Sci. Transl. Med. 2012;4:118ra11. doi: 10.1126/scitranslmed.3002629. (3) Cussonneau et al. Concurrent BMP Signaling Maintenance and TGF-β Signaling Inhibition Is a Hallmark of Natural Resistance to Muscle Atrophy in the Hibernating Bear. Cells. 2021. 10(8):1873. doi: 10.3390/cells10081873.

C37

Neurovascular coupling during dynamic upper body resistance exercise in healthy individuals

Stephanie Korad[1], Toby Mundel[2,3], Blake Perry[1]

[1]School of Health Sciences, Massey University, Wellington, New Zealand, [2]School of Sport, Exercise and Nutrition, Massey University, Palmerston North, New Zealand, [3]Department of Kinesiology, Brock University, St Catherines, Canada

During dynamic exercise many of the regulators of cerebral blood flow (CBF) are concomitantly perturbed. These regulators include neurovascular coupling (NVC), arterial carbon dioxide content, arterial blood pressure, sympathetic nerve activity, and cerebral autoregulation (CA). Neurovascular coupling refers to the matching of local CBF to neuronal activity. That is, when neuronal activity increases, so does local blood flow. During unilateral static handgrip exercise blood velocity in the middle cerebral artery (MCAv) contralateral to the exercising limb increases, indicative of NVC. However, it is unknown whether this persists during dynamic resistance exercise (RE). This study aimed to examine the cerebral haemodynamic response to unilateral dynamic upper body RE in healthy individuals. We hypothesied that during unilateral dynamic upper body RE, there will be no differences between contralateral and ipsilateral MCAv due the overriding influence of arterial carbon dioxide concentration and blood pressure. The current study could provide valuable insights for the safe prescription of dynamic RE to those who have suffered cerebrovascular injury. Thirty (female = 16, mean ± SD: age, 26 ± 6 years, height 175 ± 10cm, weight 74 ± 15kg, BMI 24 ± 5kg/m^2) healthy individuals completed 4 sets of 10 paced repetitions (15-beats-per-minute) of unilateral bicep curl exercise at 60% of predicted 1 repetition maximum (60% of 1RM 7 ± 3kg). Beat-to-beat blood pressure, bi-lateral MCAv, and the partial pressure of end-tidal carbon dioxide ($P_{ET}CO_2$ – as a proxy for arterial CO_2) were measured throughout. One-way ANOVA was used to analyse cardiovascular variables, and two-way ANOVA was used to analyse dependent cerebrovascular variables (side x sets, 2x4). Typical cerebrovascular and cardiovascular responses during RE are shown in Figure 1. Within exercise bilateral MCAv, cerebral conductance index, and pulse velocity decreased across the exercise sets (all $P < 0.001$), but no significant interaction effect was observed (all $P > 0.221$) for any dependent variables. Despite the recruitment of a small muscle mass during the bicep curl, we observed sinusoidal fluctuations in MAP typical of dynamic RE. Furthermore, although not significant (all $P > 0.316$), average $P_{ET}CO_2$ was ~2 mmHg lower during exercise. The current data indicates no differences between contralateral and ipsilateral MCAv during unilateral dynamic RE, consistent with our hypothesis, but contradicting findings of static RE studies. The effects of NVC were not discernible in the MCAv data, possibly obfuscated by the small reduction in $P_{ET}CO_2$ and the fluctuating MAP. Future studies are required to attempt to discern the underlying physiology of local and global CBF during dynamic RE.

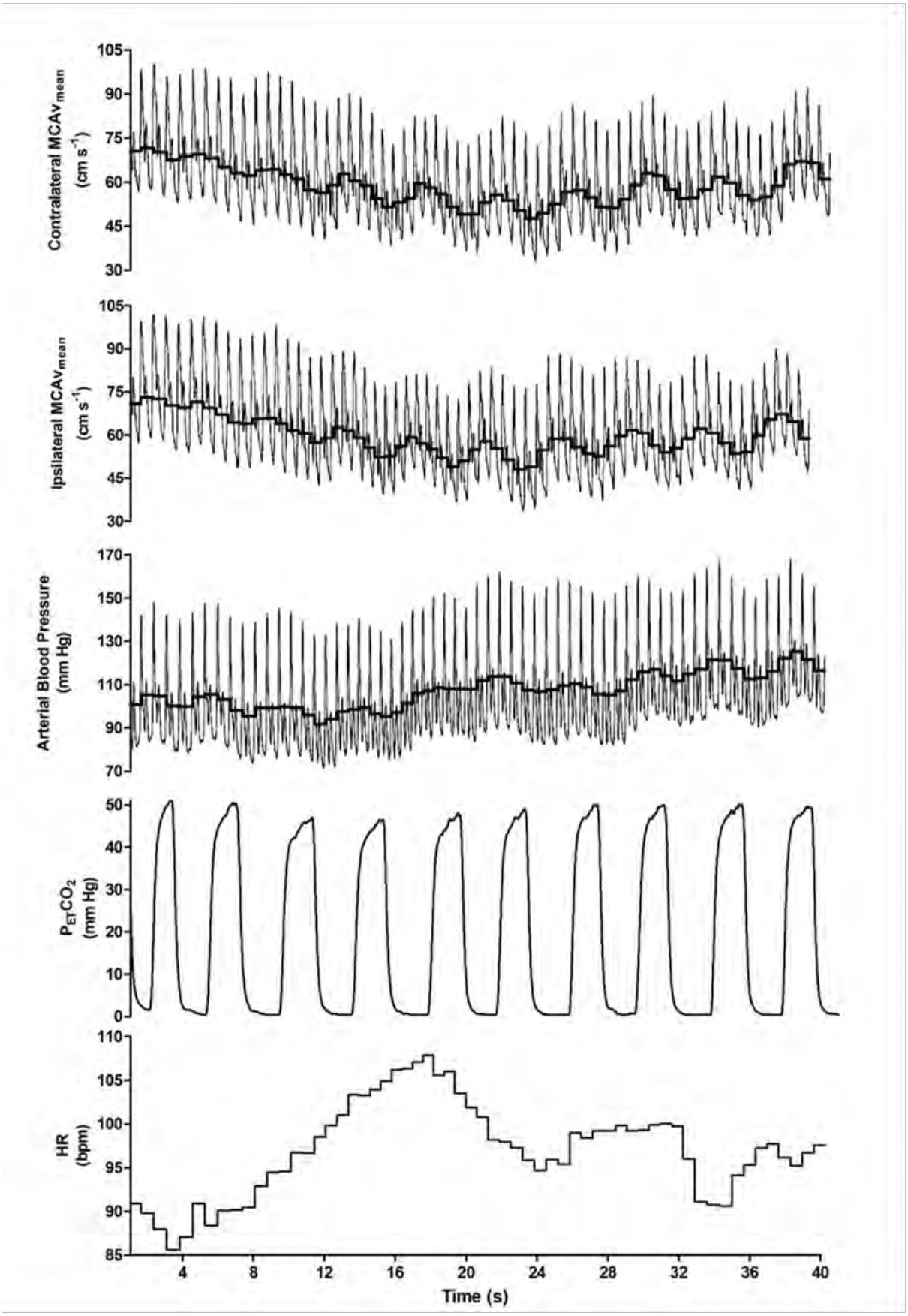
Contralateral MCAv$_{mean}$ (cm s^{-1})
105
90
75
60
45
30
Ipsilateral MCAv$_{mean}$ (cm s^{-1})
105
90
75
60
45
30
Arterial Blood Pressure (mm Hg)
170
150
130
110
90
70
$P_{ET}CO_2$ (mm Hg)
50
40
30
20
10
0
HR (bpm)
110
105
100
95
90
85
4
8
12
16
20
24
28
32
36
40
Time (s)

C38

Comparison of ectopic fat deposition between children with and without obesity: Influence of sex and physical activity level

Ryan G. Larsen[1], Charlotte N. Eggertsen[2,3,4], Jonas Gelardi[1], Jan C. Brønd[6], Aase Handberg[4,5], Esben T. Vestergaard[7,8], Jens B. Frøkjær[9], Søren Hagstrøm[2,3,4]

[1]ExerciseTech, Department of Health Science and Technology, Aalborg University, Aalborg, Denmark, [2]Department of Pediatrics and Adolescent Medicine, Aalborg University Hospital, Aalborg, Denmark, [3]Steno Diabetes Center North Denmark, Aalborg University Hospital, Aalborg, Denmark, [4]Department of Clinical Medicine, Aalborg University Hospital,, Aalborg, Denmark, [5]Department of Clinical Biochemistry, Aalborg University Hospital, Aalborg, Denmark, [6]Department of Sport Science and Clinical Biomechanics, University of Southern Denmark, Odense, Denmark, [7]Department of Pediatrics and Adolescent Medicine, Aarhus University Hospital, Aarhus, Denmark, [8]Department of Clinical Medicine, Aarhus University, Aarhus, Denmark, [9]Department of Radiology, Aalborg University Hospital, Aalborg, Denmark

Introduction: According to the theory of lipitoxicity, ectopic fat deposition (i.e., storage of triglycerides in non-adipose tissues, such as muscle, liver, pancreas) can lead to inflammation, insulin resistance and beta-cell dysfunction (1, 2). A previous study reported greater fat deposition in skeletal muscle and liver in children with obesity compared to their lean counterparts (3). However, the role of weight status (obesity vs. normal weight) on pancreatic fat deposition in children is yet unclear. In addition, little is known about the roles of sex and physical activity level in modulating ectopic fat deposition in children. We tested the hypotheses that children with obesity exhibit greater fat deposition in psoas muscle, liver, and pancreas compared to children with normal weight, matched for age and sex. We also investigated if sex and physical activity level modulate fat deposition in these organs.

Methods: 3T MR scanning with multi-echo Dixon imaging was used to acquire proton density fat fraction (PDFF) maps in 48 children (9-16 years; 33 boys, 15 girls) with obesity (body mass index, BMI > 90 percentile for age and sex) and in 30 age-matched children with normal weight (18 boys, 12 girls). From the PDFF maps, liver, psoas muscle and pancreas were outlined to obtain fat fraction in each specific organ. To assess physical activity level, participants wore a 3-axis accelerometer on the thigh for seven consecutive days. Daily minutes spent in sedentary, light, moderate and vigorous intensity were quantified. Fat fractions and physical activity categories were analyzed using 2-way (group, sex) repeated measures ANOVA. Associations between physical activity level and fat fractions were explored using Pearson's correlation.

Results: Compared to normal weight, children with obesity showed higher fat fraction in liver (6.3±6.9% vs. 1.7±0.7; $p<0.001$), psoas (2.8±1.6% vs. 1.1±0.6%; $p<0.001$) and pancreas (4.9±2.8% vs. 1.7±0.7%; $p<0.001$) with no effects or interactions of sex. Daily minutes spent in moderate (29.0±13.7 vs. 43.1±19.5; $p<0.001$) and vigorous (8.2±7.6 vs. 21.9 ±13.2; $p<0.001$) intensity were lower in children with obesity compared with normal weight, with no effects or interactions of sex. Daily minutes of moderate-to-vigorous intensity was inversely associated with fat fraction in liver ($r=-0.27$, $p<0.05$), psoas ($r=-0.34$, $p<0.01$), and pancreas ($r=-0.50$, $p<0.01$).

Conclusion: Children with obesity exhibited greater fat deposition in liver, psoas muscle and pancreas compared to their lean counterparts. While sex did not play a role in modulating fat deposition, time spent in moderate-to-vigorous intensity activities were inversely associated with fat fraction in each organ. Future studies are required to 1) elucidate biomarkers that can identify children who display a critical amount of ectopic fat deposition, and 2) explore interventions effective in reducing ectopic fat deposition in children with obesity.

1) Plötz T and Lenzen S. Mechanisms of lipotoxicity-induced dysfunction and death of human pancreatic beta cells under obesity and type 2 diabetes conditions, Obesity reviews, 2024, online ahead of print 2) Rada P et al. Understanding lipotoxicity in NAFLD pathogenesis: is CD36 a key driver? Cell Death & Disease, 2020, 11(9):802 3) Fonvig CE et al. 1H-MRS Measured Ectopic Fat in Liver and Muscle in Danish Lean and Obese Children and Adolescents, Plos One, 2015, 10(8): e0135018

C39

High-intensity continuous exercise elevates I-FABP2 levels equally across 30 and 60-minute durations in healthy males.

Lewis R Mattin[1], Victoria J McIver[2], Adora MW Yau[3], Gethin H Evans[3]

[1]School of Life Sciences, University of Westminster, London, UK, London, United Kingdom, [2]Department of Sport, Exercise and Rehabilitation, Northumbria University, Newcastle, UK, Newcastle, United Kingdom, [3]Department of Life Sciences, Manchester Metropolitan University, Manchester, UK, Manchester, United Kingdom

Introduction: Intestinal fatty acid binding protein two (I-$FABP_2$) is a small 15 KDa cytosolic protein expressed in epithelial cells of the mucosal layer of the small and large intestines [1]. When damage occurs, I-$FABP_2$ is released, and plasma concentrations increase [2]. Notably, I-$FABP_2$ is not expressed in any other tissues. Therefore, I-$FABP_2$ is used to evaluate gut wall integrity and intestinal injury, contributing to gastrointestinal complications and delayed nutrient delivery [1-4]. However, in trained participants, mucosal damage increases in response to exercise > 70% $\dot{V}O_{2Max}$ for durations of ~60 minutes [2, 4, 5]. Therefore, this study aimed to investigate the effect of high-intensity continuous exercise at two different durations, 30 and 60 minutes, on I-$FABP_2$ responses in healthy male participants. **Method:**Fourteen healthy males (Mean ± SD; age 27 ± 6 years; height 179 ± 9 cm; body mass 79 ± 10 kg; body fat 18.5 ± 4.1 %; BMI 24.9 ± 2 kg/m^2; $\dot{V}O_{2peak}$ 42 ± 9 ml/kg/min). Completed two ~4-h trials in a randomised order. Diet was standardised 24-h before experimental trials. Participants arrived at the laboratory following an overnight fast before completing a 60-min continuous cycle (EX-60) or a split 30-min morning and 30-min afternoon cycle (EX-30) at the same intended intensity of ~70% $\dot{V}O_{2Max}$. Participants then received breakfast at 75-min (Semi-skimmed milk), which amounted to 30% of the estimated trial energy expenditure (ETEE), with the total volume standardised to 500ml with water. Participants then recovered for 2-h (90-210 min) followed by the second 30-min exercise bout from 210-240-min (EX-30 second bout). Heart rate (HR) was recorded every 5-min, and REP every 10-min during all exercise periods. I-$FABP_2$ was measured at baseline (0), Pre-breakfast (75-min), and Post-second EX (270-min). **Results:** There were no differences in Pre-trial energy intake between EX-60 and EX-30 (2571 ± 1173 Kcal Vs 2547 ± 1311 Kcal; p = 0.779). There was no main effect for I-$FABP_2$ AUC for EX-60 vs EX-30, respectively (p = 0.400). No main effect for trial (p =0.252) nor trial x time interaction (p =0.780) was observed. However, an effect for time (p <0.001) was identified for I-$FABP_2$. Post-hoc tests revealed I-$FABP_2$ increased from baseline to Post-EX (75-min) respectively EX-60 (485 ± 301 vs 1334 ± 626 pg.ml^{-1}; p <0.001) and EX-30 (572 ± 325 vs 1454 ± 792 pg.ml^{-1}) and baseline to post-second EX (270 min) highly significant in both trials (p <0.001). REP was significantly different across all measurements during exercise (p <0.001). There were no differences in HR averaged over 60-min EX-60 and EX-30 (156 ± 14 vs 154 ± 14 bpm; p = 0.534). **Conclusion**: The results of this study demonstrate that 30 min of high-intensity exercise was sufficient to cause an increased intestinal cellular injury, which caused cell membrane integrity to be compromised following strenuous exercise to the same extent as 60 min when a health population is used. Therefore, the effect of I-$FABP_2$ may depend upon training status, and an individualised approach should be warranted.

1. Agellon LB et al. (2007). Molecular and Cell Biology of Lipids, 1771 (10). 2. Pugh JN et al. (2017). Appl Physiol Nutr Metab, 42 (9). 3. Lau E et al. (2016). Nutr Metab (Lond), 13 (31). 4. van Wijck K et al. (2011). PLoS One, 6 (7). 5. Van Wijck K et al. (2012). Med Sci Sports Exerc, 44 (12).

C40

The Impact of Chronic Electronic Cigarette Use on Blood Pressure Responses to Exercise

Maddie Roscoe[1], Rhiannon Price-Wickenden[1], Mared Tomkinson[1], Cory Richards[2], Thomas Griffiths[2], Z Adams[1,2], Lydia Simpson[1], Rachel Lord[2], Benjamin Chant[1], Emma Hart[1]

[1]School of Physiology, Pharmacology and Neuroscience, University of Bristol, Bristol, United Kingdom, [2]Cardiff Metropolitan Univeristy, Cardiff, United Kingdom

Over recent years, there has been an unprecedented uptake in the use of electronic cigarettes (e-cigarettes) as an alternative to tobacco smoking. They are often marketed as a 'safer' option, however, there is a significant lack of research investigating their impact on physiological health, especially long-term. Assessing increases in systolic blood pressure (SBP) during exercise is an important diagnostic tool for predicting the likelihood of a future cardiovascular events. Current literature has only investigated the effect of vaping on SBP at rest. This study aims to evaluate changes in SBP during metaboreflex isolation using post-exercise ischemia (PEI) and during cardiopulmonary exercise testing (CPET). The study was approved by the University of Bristol Ethics Committee and conformed to the Declaration of Helsinki. Seventeen healthy, non-tobacco smoking participants were recruited, twelve controls (6 males) and five regular e-cigarette users (4 males) (defined as ≥5 days per week for >6 months). Vapers were asked to refrain from vaping 8 hours prior to each study visit (confirmed via urine cotinine test). To start, 2-minutes of baseline data was recorded followed by an isometric handgrip exercise at 40% maximal voluntary contraction for 2-minutes, with an occlusion at 90 seconds using an inflated cuff (>220 mmHg). This remained inflated for a further 2 minutes and 30 seconds to isolate the effects of the metaboreflex during PEI. This was followed with a 2-minute recovery period. Beat-to-beat BP was measured continuously via finger photo-plethysmography (Finapres) and heart rate (HR) measured via 3-lead ECG. After a 15-minute rest period, participants then completed a ramped incremental exercise test to volitional exhaustion on a cycle ergometer. BP was recorded every 1-minute throughout baseline, unloaded and loaded cycling and during recovery. For all data, absolute and change from baseline values were analysed over 30s increments. The change in SBP from baseline to the end of PEI (last 30s) or to peak SBP during CPET (as defined by the final 30s of exercise) were compared between groups using an unpaired t-test. Data are mean ± SD. There was no difference in age (controls; 21±1 years vs. vapers; 22±2 years, P=0.2339), body mass index (22.9±1.4 kg/m^2 vs. 22.3±4.6 kg/m^2, P=0.6962) and resting SBP (125±13mmHg vs. 121±12 mmHg, P=0.5870). There was no difference observed between groups in A) the SBP change from baseline to the end of PEI (Δ21.0±19.6 mmHg vs. 29.9±22.2 mmHg, P=0.3997) and B) change from baseline to peak SBP during CPET (Δ74.9±24.9 mmHg vs. 88.3±25.2 mmHg, P=0.2566). This study suggests that long-term vaping may not impact the SBP response to exercise or metaboreflex activation.

C41

Characterising the Cellular Physiology of a Novel Phospholipase Target in Skeletal Muscle within the Aetiologies of Obesity and Diabetes

Rashmi Sivasengh[1], Iris Pruñonosa Cervera[2], Nicholas M. Morton[3], Brendan M. Gabriel[1]

[1]University of Aberdeen, Aberdeen, United Kingdom, [2]University of Edinburgh, Edinburgh, United Kingdom, [3]School of Science and Technology, Nottingham Trent University, Nottingham, United Kingdom

Obesity increases the risk for diabetes and cardiovascular disease. Genetic predisposition exacerbates environmental drivers of obesity such as energy-dense diets and a sedentary lifestyle. We have used divergently selected Fat (23% fat) and Lean (4% fat) lines of mice to identify the genes underlying adiposity. A stratified approach using quantitative trait loci (QTL; heritable genetic intervals segregating with adiposity in Fat x Lean F2 populations), transcriptomics, and comparative cross-species bioinformatics identified candidate obesity genes (Morton et al., 2016). A specific phospholipase A2 isoform (we name here PlaX), positioned in obesity (Fob)-1 QTL, exhibited ~5-fold elevated mRNA levels in the skeletal muscle of Fat mice compared to Lean mice. PlaX has been previously linked to the regulation of intracellular membrane vesicle trafficking and generation of lipid signalling mediators (Prunonosa Cervera *et al.*, 2021). Overexpression of PlaX in C2C12 myotubes impaired cellular energetics and increased levels of the active form of AMP-activated protein kinase (AMPK). This led us to hypothesize that skeletal muscle PlaX overexpression may drive obesity by compromising myocyte energetics. To characterize the role of PlaX in skeletal muscle, we have overexpressed PlaX in L6 myotubes (n=3) using lentiviral transduction and performed RNA-sequencing on the Illumina NextSeq 2000 platform. As expected, Plax was most significantly overexpressed with a +6.1886-fold change (Adj.p= 5.84e-14) in overexpressed cells (differential gene expression analysis). Several genes with differential expression in PlaX overexpression cells were linked to mitochondrial respiration and metabolism. These included Pdk4, which was down regulated with -1.02327 fold-change (adj.p value 0.0012); and Mitochondrial calcium uptake gene (Micu1) which was down regulated with a -0.328-fold change (Adj.P= 1.16e^-11). It is known that Mitochondrial calcium uptake 1 (Micu1) negatively regulates thermogenesis and deletion of Micu1 in adiposity impairs thermogenesis and may lead to increased risk of obesity and metabolic dysfunction. Anti-Flag magnetic beads were used to perform Immunoprecipitant (IP) pull down to identify PlaX binding partners. As expected, PlaX was overexpressed in IP eluant >1*10^8. We performed Gene ontology on proteins detected in PlaX eluant (which were not detected in GFP and not treated controls) and found mitochondrial cellular compartments were overexpressed (Differentially expressed protein analysis, n=3, FDR-adjusted (adj.) p<0.02). Our IP and RNA-Sequencing data indicate the PlaX has a regulatory role on mitochondrial metabolism, and this may be a mechanism driving increased adiposity. In summary, our genetic strategy has identified a novel potential skeletal muscle driver of obesity that could be a tractable target for therapeutic development.

1. Azevedo PG de, Miranda LR, Nicolau ES, Alves RB, Bicalho MAC, Couto PP, Ramos AV, Souza RP de, Longhi R, Friedman E, Marco L De & Bastos-Rodrigues L (2021). Genetic association of the PERIOD3 (PER3) Clock gene with extreme obesity. Obesity Research & Clinical Practice 15, 334–338. 2. Cervera IP, Gabriel BM, Aldiss P & Morton NM (2021). The phospholipase A2 family's role in metabolic diseases: Focus on skeletal muscle. Physiological Reports; DOI: 10.14814/PHY2.14662.

3. Massart J, Sjögren RJO, Egan B, Garde C, Lindgren M, Gu W, Ferreira DMS, Katayama M, Ruas JL, Barrès R, O'Gorman DJ, Zierath JR & Krook A (2021). Endurance exercise training-responsive miR-19b-3p improves skeletal muscle glucose metabolism. Nature Communications 2021 12:1 12, 1–13. 4. Morton NM et al. (2016). Genetic identification of thiosulfate sulfurtransferase as an adipocyte-expressed anti-diabetic target in mice selected for leanness. Nat Med 22, 771–779.

C42

Iron-catalysed free radical formation underpins the systemic vasculopathic complications in chronic mountain sickness

Damian Miles Bailey[1], Marcel Culcasi[2], Teresa Filipponi[1], Julien Brugniaux[3], Benjamin Stacey[1], Christopher Marley[1], Rodrigo Soria[4], Stefano Rimoldi[4], David Cerny[4], Emrush Rexhaj[4], Lorenza Pratali[5], Carlos Salinas Salmòn[6], Carla Murillo Jáuregui[6], Mercedes Villena[6], Francisco Villafuerte[7], Antal Rockenbauer[8], Sylvia Pietri[2], Urs Scherrer[4], Claudio Sartori[9]

[1]University of South Wales, Glamorgan, United Kingdom, [2]Aix Marseille University, Marseille, France, [3]Grenoble Alpes University, Grenoble, France, [4]University Hospital Bern, Bern, Switzerland, [5]Institute of Clinical Physiology, Pisa, Italy, [6]Instituto Bolivano de Biologia de Altura, La Paz, Bolivia, Plurinational State of, [7]Universidad Peruana Cayetano Heredia, Lima, Peru, [8]Research Center for Natural Sciences, Budapest, Hungary, [9]University Hospital, Lausanne, Switzerland

Background: Chronic mountain sickness (CMS) is a high-altitude maladaptation syndrome that affects between 5-10 % of the world's estimated 140 million highlanders who permanently reside >2,500 meters above sea-level (Leon-Velarde et al. 2005). It is characterised by excessive erythrocytosis, severe hypoxaemia and elevated systemic oxidative-nitrosative stress (OXNOS) subsequent to a free radical-mediated reduction in vascular nitric oxide (NO) bioavailability (Bailey et al. 2013; Bailey et al. 2019). To better define underlying molecular mechanisms, dietary risk factors and vascular consequences, we compared healthy male lowlanders (80 m, n = 10) against age/sex-matched highlanders born and bred in La Paz, Bolivia (3,600 m) with (CMS+, n = 10) and without (CMS-, n = 10) clinically diagnosed CMS.

Methods: Ethical approval protocol was obtained from the Institutional Review Boards for Human Investigation at the University of San Andres, La Paz, Bolivia (CNB #52/04), Universidad Peruana Cayetano Heredia, Lima, Péru (#101686), University of Lausanne, Lausanne, Switzerland (#89/06, #94/10), and University of South Wales, Glamorgan, UK (#4/07), prior to registration in a clinical trials database (NCT01182792). Cephalic venous blood was assayed for systemic OXNOS using electron paramagnetic resonance spectroscopy and reductive ozone-based chemiluminescence (Bailey et al. 2019). Nutritional intake was assessed via dietary recall. Systemic vascular function and structure were assessed via flow-mediated dilatation, aortic pulse wave velocity and carotid intima-media thickness using duplex ultrasound and applanation tonometry. Following confirmation of distribution normality (Shapiro-Wilk *W* tests), data were analysed using one-way ANOVAs with post-hoc Bonferroni-corrected independent samples *t*-tests. Relationships between variables were assessed using Pearson Product Moment Correlations.

Results: Basal systemic OXNOS was permanently elevated in highlanders (P = <0.001 vs. lowlanders) and further exaggerated in CMS+, reflected by increased hydroxyl radical spin adduct formation (P = <0.001 vs. CMS-) subsequent to liberation of free 'catalytic' iron consistent with a Fenton and/or nucleophilic addition mechanism(s). This was accompanied by elevated global protein carbonylation (P = 0.046 vs. CMS-) and corresponding reduction in plasma nitrite (P = <0.001 vs. lowlanders). Dietary intake of vitamins C and E, carotene, magnesium and retinol were lower in highlanders and especially deficient in CMS+ due to reduced consumption of fruit and vegetables (P = <0.001 to 0.028 vs. lowlanders/CMS-). Systemic vascular function and structure

were also impaired in highlanders (P = <0.001 to 0.040 vs. lowlanders) with more marked dysfunction observed in CMS+ (P = 0.035 to 0.043 vs. CMS-) in direct proportion to systemic OXNOS (r = -0.692 to 0.595, P = <0.001 to 0.045).

Conclusions: Collectively, these findings suggest that lifelong exposure to iron-catalysed systemic OXNOS, compounded by a dietary deficiency of antioxidant micronutrients, likely contributes to the systemic vasculopathic complications and increased morbidity/mortality in CMS+.

Leon-Velarde F et al. (2005). High Alt Med Biol 6, 147-157. Bailey DM et al. (2013). Chest 143, 444-451. Bailey DM et al. (2019). J Physiol 597, 611-629.

C43

The role of neural input and microvascular blood flow as mediators of neuromuscular control

Eleanor Jones[1], Yuxiao Guo[1], Philip Atherton[1], Bethan Phillips[1], Mathew Piasecki[1]

[1]Centre of Metabolism and Ageing Physiology (COMAP), University of Nottingham, Derby, United Kingdom

Introduction
Force steadiness (FS), the ability to maintain a constant level of force output is known to progressively decrease during prolonged isometric contractions [1,2] which is partly mediated by the level of common synaptic input to motor units (MU). Ischemia, in which occlusion of the limb microvasculature reduces the delivery of oxygen and nutrients may also contribute to performance fatigue and reduced FS. However, the extent of the influence of each remains undefined. The aim of this study was to determine the effects of vastus lateralis (VL) neural input and microvascular blood flow on FS during a knee extensor fatiguing contraction.

Methods
Ten young volunteers (3 females; 30 ± 6 years) completed a 3-minute isometric leg extension at 30% maximum voluntary contraction (MVC), with data collected during the first and final 30-seconds (s) of the contraction. High-density surface electromyography (HD-sEMG) was used to identify individual MU potentials (MUPs) from the VL. FS was defined as the coefficient of variation (CoV) of force and compared between the first and final 30s of the contraction. Estimates of common synaptic inputs were made using the magnitude-squared coherence in the delta bandwidth (0–5 Hz) [3]. Microvascular blood volume (MBV) was determined from the plateau phase of a non-linear regression of echo acoustic intensity (AI) simultaneously recorded using contrast enhanced ultrasound (CEUS)[4]. Between time point data for all parameters was compared using paired t-tests with significance assumed as $p<0.05$.

Results
10.4±8.5 (Mean±SD) MUs per person were identified in the first 30s and 10.3±8.1 in the last 30s. CoV force increased from the first to the last 30s of the fatiguing contraction (CoV: 3.13±0.74 vs. 4.97±1.72%; p=0.005) as did MBV (AI: 6.66±0.72 vs. 7.72±1.50 au; p=0.004) but delta coherence (Z-score: 3.40±1.83 vs. 3.40±1.56; p=0.996) did not change.

Conclusion
As expected, FS decreased during an isometric contraction of the knee extensors with an increase in MBV also observed. However, no changes were observed in the common synaptic input to MUs. These findings suggest that during an isometric contraction muscle blood flow may have a greater influence on FS at the onset of fatigue than neural properties. These findings can translate into

understanding ways to improve athletic performance as well as ameliorating functional impairment in clinical populations therefore, further investigation is needed into the neurophysiological factors involved in maintaining force control during fatigue.

1. Enoka RM, Farina D. Force steadiness: From motor units to voluntary actions. Physiology. 2021;36: 114–130. doi:10.1152/physiol.00027.2020 2. Martinez-Valdes E, Negro F, Falla D, Dideriksen JL, Heckman CJ, Farina D. Inability to increase the neural drive to muscle is associated with task failure during submaximal contractions. J Neurophysiol. 2020;124: 1110–1121. doi:10.1152/jn.00447.2020 3. Alix-Fages C, Jiménez-Martínez P, de Oliveira DS, Möck S, Balsalobre-Fernández C, Del Vecchio A. Mental fatigue impairs physical performance but not the neural drive to the muscle: a preliminary analysis. Eur J Appl Physiol. 2023; 508212. doi:10.1007/s00421-023-05189-1 4. Mitchell WK, Phillips BE, Williams JP, Rankin D, Smith K, Lund JN, et al. Development of a new sonovueTM contrast-enhanced ultrasound approach reveals temporal and age-related features of muscle microvascular responses to feeding. Physiol Rep. 2013;1. doi:10.1002/phy2.119

C44

Influence of cardiorespiratory fitness on RPE and Playerload in simulated mixed martial arts bouts

Christopher Kirk[1], David Clark[2], Carl Langan-Evans[3]

[1]Sheffield Hallam University, Sheffield, United Kingdom, [2]Robert Gordon University, Aberdeen, United Kingdom, [3]Liverpool John Moores University, Liverpool, United Kingdom

Mixed martial arts (MMA) may potentially be classified as a high intensity aerobic endurance event (1). The influence of aerobic capacity ($\dot{V}O_2$max) on MMA performance is, however, currently unknown. The aim of this study was to compare the laboratory measured aerobic capacities of MMA participants to the external load, internal intensity and external intensity of MMA sparring bouts to examine the influence of aerobic fitness on performance. A cohort of n=10 male MMA participants (age = 24±2.8 years; mass = 74.3±8.2kg; stature = 176.8±7.9cm) completed a treadmill based graded exercise test (GXT) to measure their absolute ($L \cdot min^{-1}$) and relative ($ml \cdot kg \cdot min^{-1}$) $\dot{V}O_2$max. Participants also took part in a 3x5mins MMA sparring bout whilst equipped with a Catapult Optimeye S5 accelerometer which recorded Playerload (PLd_{ACC}) as external load and Playerload per minute ($PLd_{ACC} \cdot min^{-1}$) as external intensity(2) throughout. Sessional rating of perceive exertion (sRPE) was recorded as internal intensity at the end of each round(3). sRPE of each round was classified as low intensity (≤ 4AU); moderate intensity (5 – 6AU); high intensity (≥ 7AU) as applied previously(4). All data were collected following institutional ethical approval and informed consent. The cohort's mean $\dot{V}O_2$max = 53.1±5.9 $ml \cdot kg \cdot min^{-1}$. The cohort's median $\dot{V}O_2$max (53.3 $ml \cdot kg \cdot min^{-1}$) was used to split the cohort into top 50% and bottom 50% groups. Top 50% group $\dot{V}O_2$max = 57.7±3.6 $ml \cdot kg \cdot min^{-1}$; 4.1±0.5 $L \cdot min^{-1}$. Bottom 50% group $\dot{V}O_2$max = 48.5±3.6 $ml \cdot kg \cdot min^{-1}$; 3.8±0.4 $L \cdot min^{-1}$. Bayesian repeated measures ANOVA ($BF_{10} \geq 3$) were used to determine any differences in external/internal intensity between groups, between rounds, and between minutes(5). All analyses were completed using JASP 0.18.3 (JASP Team, NETHERLANDS). Round*group differences in sRPE were found to be decisive with a large effect (BF_{10} = 143, ω^2 = 0.15) (Figure 1). The top 50% group were found to maintain moderate sRPE throughout sparring (round 1 = 5.2±1.3AU; round 2 = 5.6±1.3AU; round 3 = 6.4±1.9AU). The bottom 50% group's sRPE moved from moderate in round 1 (4.6±1.1AU) and round 2 (6.8±1.3AU) to high in round 3 (8.6±1.1AU). Whilst the top 50% group recorded greater PLd_{ACC} and $PLd_{ACC} \cdot min^{-1}$ than the bottom 50% group in each round, these differences were not statistically relevant between groups or rounds. When analysing PLd_{ACC} there was a moderate minute*group difference with a medium effect (BF_{10} = 3, ω^2 = .11). Resulting post hoc between groups differences were decisive with a medium effect (BF_{10} = 380, ω^2 = .12) with the top 50% group recording greater PLd_{ACC} for most of rounds 1 and 2, and displaying an 'end spurt' in round 3 (Figure 2). These results indicate having a $\dot{V}O_2$max <53 $ml \cdot kg \cdot min^{-1}$ is related to increased internal intensity in MMA sparring. Participants with $\dot{V}O_2$max above this appeared capable of maintaining greater and qualitatively more consistent external intensity throughout the first and second rounds of sparring. These data support the aerobic nature of MMA and may provide minimum aerobic fitness levels to aim for during competition preparation.

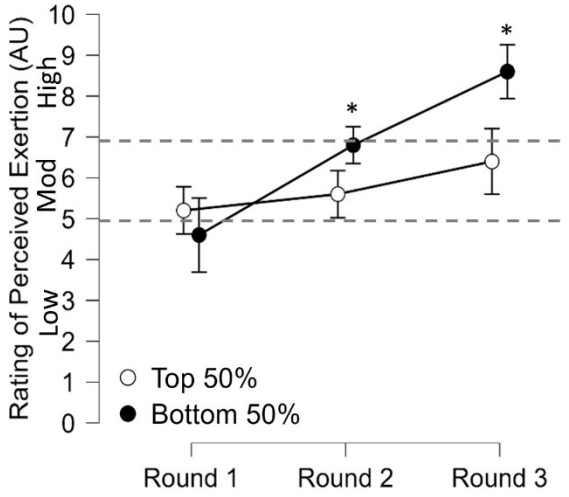

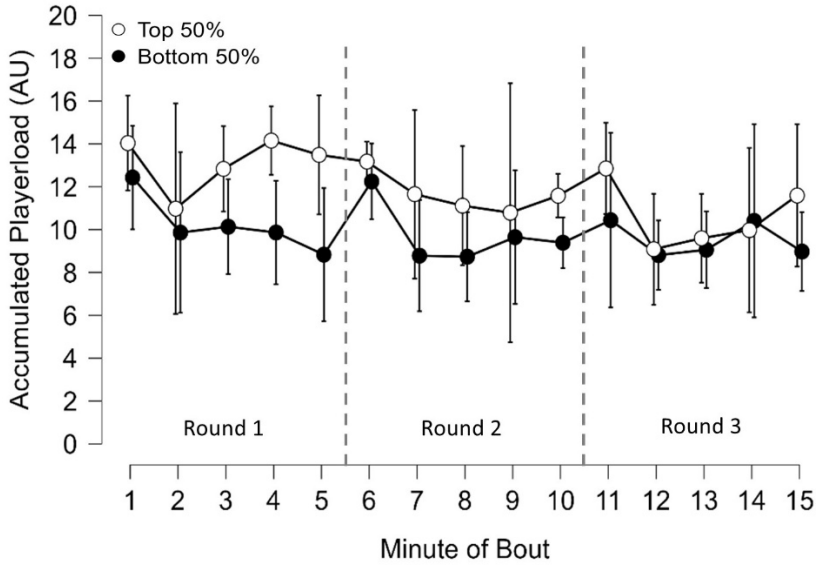

1. Draper N, Marshall H. High-intensity aerobic endurance sports. In: Draper, Nick and Marshall, Helen, editor. Exercise Physiology for Health and Sports Performance. New York: Routledge; 2013. p. 322 – 350. 2. McLean BD, Cummins C, Conlan G, Duthie G, Coutts AJ. The fit matters: influence of accelerometer fitting and training drill demands on load measures in rugby league players. Int J Sports Physiol Perform. Human Kinetics; 2018;13(8):1083–9. 3. Kirk C, Langan-Evans C, Clark D, Morton J. The relationships between external and internal training loads in mixed martial arts. Int J Sports Physiol Perform. 2024; 4. Kirk C, Langan-Evans C, Clark D, Morton J. Quantification of training load distribution in mixed martial arts athletes: A lack of periodisation and load management. PLoS One. 2021;16(5). 5. Van Doorn J, van den Bergh D, Bohm U, Dablander F, Derks K, Draws T, et al. The JASP Guidelines for Conducting and Reporting a Bayesian Analysis. PsyArXiv; 2019;

C45

Metformin inhibits glucose-uptake regulating transcription factor NR4A3 expression after exercise.

Brenda J. Peña Carrillo[1], Rasmus Kjøbsted[2], Jonas M Kristensen[2], Jørgen F.P. Wojtaszewski[2], Brendan M. Gabriel[1]

[1]University of Aberdeen, Aberdeen, United Kingdom, [2]August Krogh section for molecular physiology, Institute for Nutrition, Exercise and Sports, University of Copenhagen, Copenhagen, Denmark

Metformin is the most prescribed initial anti-hyperglycaemic medication for people with Type 2 Diabetes. Exercise also has many beneficial health effects and is often recommended concomitantly. Although exercise also improves glycaemia, this effect is inhibited when undertaken alongside metformin ingestion [1,2]. Metformin intake also appears to further inhibit the beneficial response to exercise, including ablating improvements in insulin sensitivity and skeletal muscle mitochondrial protein synthesis and respiration [3,4]. Therefore, we propose that the skeletal muscle transcriptional response to exercise is disrupted by metformin. In this study, we hypothesise that metformin alters the transcriptomic response to exercise, and that this plays a role in the metformin inhibition of the beneficial exercise response. To test this, we analysed skeletal muscle biopsies from a previous study [5]. In this study, seven healthy lean male participants completed one bout of single-leg exercise with a contralateral non-exercising control-leg after acute metformin/placebo supplementation in a crossover design. After an overnight fast, muscle biopsies from the vastus lateralis were obtained in both legs after 1 hr of rest. Thereafter, 1.5 g metformin/placebo was ingested together with a standardized breakfast, the following 4½ hr were spent lying on a bed, after 2 hr a second metformin dose of 1.5 g metformin/placebo was ingested, at 4½ hr a second needle biopsy in both legs was taken. Immediately after this, the participant performed one-legged knee extensor exercise for 40 min with an intensity of 80% PWL (peak work-load) and a third biopsy was taken from both legs. RNA sequencing analysis was performed on biopsy samples from the rest and exercised leg from metformin/placebo groups, after 1 hr of rest, after 4½ hr (after metformin/placebo supplementation), and after exercise. This analysis revealed that metformin supplementation inhibited the transcriptomic response to exercise by reducing the total number of differentially expressed genes in response to exercise. After exercise, 81 genes were upregulated in response to exercise in both the metformin and placebo trials. 53 genes were uniquely upregulated in the placebo trial, while only 17 genes were uniquely upregulated in the Metformin trial. Importantly, the transcription factor NR4A3 was upregulated in response to exercise during the placebo trial (adj.p=0.011), but not when participants consumed metformin (adj.p=0.234). In HSMM (Human skeletal muscle myotubes), metformin (10μM) did not change *NR4A3* expression (RT-qPCR, 1.2-fold-change, p=0.536) compared to the control. As expected, the exercise mimetic Ionomycin (8μM) significantly increased *NR4A3* expression (4.3-fold-change, p<0.001), while concomitant metformin incubation significantly reduced the relative *NR4A3* response (2.4-fold-change, p=0.002). In summary, we propose that the *NR4A3* response to exercise is inhibited by metformin and that this may be a mechanism inhibiting exercise training-induced adaptations and skeletal muscle insulin sensitisation during metformin treatment.

1. Boulé NG, et al. (2011) Metformin and exercise in type 2 diabetes: examining treatment modality interactions. Diabetes Care 34(7):1469–1474. https://doi.org/10.2337/DC10-2207. 2. Peña Carrillo, BJ, et al. (2024). Morning exercise and pre-breakfast metformin interact to reduce glycaemia in people with Type 2 Diabetes: a randomized crossover trial. MedRxiv 2023-09. https://doi.org/10.1101/2023.09.07.23295059. 3. Das S, et al. (2018) Effect of metformin on exercise capacity: A meta-analysis. Diabetes Res Clin Pr 144:270–278. https://doi.org/10.1016/j.diabres.2018.08.022. 4. Konopka AR, et al. (2019) Metformin inhibits mitochondrial adaptations to aerobic exercise training in older adults. Aging Cell 18(1):e12880. https://doi.org/10.1111/acel.12880. 5. Kristensen JM, et al. (2019) Metformin does not compromise energy status in human skeletal muscle at rest or during acute exercise: A randomised, crossover trial. Physiol Rep 7(23). https://doi.org/10.14814/phy2.14307.

C46

Insights into the Transforming Growth Factor superfamily specific modulation: unravelling the impact of hibernating bear serum in primary human muscle cells

Chloé Richard[1], Guillaume Fourneaux[1], Alexandre Geffroy[2], Gwendal Cueff[1], Christophe Tatout[3], Alina L Evans[4], Jonas Kindberg[5], Guillemette Gauquelin-Koch[6], Etienne Lefai[1], Fabrice Bertile[2], Lydie Combaret[1]

[1]Université Clermont Auvergne, INRAE, Unité de Nutrition Humaine, UMR 1019, Clermont-Ferrand, France, [2]Université de Strasbourg, CNRS, IPHC UMR 7178, Strasbourg, France, [3]Université Clermont Auvergne, CNRS, Inserm, iGReD, Clermont-Ferrand, France, [4]Department of Forestry and Wildlife Management, Inland Norway University of Applied Sciences, Campus Evenstad, NO-2480, Koppang, Norway, [5]Norwegian Institute for Nature Research (NINA), Trondheim, Norway, [6]Centre National d'Etudes Spatiales, CNES, 75001, Paris, France

Muscle atrophy observed in several physio-pathological situations has harmful consequences for the patients and results from an imbalance between protein synthesis and proteolysis. Despite a thorough understanding of molecular events involved in muscle atrophy, primarily through using rodent and human models, no proven effective treatment exists to date (1). In our group, we use the brown bear model, which does not display muscle atrophy during hibernation, although prolonged fasting and physical inactivity. This muscle atrophy resistance is correlated with inhibition of the pro-atrophic TGF-β (Transforming Growth Factor) signalling and maintenance of the hypertrophic BMP (Bone Morphogenetic Protein) signalling (2). We also showed that winter-hibernating bear serum (WBS) induces hypertrophy in human myotubes (3).

The study aimed to further investigate WBS effects on human myotubes by analysing transcriptome changes (mRNA sequencing) after 48h cultivation with 5% SBS (summer-active bear serum) or WBS (n=3, DESEQ2 analysis). Subsequently, we selected some differentially expressed genes (DEGs) identified above within the BMP pathway and analysed their protein levels (n=8-9, ratio paired t-test). Finally, we investigated the impact of bear serum on human myotubes response (n=6) to increasing doses of BMP7 (0 to 2µg/ml) or TGF-β 3(0 to 100ng/ml) for 30 min. We thus analyzed SMAD3 or SMAD1/5 phosphorylation, indicative of TGF-β or BMP pathway activation, respectively (2-way ANOVA). Data are means +/-SEM and statistical significance threshold was set at 0.05.

We identified 352 DEGs in human myotubes cultivated with WBS versus SBS. Gene Ontology analysis revealed enrichment in pathways related to muscle function, extracellular matrix remodelling and regulation of BMP signalling. Specifically, mRNA levels for several BMP signalling inhibitors (*SMAD6*, *CHRDL2*, *GREM1/2*) and activators (*ENG*, *SCUBE3*) decreased by 20-58% in WBS compared to SBS conditions. In addition, several BMP-regulated genes were also downregulated by 40-70% in WBS (*ID1*, *ID3*, *SMAD6, SAMD11*). We further report here that ENG and GREM1 protein levels were also downregulated by 18-37% in WBS versus SBS conditions. We showed that BMP7 treatment induces dose-dependent SMAD1/5 phosphorylation in human myotubes, beginning at 0.1µg/ml in SBS conditions and 0.5µg/ml in WBS. The maximal induction was nevertheless identical in both conditions. Similarly, the response of human myotubes to TGF-β3 treatment was also lower in WBS conditions compared to SBS conditions. SMAD3

phosphorylation showed a dose-dependent increase, starting at 1ng/ml in SBS and 10 ng/ml in WBS. By contrast to the BMP challenge, the induction remained consistently lower across all concentrations, including the higher one (100ng/ml).

Overall, we show a transcriptomic reprogramming of human myotubes cultivated with WBS, including BMP signalling pathway regulation. The reduced responsiveness of both TGFb and BMP pathways to their ligands in the presence of WBS aligns with the hypometabolism previously reported in these myotubes (3) or hibernating brown bear muscle (4). Conversely, the lower induction of TGFβ signalling for all concentrations, contrasted with the consistent plateau of BMP induction at high doses, suggests that WBS may modulate the TGFβ/BMP balance towards the BMP pathway. These data are consistent with the specific TGF-β/BMP balance depicted in atrophy-resistant muscles from the hibernating brown bear (2).

(1) Peris-Moreno et al. Ubiquitin Ligases at the Heart of Skeletal Muscle Atrophy Control. Molecules. 2021 Jan 14;26(2):407. doi: 10.3390/molecules26020407. (2) Cussonneau et al. Concurrent BMP Signaling Maintenance and TGF-β Signaling Inhibition Is a Hallmark of Natural Resistance to Muscle Atrophy in the Hibernating Bear. Cells. 2021. 10(8):1873. doi: 10.3390/cells10081873. (3) Chanon et al. Proteolysis inhibition by hibernating bear serum leads to increased protein content in human muscle cells. Sci Rep. 2018. 8(1):5525. doi: 10.1038/s41598-018-23891-5. (4) Chazarin et al. Metabolic reprogramming involving glycolysis in the hibernating brown bear skeletal muscle. Front Zool. 2019 May 6;16:12. doi: 10.1186/s12983-019-0312-2.

C47

The Role of Extracellular Matrix Components in Determining Skeletal Muscle Fiber Types: An Investigation with C2C12 Myoblasts

Yhusi Karina Riskawati[1,3], Hsi Chang[2], Chuang-Yu Lin[4]

[1]International PhD Program for Cell Therapy and Regenerative Medicine, College of Medicine, Taipei Medical University, Taipei, Taiwan, Province of China, [2]Department of Pediatrics, School of Medicine, College of Medicine, Taipei Medical University, Taipei, Taiwan, Province of China, [3]Physiology Department, Faculty of Medicine, Universitas Brawijaya, Malang, Indonesia, [4]Department of Biomedical Science and Environmental Biology, Kaohsiung Medical University, Kaohsiung, Taiwan, Province of China

Introduction Muscle functionality and adaptability depend on the precise specification of muscle fiber types, a process that directly influences contraction dynamics and overall performance. While the critical role of extracellular matrix (ECM) components in muscle development is recognized, the specific mechanisms through which ECM influences the differentiation of myoblasts into distinct muscle fiber types remain inadequately explored. This gap in knowledge, particularly regarding how different ECM cues guide the activation of myogenic regulatory factors (MRFs) and mediate fiber type-specific transitions, limits our understanding of muscle physiology and the development of targeted therapeutic interventions. Addressing this gap, our study delves into the modulation of C2C12 myoblast differentiation by ECM components present in Matrigel™, aiming to elucidate the intricate processes of muscle contraction regulation and fiber type specification. Through this investigation, we seek to contribute to the broader comprehension of muscle tissue engineering and the potential for ECM-based strategies in regenerative medicine.

Method C2C12-GFP myoblasts were differentiated on a Matrigel™ substrate, enabling the assessment of myotube formation. The expression patterns of key MRFs were evaluated via quantitative PCR (qPCR), while the expression of myosin heavy chain (MyHC) genes and proteins, indicative of fast and slow skeletal muscle fibers, was analyzed using Western blotting and immunocytochemistry. RNA sequencing was employed to dissect the signaling pathways and gene expression profiles underlying muscle fiber type differentiation in response to ECM cues.

Results Observations from Day 7 post-differentiation highlighted a pronounced shift towards fast-type myotube predominance, with decreased Pax7 and increased Myogenin expressions reflecting advanced differentiation stages. This trend was validated through Western blot and immunofluorescence analyses, revealing an altered expression ratio favoring fast-type over slow-type myotube proteins. qPCR analysis corroborated these findings, demonstrating upregulation of the MYH4 gene and downregulation of MYH7, alongside modulations in HIF-1α and PGC-1α levels. RNA sequencing analysis utilizing Gene Ontology (GO) and the Kyoto Encyclopedia of Genes and Genomes (KEGG) databases to analyze differentially expressed genes (DEGs), revealed a gene expression profile distinct from controls, with pathway analyses emphasizing activity within specific pathways such as C5 isoprenoid biosynthesis and inositol phosphate metabolism. Central genes to these pathways, including Cenpf, Brca1, and Nek2, were pinpointed as potential targets for modulating muscle fiber type differentiation.

Conclusions The ECM components in Matrigel™ play a significant role in steering C2C12 myoblast differentiation towards specific muscle fiber types, with significant implications for muscle contraction and overall muscle health. Our study enhances the understanding of the molecular landscape governing muscle fiber specificity and opens avenues for targeted strategies in muscle repair and regeneration. By elucidating the mechanisms through which ECM influences muscle cell fate, we contribute to the broader knowledge base in muscle physiology, offering insights into optimizing muscle function and combating muscle-related diseases.

1. Hoppeler, H., Molecular networks in skeletal muscle plasticity. Journal of Experimental Biology, 2016. 219(2): p. 205-213. 2. Oskolkov, N., et al., High-throughput muscle fiber typing from RNA sequencing data. Skelet Muscle, 2022. 12(1): p. 16. 3. Zhang, W., Y. Liu, and H. Zhang, Extracellular matrix: an important regulator of cell functions and skeletal muscle development. Cell & Bioscience, 2021. 11(1): p. 65. 4. Yasuda, T., et al., Mitochondrial dynamics define muscle fiber type by modulating cellular metabolic pathways. Cell Reports, 2023. 42(5): p. 112434. 5. Grefte, S., et al., Matrigel, but not collagen I, maintains the differentiation capacity of muscle derived cells in vitro. Biomedical Materials, 2012. 7(5): p. 055004.

C48

Retinal cone-driven responses to flickering stimuli recorded from over 2000 adults: associations with age, sex and ethnicity

Muhammad Hamza Ahmed[1], Xiaofan Jiang[1,2,3], Isabelle Chow[2,3], Diana Kozareva[2,3], Pirro Hysi[2,3], Christopher Hammond[2,3], Omar Mahroo[1,2,3]

[1]Institute of Ophthalmology, University College London, London, United Kingdom, [2]Department of Twin Research and Genetic Epidemiology, King's College London, London, United Kingdom, [3]Section of Ophthalmology, King's College London, St Thomas' Hospital Campus, London, United Kingdom

Purpose

The peak time of the electroretinogram (ERG) response to flicker is a sensitive measure of human panretinal cone system function in health and disease. Here, we analysed responses in over 2000 healthy adult twins, with the aim of exploring associations with age, sex and ethnicity.

Methods

Participants were recruited from the TwinsUK cohort and underwent non-mydriatic light-adapted ERG recordings using a portable device (RETeval system, LKC Technologies) in conjunction with specialised skin electrodes. The study had Research Ethics Committee approval and conformed to the tenets of the Declaration of Helsinki. The device delivered white full-field flickering stimuli (28.3 Hz) on a white background. Pupil diameter was automatically measured and adjusted for, such that the retinal illuminance of stimuli (85 Td.s) and background (850 Td) were equivalent to that delivered by international standard stimuli through a dilated pupil. Flicker ERG peak times were averaged across both eyes for each participant. Participants were excluded where reliable recordings were unavailable from either eye or if the interocular difference in peak time exceeded 2 ms. When both members of a twin pair were included, peak times were averaged for both twins (to avoid confounding due to intrapair correlation). Correlation with age was quantified and comparisons (age-adjusted where appropriate) were made between sexes and ethnicities.

Results

Recordings were analysed from 2395 participants (83% female, 94% of white ethnicity), including 852 full twin pairs. Mean (SD) age was 55.7 (16.3) years; median age was 60. Mean (SD) flicker ERG peak time was 25.6 (1.2) ms; the median was 25.4 ms. Peak times showed a highly significant ($p<0.0001$) positive correlation with age; the Spearman correlation coefficient was 0.52. The relationship with age was non-linear, such that the increase in peak time per year was greater for older age groups. Male and female participants had similar mean ages, and the difference between averaged peak times across sexes was not significant ($p=0.059$). Where ethnicity was recorded,

806 pairs identified as white, 14 pairs as black, and 12 pairs as Asian. Age-adjusted comparisons revealed the following significant differences: compared with black participants mean peak time was shorter for white participants (p=0.000086) and shorter for Asian participants (p=0.0097). Other comparisons did not reach significance.

Conclusions

The highly significant association between ERG flicker peak times and age suggests possible slowing of retinal processing with age. The relationship was not linear. We also found a difference between ethnicities that invites further investigation, and suggests potential importance of development of ethnicity-specific reference ranges.

C49

The impact of fatiguing exercise on corticospinal function in relapse-remitting multiple sclerosis

Gemma Brownbill[1], Jeanne Dekerle[2], Mara Cercignani[3], James Stone[1]

[1]Brighton and Sussex Medical School, Brighton, United Kingdom, [2]Brighton University, Brighton, United Kingdom, [3]Cardiff University, Cardiff, United Kingdom

Background: Multiple sclerosis (MS) is an autoimmune demyelinating disease that disrupts corticospinal functioning. Transcranial magnetic stimulation (TMS) of the motor cortex allows assessment of both corticospinal excitability, inhibition, and conduction time via recordings of motor evoked potentials (MEPs) and silent periods (SPs), respectively. A change indicates a central origin of neuromuscular fatigue. Research has shown that corticospinal integrity is impaired at rest in MS. This study investigated how sustained isometric exercises of the wrist extensors affects corticospinal responses in people with relapsing-remitting MS compared to healthy controls.

Methods: 22 people with relapse-remitting MS (3 males; Expanded Disability Status Scale < 3.5) and 22 healthy matched controls (CG) performed an all-out 3-minute effort, and 8 minutes later, a 5-minute submaximal effort (17.2 ± 6.6 % Maximal Voluntary Contraction (MVC)). Active motor threshold (AMT) was quantified as the minimum stimulator output to evoke 3/6 MEP > 0.5mV at 20% MVC. Ten single-pulse TMS (120% AMT) were delivered to the primary motor cortex during a 10% MVC, before the 3-minute all-out effort, immediately after, and 9 minutes following the 5-minute submaximal exercise bout. Surface electromyography was recorded from the extensor carpi radialis longus (ECRL) and extensor carpi radialis brevis (ECRB) muscles. MEP amplitude, latency, and silent period (SP were measured for each MEP. Student t-tests and linear mixed models were used to assess group, time, and interaction effects. Critical *p* value was set at 0.05. Ethical approval was obtained by the Health Research Authority (IRAS: 260176).

Results: AMT was significantly higher in the MS group (MS: 55 ± 10 % of maximum stimulator output (MSO); CG: 47 ± 8 % of MSO ($t_{(21)}$ = -3.66, p = .001). Averages and standard deviations for both groups at each time point for all variables can be viewed in Table 1. A significant effect of time was found for ECRB SP only ($F_{(2, 70.7)}$ = 3.77, p = .02). MEP latency and SP were overall longer and absolute ECRB MEP amplitude smaller for the MS group (ECRL latency: $F_{(1, 29.3)}$ = 8.51, p = .007; ECRL SP: $F_{(1, 20.3)}$ = 4.67, p = .04; ECRB latency: $F_{(1, 37.6)}$ = 6.79, p = .01; ECRB SP: $F_{(1, 24.2)}$ = 7.08, p = .01; ECRB MEP amplitude: $F_{(1, 36.7)}$ = 7.82, p = .01). No group x time interactions were observed (p > .05).

Conclusion: These findings support the notion of impaired corticospinal function in MS, as evidenced by the higher AMT, longer SP, delayed MEP latencies and smaller MEP amplitudes in the MS group both at rest and following exercise of the wrist extensors. Exercise did not induce changes in corticospinal excitability or inhibition exclusive to the MS group.

Table 1. Mean ± standard deviation for motor evoked potential (MEP) amplitude, silent period (SP) and latency for the extensor capri radialis longus (ECRL) and extensor capri radialis brevis (ECRB).

Dependent variable	Muscle	Group	Pre-exercise	Post-exercise	Post-recovery
MEP amplitude (mV)	ECRL	CG (n = 22)	1.48 ± 1.02	1.56 ± 1.07	1.49 ± 1.04
		MS (n = 20)	0.95 ± 0.57	1.16 ± 0.71	1.16 ± 0.54
	ECRB	CG (n = 22)	1.87 ± 1.07	2.14 ± 1.21	1.99 ± 0.98
		MS (n = 20)	1.12 ± 0.53	1.32 ± 0.64	1.46 ± 0.70
MEP SP (ms)	ECRL	CG (n = 20)	139 ± 17.4	136 ± 21.9	131 ± 21.6
		MS (n = 16)	159 ± 43.5	161 ± 48.7	154 ± 30.0
	ECRB	CG (n = 21)	137 ± 20.0	136 ± 20.6	129 ± 21.4
		MS (n = 18)	163 ± 37.1	164 ± 51.9	157 ± 32.0
MEP latency (ms)	ECRL	CG (n = 22)	14.1 ± 1.2	14.3 ± 1.3	14.1 ± 1.3
		MS (n = 22)	16.2 ± 2.7	16.1 ± 3.0	15.8 ± 2.6
	ECRB	CG (n = 22)	14.5 ± 1.7	14.6 ± 1.8	14.5 ± 2.0
		MS (n = 21)	16.3 ± 2.3	16.3 ± 2.7	16.3 ± 2.7

C50

The Human Taste Code

Göran Hellekant[5,6]

[1]University of Wisconsin-Madison School of Veterinary Medicine Department of Biomedical Sciences 1656 Linden Drive Madison, WI 53706, USA Retired Professor University of Minnesota Duluth Campus School of Medicine Department of Biomedical Sciences 1035 University Drive Duluth, MN 55812, USA Guest Senior Professor Swedish University of Agricultural Sciences School of Veterinary Medicine Department of Animal Breeding and Genetics Uppsala, Sweden, Madison WI, United States, [2]Swedish University of Agricultural Sciences School of Veterinary Medicine Department of Animal Breeding and Genetics Uppsala, Sweden Guest Senior Professor Swedish University of Agricultural Sciences School of Veterinary Medicine Department of Animal Breeding and Genetics Uppsala, Sweden, Uppsala, Sweden, [3]University of Wisconsin-Madison, Madison, United States, [4]Swedish University of Agricultural Sciences, Uppsala, Sweden, [5]University of Wisconsin-Madison, Madison, United States, [6]Swedish University of Agricultural Sciences, Uppsala, Sweden

Background: Since antiquity human taste has been divided into 4-5 taste qualities. However, responses in taste fibers of other animal species have only partly clustered according to human qualities. We realized taste qualities vary according to phylogeny, where species closer to humans show higher fidelity to human taste qualities.

Methods/Results: We compared psychophysical data and taste nerve recording from humans to behavioral tests and single taste fiber recordings in chimpanzee, rhesus and marmoset. Our data show how, with phylogenetic closeness to humans, taste fibers responded more exclusively to taste stimuli within each human taste quality. We then used the human sweet taste modifiers, miraculin and gymnemic acid. In human, miraculin adds sweet to sour taste and doubles nerve responses to acids. After miraculin nonhuman primates also doubled acid intake while both acid-specific and sweet-specific single taste fibers responded to acids. In human gymnemic acid eliminates sweet quality. In chimpanzee gymnemic acid abolished taste fiber responses to sweet without affecting responses to other tastes.

Analytical and statistical tools: Clusters of taste fibers in both CT and NG were identified with hierarchical cluster analysis. Responses to all stimuli were taken into consideration and the analysis considers each stimulus as an independent variable and a Pearson correlation coefficient is calculated between the responses. The results of hierarchical cluster analysis were presented as a Dendrogram. Multidimensional Scaling presented the single fiber results in a multidimensional space for further analyses.

The animal research was conducted in accordance with the principle and guidelines established by the Association for the Assessment and Accreditation of Laboratory Animal Care International (AAALAC) and procedures were approved by the local Institutional Animal Care and Use Committee (IACUC) from the University of Wisconsin-Madison, WI, USA (marmoset and rhesus monkey) and Laboratory for Experimental Medicine and Surgery in Primates, New York Medical Center, NY, USA. (chimpanzee).

Conclusions: Information from each type of taste receptor cell reaches a specific cortical taste area where it gives rise to taste qualities; taste is created in the cortical region where taste fibers deliver action potentials, thus satisfying the criteria of labeled-line coding which follows Mueller's law of specific nerve energy for pain, touch, and temperature where sensation is created in the cortex after conveyance by sensory fibers. In humans these cortical areas give rise to the taste qualities, sweet, sour, bitter, salt and umami. It is likely that this principle applies to other mammals, but their taste qualities differ due to species differences in taste receptor structure.

Hellekant G, Ninomiya Y, Danilova V: Taste in chimpanzees II: single chorda tympani fibers. Physiol Behav 1997, 61(6):829-841. Hellekant G, Ninomiya Y, Danilova V: Taste in chimpanzees III: Labeled line coding in sweet taste. Physiol Behav 1998, 65(2):191-200. Lee H, Macpherson LJ, Parada CA, Zuker CS, Ryba NJP: Rewiring the taste system. Nature 2017, 548(7667):330-333.

C51

Chronic vagus nerve stimulation reduces muscle sympathetic nerve activity in drug-resistant epilepsy

Mikaela Patros[1], Shobi Sivathamboo[1], Hugh Simpson[1], Terence J O'Brien[1], Vaughan G Macefield[1]

[1]Department of Neuroscience, School of Translational Medicine, Monash University, Melbourne, Australia

Background:

Vagus Nerve Stimulation (VNS), delivered via surgically implanted cuff electrodes on the left cervical vagus, is used to treat drug-resistant epilepsy (DRE). VNS is believed to act on the brain to reduce seizures by chronic neuromodulation, but it is not known what effects it has on other systems, including the sympathetic nervous system. Here we tested the hypothesis that chronic VNS reduces muscle sympathetic nerve activity (MSNA).

Methods:

Nineteen patients between the ages of 18-66 years with a diagnosis of DRE were recruited from the Alfred Health epilepsy clinics. Spontaneous bursts of MSNA were recorded via a tungsten microelectrode inserted percutaneously into a muscle fascicle of the common peroneal nerve. MSNA recordings were obtained from 11 DRE patients with implanted VNS devices who had been stimulated chronically (>6 months stimulation) and 8 DRE patients yet to receive a VNS implant. Baseline recordings were obtained in existing VNS patients, lying supine with their VNS device stimulating at their clinically set parameters (1.125-3.5 mA, 20 Hz, 250μs, duty cycle 10%-35%).

Results:

Patients without VNS (n=8) had a mean of 26.6 ± 9.5 (SD) bursts/min at rest, while those treated with VNS (n=11) had a mean of 13.1 ± 7.9 SD bursts/min, measured between trains of VNS. Although VNS did not appear to affect MSNA acutely, MSNA was significantly lower in patients following chronic VNS (p=0.0017).

Conclusions:

While VNS appeared to have no acute effects on MSNA at rest, nor during manouevres that increase MSNA, such as passive head-up tilt, MSNA was reduced in patients with chronic VNS treatment compared to those without. Chronic VNS treatment may have a protective effect on cardiovascular risk by reducing sympathetic activity. This may contribute to the mechanism behind risk-reduction for sudden unexplained death in epilepsy (SUDEP) in VNS-treated patients (Ryvlin et al., 2018).

Ryvlin P, So EL, Gordon CM, Hesdorffer DC, Sperling MR, Devinsky O, Bunker MT, Olin B, Friedman D. Long-term surveillance of SUDEP in drug-resistant epilepsy patients treated with VNS therapy. Epilepsia. 2018; 59: 562-572.

C52

The loss of Ca2+ -activated Cl- channel, TMEM16A worsens the ischemic stroke-reperfusion outcome

Elizaveta Melnikova[1], Ida Damsgaard Larsen[1], Line Mathilde Brostrup Hansen[1], Dmitry Postnov[2], Christian Aalkjær[1], Vladimir Matchkov[1]

[1]Aarhus University, Aarhus, Denmark, [2]Department of Clinical Medicine - Center of Functionally Integrative Neuroscience (CFIN), Aarhus, Denmark

The brain is the most active and highly metabolically demanding organ (1). Oxygen delivery is carried out through strictly controlled cerebral perfusion via local redistribution of blood flow under variations in neuronal activity. There is an intimate relationship between cerebral vasculature and neuronal tissue, where changes in local perfusion affect supplied cells and vice versa, glia and neurons influence adjacent blood flow (2). Anoctamin-1 (TMEM16A) belongs to the family of Ca^{2+}-activated Cl^- channels (3) and is suggested to act as a central regulator of neuromodulation. Tmem16A is activated by intracellular Ca^{2+}ions, leading to Cl^- influx and subsequent depolarization of smooth muscle cells (3). This enables an amplification loop for voltage-dependent Ca^{2+}-influx and cerebrovascular contraction. This reinforces the idea of TMEM16A implication for ischemic stroke outcome. Ischemic Stroke is caused by a rapid loss of blood supply to a part of the brain due to thromboembolic occlusion in cerebral circulation (4). Understanding the mechanisms contributing to the harmful action of stroke reperfusion is of great importance for new treatment paradigms to improve stroke survival and outcome.

We aim to evaluate the importance of cerebrovascular TMEM16A for neuroprotection during ischemic stroke.

Procedures were performed according to the guidelines from Directive 2010/63/EU of the European Parliament on the protection of animals used for scientific purposes and approved by the Animal Experiments Inspectorate of the Danish Ministry of Environment and Food.

We used 3.5-6 months old, smooth-muscle-specific conditional TMEM16A knockout (KO) male mice. Mice expressed TMEM16A gene floxed around exon7 and Cre recombinase with estrogen receptor type 2 under control of smooth muscle myosin heavy chain promoter. Age-matched male mice expressing Cre only were used as a control. All mice were treated with tamoxifen injections to induce smooth-muscle-specific knockout. Cerebral blood flow was assessed with Laser Speckle Contrast Imaging. Ischemic stroke was induced with a transient middle cerebral artery occlusion (tMCAO) for 60 min in mice anesthetized with isoflurane. Stroke severity was analyzed with post-mortal 2,3,5-triphenyltetrazolium (TTC) staining.

tMCAO reduced blood flow in the ipsilateral hemisphere for both KO (n=7-8) and controls (n=8;p<0.05; *fig*.1a), with TMEM16A KO mice having an attenuated flow reduction (< 80% compared to the controls (p >0.01; *fig*.1a). No difference between KO and control mice in brain perfusion was observed 24 hours after reperfusion (p <0.05; *fig*.1a). When blood flow changes during MCA occlusion were analyzed in detail, a larger area of severe blood flow drop (<80%) was

seen in TMEM16A KO mice over the occlusion period (p >0.01)(f*ig*.1a). TTC staining suggested a larger infarct volume in KO (n=7) than in control mice (n=7-8; p=0.125; f*ig*.2).

We found that smooth muscle-specific knockout of TMEM16A worsens ischemic stroke-reperfusion outcomes in mice. We suggest this occurs due to diminished cerebral blood flow control in TMEM16A knockout mice and their abnormal vascular tone. This proposes that under ischemic conditions, when there is an imbalance in ion concentrations, TMEM16A is an important component for vascular tone optimization. Our results indicate that TMEM16A may be a potential pharmacological target in improving stroke outcomes.

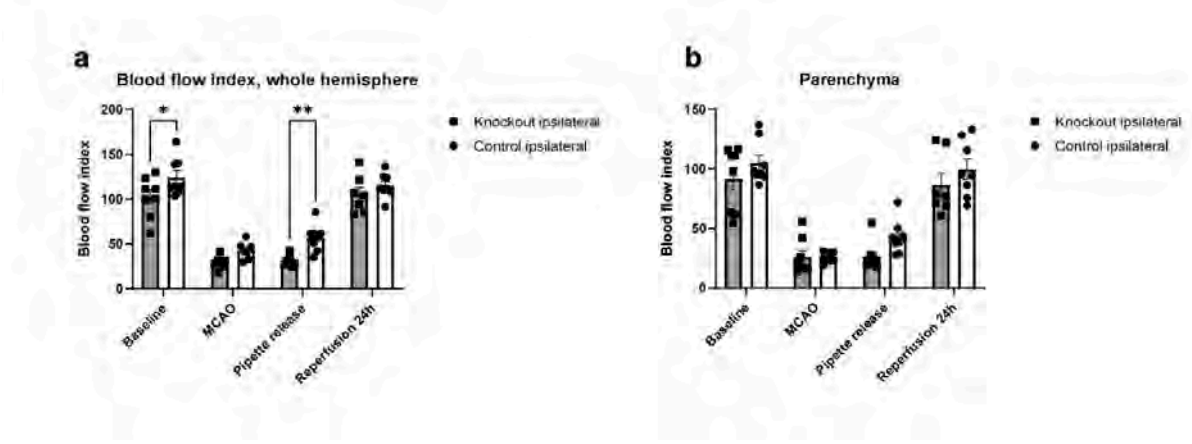

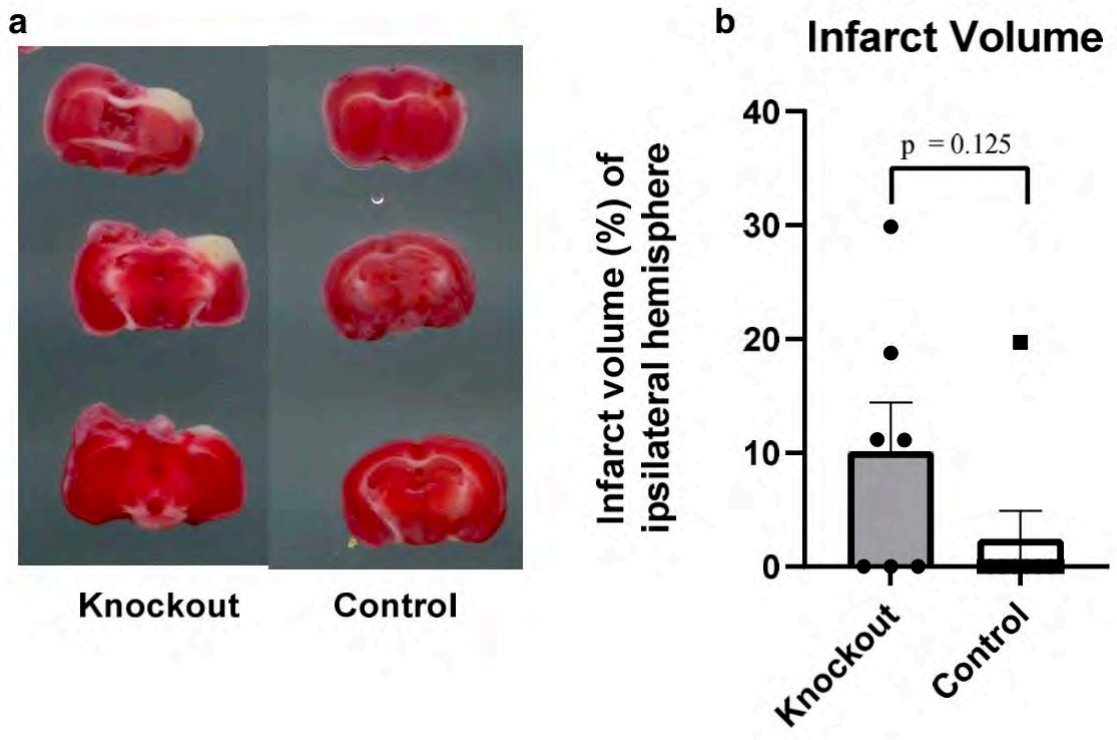

1) Mireille Bélanger et. al. Volume 14, Issue 6, December 2011, Pages 724-738. 2) Costantino Iadecola. Neuron. 2017 Sep 27; 96(1): 17–42. 3) Weiliang Bai et. al. J Adv Res. 2021 Nov; 33: 53–68. 4) Eng H. Lo et. Al. Nature Reviews Neuroscience, volume 4, pages 399–414 (2003).

C53

G155D mutation associated with Autosomal Dominant Nocturnal Frontal Lobe Epilepsy alters the structure-function relationship of Calcium Binding Protein 4.

Vanessa Morris[2], Dan Rigden[2], Caroline Dart[2], Nordine Helassa[2]

[1]University of Liverpool, Liverpool, United Kingdom, [2]Department of Biochemistry, Cell and Systems Biology, Institute of Systems, Molecular and Integrative Biology, University of Liverpool, Liverpool, United Kingdom

Introduction – Autosomal dominant frontal lobe epilepsy (ANDFLE) is a form of partial epilepsy disorder characterised by frequent focal seizures with usual onset at around 10 years of age. Currently, 30 % of ADNFLE patients do not respond to treatment. Calcium Binding Protein 4 (CaBP4) regulates the activity of voltage-dependent calcium channels including Cav1.3 and Cav1.4. Cav1.4 is predominantly expressed in photoreceptor synaptic terminals and plays a crucial role in maximal glutamate release under low light conditions. The point mutation G155D in CaBP4 has been associated with ADNFLE, yet its impact on the structure-function relationship of CaBP4 is still unknown.

Methods – Computational biology tools (AlphaFold and DynaMut) alongside circular dichroism (CD) were utilised to examine the G155D induced modifications to secondary and tertiary structure. Predicted changes to protein stability were also considered using computational tools (DynaMut). Susceptibility to protease digestion (SDS-PAGE) and thermostability (CD) were also used to investigate the impact of G155D on protein stability. The impact of the G155D mutation on CaBP4's calcium affinity was evaluated through intrinsic fluorescence spectroscopy (tyrosine). Isothermal titration calorimetry (ITC) assessed whether G155D caused changes to CaBP4's affinity for the IQ domains of voltage-dependent calcium channels (Cav1.2, Cav1.3, Cav1.4).

Results and Conclusions – Under both calcium-bound (n = 5) and calcium-free conditions (n = 5), the G155D variant exhibited a decrease of 10 ± 1% in alpha-helical content and a 5 ± 1% increase in unordered structure. DynaMut predictions revealed a notable increase in flexibility within the region of the G155D mutation and an elevated number of intra-molecular interactions. Susceptibility to protease digestion showed that the G155D mutation destabilised the protein in both calcium-bound (n = 7) and calcium-free conditions (n = 5). The G155D variant also displayed a significant reduction in thermostability with V_{50} values dropping from 44.0 ±0.8 °c to 37.9 ± 0.5 °c in calcium-free conditions (n = 6) and from 82.5 ± 1.3 °c to 76.2 ± 1.2 °c when calcium-bound (n = 6). Equilibrium calcium titrations showed a 2-fold reduction in Ca^{2+} affinity (n = 3) for the G155D variant. There was also reduced affinity seen between the G155D protein and all the voltage-dependent calcium channels' IQ domains. For the Cav1.2 IQ domain there was a 3.6-fold reduction in affinity from K_d CaBP4 = 1.85 M (n = 2) to K_d G155D = 6.59 M (n = 4). Meanwhile for both Cav1.3 and Cav1.4 there was a 4.7 fold reduction in affinity from K_d CaBP4 = 1.85 M (n = 5) to K_d G155D = 8.67 M (n = 7) and from K_d CaBP4 = 1.59 M (n = 5) to K_d G155D = 7.41 M (n = 6) respectively. To summarize, our findings indicate that the ADNFLE-associated mutant G155D has a significant impact on the structure, stability and binding affinity of CaBP4. This study marks the beginning of understanding the mechanism in which the G155D point mutation in CaBP4 leads to ADNFLE.

C54

The influence of the menopause and hormone replacement therapy on cortical neuroplasticity

Paul Ansdell[1], Padraig Spillane[1], Mollie O'Hanlon[2], Elisa Nédélec[2], Thomas Inns[2], Markus Hausmann[3], Stuart Goodall[1], Katy Vincent[4], Charlotte Stagg[4], Jessica Piasecki[2]

[1]Northumbria University, Newcastle Upon Tyne, United Kingdom, [2]Nottingham Trent University, Nottingham, United Kingdom, [3]Durham University, Durham, United Kingdom, [4]University of Oxford, Oxford, United Kingdom

Rationale: Previous research has demonstrated the neuroactive effects of ovarian hormones across the menstrual cycle [1], however it remains less clear how the cessation of hormone production across the menopause influences motor cortical properties. Additionally, it is currently unknown how nervous system adaptation (neuroplasticity) is mediated by endogenous and exogenous hormones across the human lifespan.

Methods: Participants' menopausal status was classified according to NICE guidelines on the diagnosis and management of menopause, with 12 pre-menopausal (age: 29 ± 7 years), 7 peri-menopausal (49 ± 4 years), 5 post-menopausal females (54 ± 5 years), and 7 females using HRT (54 ± 4 years) taking part in the study. Participants underwent a baseline neurophysiological assessment, including electrical stimulation of the median nerve and transcranial magnetic stimulation of the motor cortex to assess corticospinal excitability and intracortical inhibition and facilitation (SICI and ICF). Then, a paired associative stimulation (PAS) protocol was performed with electrical stimulation at 300% perceptual threshold delivered 25 ms prior to TMS at 120% motor threshold. 200 paired stimuli were delivered at 0.2 Hz, which were then followed with repeated neurophysiological assessments immediately, 10-, 20- and 30-minutes after PAS.

Results: No differences between groups were observed at baseline for corticospinal excitability ($p = 0.322$), SICI ($p = 0.570$) or ICF ($p = 0.961$). In response to the PAS protocol, only the pre-menopausal group experienced a significant increase in corticospinal excitability (+69%, $p < 0.001$), compared to peri- (+38%, $p = 0.136$) and post-menopausal females (+4%, $p = 0.868$). HRT users experienced a +53% increase in corticospinal excitability, however, this did not reach statistical significance ($p = 0.084$).

Conclusions: Motor cortical neuroplasticity was only evident in pre-menopausal females, implying that the cessation of ovarian hormone production impairs the nervous system's ability to adapt to novel stimuli. HRT could present an exogenous method of attenuating this menopause-related effect, which has implications for functional capacity in health and disease.

[1] Piasecki et al. (2024) Exerc Sports Sci Rev 52(2): p54-62

C55

Expiratory muscle activation pattern during exposure to hypoxia and hypercapnia

Letícia Mendes[1], Beatriz Vieira[1], Isabela Leirão[1], Daniel Zoccal[1]

[1]Department of Physiology and Pathology, School of Dentistry of Araraquara, São Paulo State University, Araraquara, Brazil

The coordination of respiratory muscle activity is essential to move air in and out of the lungs. At rest, inspiration is an active process with contractions of diaphragmatic (DIA) and external intercostal muscles (eIC), while the expiratory airflow is generated by elastic recoil forces of the thorax and lungs. Exposure to reduced oxygen (hypoxia) or elevated carbon dioxide levels (hypercapnia) transforms expiration into an active process, with the recruitment of abdominal (ABD) and internal intercostal muscles (iIC) that increase the expiratory flow. It remains unclear how the ABD and iIC muscles are coordinated during active expiration and how their entrainment modifies the expiratory flow to improve pulmonary ventilation. In the present study, we examined the ABD and iIC muscle activity patterns and the corresponding alterations in the expiratory flow during conditions of hypoxia and hypercapnia. Electrodes were implanted in the DIA, eIC, iIC, and ABD muscles of anesthetized (urethane, 1.2 mg/kg, i.v.) adult male Holtzman rats (n=8, 250-300 g). These animals also received a snout mask that allowed exposure to gas mixtures while monitoring nasal airflow. Experiments were performed under anesthesia. Physiological parameters were recorded under resting conditions and during 10-min exposure to hypoxia (7% O_2) and hypercapnia (7% CO_2). All procedures were approved by the institutional Ethics Committee (#17/2020). Values are expressed as mean±SD and compared using one-way ANOVA followed by Bonferroni or Friedman post-tests. Under resting conditions, DIA and eIC showed synchronized bursts during the inspiratory phase, ABD and iIC were silent, and the expiratory flow peaked during the first expiration stage. Hypoxia caused an initial increase in the respiratory frequency (fR) (resting: 88±11 vs 2^{nd}-min: 113± 19 bpm, $P<0.01$), elicited a sustained increase in DIA (Δ: 25-41%) and eIC (Δ: 37-58%) burst amplitudes ($P<0.05$), and brought about phase-locked ABD (Δ: 60-120%) and iIC (Δ: 116-325%) expiratory bursts ($P<0.05$) during the initial six minutes of exposure. These hypoxia-induced respiratory motor changes were accompanied by increased airflow during the second stage of expiration. Under hypercapnic conditions, fR increased during the last 2 min of exposure (resting: 85±12 vs 10^{th}-min: 97±14 bpm, $P=0.0299$), DIA (Δ: 45-56%) and eIC (Δ: 111-128%) burst amplitudes were higher throughout the exposure time ($P<0.05$), and ABD (Δ: 105-144%) and iIC (Δ: 219-255%) expiratory activities were higher during the last four minutes of exposure ($P<0.02$). The respiratory motor responses to hypercapnia did not change the airflow pattern, peaking during the first stage of expiration as noted during resting conditions. Our data indicate that hypoxia and hypercapnia exposures evoke entrained ABD and iIC bursts during the expiratory phase. However, their recruitment timing differs between gas conditions, occurring earlier under hypoxia than in hypercapnia. Moreover, their impact on the expiratory airflow is different, indicating that the adjustments of active expiration on the pulmonary mechanics involve stimulus-dependent recruitment of additional respiratory muscles.

C56

Unveiling the unseen: an in-depth exploration of fetal brain metabolism with magnetic resonance spectroscopy

Jordan Minns[1,2], Jack Darby[1,2], Stacey Holman[1,2], Brahmdeep Saini[3,4,5], Georgia Williams[6], Mike Seed[3,4,5], Steven Miller[5,8], Christopher Macgowan[3,4], Jessie Guo[5], Janna Morrison[1,2]

[1]Early Origins of Adult Health Research Group, Adelaide, Australia, [2]Health and Biomedical Innovation: Clinical and Health Sciences, University of South Australia, Adelaide, Australia, [3]Translational Medicine, Hospital for Sick Children, Toronto, Canada, [4]Department of Medical Biophysics, University of Toronto, Toronto, Canada, [5]Department of Paediatrics, University of Toronto, Toronto, Canada, [6]Preclinical, Imaging and Research Laboratories, South Australian Health and Medical Research Institute, Adelaide, Australia, [7]British Columbia Women's Hospital Ambulatory Care Centre, Vancouver, Canada, [8]Department of Paediatrics, University of British Columbia & BC Children's Hospital Research Institute, Vancouver, Canada

Background: Magnetic Resonance Spectroscopy (MRS) is a non-invasive advanced imaging technique for assessing the brain's biochemical and metabolic states. For normal brain development, the fetal circulation preferentially delivers oxygen and nutrient-rich blood to the brain through unique adaptations within the fetal circulation. If these adaptations fail, poor neurodevelopment may ensue. With the overall goal of detecting altered neurodevelopment earlier in pregnancy, we aimed to develop an MRS method that overcomes the imaging complexities introduced by maternal respiration and fetal movement, to understand how variations in cerebral oxygen delivery can affect cerebral metabolism.

Methods: At 105–110 days gestation (term, 150 days), pregnant ewes (n=5) underwent fetal surgery where catheters were implanted in the fetal femoral artery and vein, and the amniotic cavity under aseptic conditions. Anaesthesia was induced with intravenous diazepam (0.3 mg/kg) and ketamine (5 mg/kg) and maintained with isoflurane (1.5%–2.5% in 100% oxygen). All ewes received an analgesic, meloxicam (0.5 mg kg−1, subcutaneously) on the day before and the day of surgery. MRI scans were performed on a 3T Siemens clinical system (Magnetom Skyraa, Siemens Healthineers, Erlangen) while the ewe was ventilated. Proton MRS was performed using PRESS at an intermediate echo time (135ms) and a voxel size 15x15x15, gated to maternal respiration. To measure blood flow and oxygenation within the major fetal vessels, phase-contrast MRI and T2 oximetry were performed as previously described (Darby *et al.*, 2020; Saini *et al.*, 2020). Measures were performed during a normoxemic (Nx) and a hyperoxemic (Hyx) fetal state, achieved by maternal hyperoxygenation and confirmed with blood gas analysis (PO_2; Siemens RAPIDPOINT). After MRI, ewes and their fetuses were humanely killed with an overdose of sodium pentobarbitone, and fetal brains were collected. Data is presented as mean±SD and analysed using a Students' t-test; $P<0.05$ is considered statistically significant.

Results: During MRI, maternal Hyx (22.933±1.712) increased fetal PO_2 compared to Nx (17.983±3.058; P=0.0061). Cerebral blood flow (P=0.6534) as well as oxygen delivery (P=0.8236) and consumption (P=0.1604) were the same in Nx and Hyx. MRS detected total choline, creatine and N-acetyl aspartate peaks, key molecules for brain metabolism and development, that were quantified utilising Tarquin. There was no significant difference in total choline, creatine or N-acetyl aspartate concentrations between Nx (2.561±0.589; 2.528±1.274; 4.142±0.875) and Hyx

(2.411±0.587; 2.438±0.773; 2.639±1.839; all P>0.05). However, Hyx (0.896±0.404) lowered the N-acetyl aspartate to choline ratio when compared to Nx (1.528±0.404; P=0.0442).

Conclusions: This study demonstrated that acute maternal hyperoxygenation elevated fetal oxygenation without affecting blood flow in the fetal circulatory system. Despite the lack of change in cerebral oxygen delivery or consumption, we showed for the first time that MRS in fetal sheep is feasible for measuring metabolic biochemicals that have a crucial role in neuronal density and function, myelin integrity and overall fetal brain metabolism. Further validation of this technique may lead to the development of a novel tool for assessing the early biochemical changes in the fetal brain of complicated pregnancies.

Darby JRT, Schrauben EM, Saini BS, Holman SL, Rajan Perumal S, Seed M, MacGowan CK & Morrison JL. (2020). Umbilical vein infusion of Prostaglandin I2 increases ductus venosus shunting of oxygen rich blood but does not increase cerebral oxygen delivery in the fetal sheep. The Journal of Physiology 598, 4957-4967. Saini BS, Darby JRT, Portnoy S, Sun L, Amerom J, Lock MC, Soo JY, Holman SL, Perumal SR, Kingdom JC, Sled JG, Macgowan CK, Morrison JL & Seed M. (2020). Normal human and sheep fetal vessel oxygen saturations by T2 magnetic resonance imaging. J Physiol 598, 3259-3281.

C57

Vastus medialis activation and knee extensor neuromuscular function across the menstrual cycle

Elisa Nédélec[1], Mollie O'Hanlon[1], Tom Inns[1], Angus Hunter[1], Mathew Piasecki[2], Jessica Piasecki[1]

[1]Nottingham Trent University, Nottingham, United Kingdom, [2]University of Nottingham, Nottingham, United Kingdom

Introduction

Estrogen and progesterone are the primary female endogenous reproductive hormones and have neuroactive excitatory and inhibitory effects, respectively [1]. However, research on the influence of fluctuating concentrations across the menstrual cycle on neuromuscular function and performance has led to conflicting findings ([2]ref). Increases in muscle force production are mediated by recruitment of progressively larger MUs and an increase in MU discharge rate. The ability to control force production is tightly connected with functional outcomes such as walking, risk of falls, and dexterity in humans; thus, being of clinical relevance in prevention of sports injuries, such as non-contact anterior cruciate ligament (ACL) injuries [3]. There are currently no data quantifying vastus medialis (VM) MU adaptation combined with menstrual cycle tracking across the human menstrual cycle. Therefore, the purpose of the study herein was to assess knee-extensor strength, force steadiness and VM activation using high density electromyography (HD-EMG) across the menstrual cycle.

Methods

Eight recreationally active eumenorrheic participants (age: 28 ± 7 years;; BMI: 23.9 ± 3.07) had their menstrual cycles tracked (mean cycle length: 29 ± 3 days; luteinizing hormone surge occurring on day 14 ± 2) prior to participation in the study. All attended for repeated identical assessments at the early follicular phase (EF), 24 to 48h pre-ovulation (Ov) and mid-luteal (ML) phases of the menstrual cycle. Maximum voluntary contraction (MVC) of the knee-extensors was recorded, and neuromuscular control was assessed through isometric trapezoid contractions (5s ramp up, 12s hold, 5s ramp down) peaking at 40% MVC, with real-time visual target feedback. During contractions, a 64 channel HD-EMG electrode was placed over the VM and RMS EMG was calculated as the highest amplitude within a 50ms window, and reported as a ratio of maximum RMS EMG. One way ANOVA was used to determine differences across timepoints with statistical significance accepted as $p < 0.05$.

Results

No statistical differences across the menstrual cycle were observed for knee extensor strength (EF:433N, Ov:418N, ML:442, p=0.500). Normalised RMS EMG did not differ across the cycle (EF:60.8, Ov:47.0, ML:56.5, p=0.139). Similarly, no statistical differences were observed in

neuromuscular control during sustained phase at 40% MVC (p=0.661), during the ascent phase (p=0.292), or the descent phase (p=0.940).

Conclusion

The current pilot data highlight minimal effect of the hormonal fluctuations of the menstrual cycle in VM activation of neuromuscular performance of the knee extensors. However, additional factors of neuromuscular performance, such as individual MU features at a range of contraction levels, should be investigated to help understand the vast discrepancy of ACL injuries incidence between men and women.

References [1] S. S. Smith and C. S. Woolley, 'Cellular and molecular effects of steroid hormones on CNS excitability', Cleve Clin J Med, vol. 71 Suppl 2, pp. S4-10, Feb. 2004, doi: 10.3949/ccjm.71.suppl_2.s4. [2] J. Piasecki et al., 'Menstrual Cycle Associated Alteration of Vastus Lateralis Motor Unit Function', Sports Medicine - Open, vol. 9, no. 1, p. 97, Oct. 2023, doi: 10.1186/s40798-023-00639-8. [3] R. J. Schmitz, K. R. Ford, B. Pietrosimone, S. J. Shultz, and J. B. Taylor, 'ACL Research Retreat IX Summary Statement: The Pediatric Athlete, March 17–19, 2022; High Point, North Carolina', Journal of Athletic Training, vol. 57, no. 9–10, pp. 990–995, Jan. 2023, doi: 10.4085/1062-6050-0219.22.

C58

Identification of novel APOE4-induced impairments to action potential firing in murine CA1 pyramidal neurons and associated rescue with clinically relevant NMDAR antagonists

Oliver G. Steele[1], Bradley Payne[1], Nicoleta Stegarescu[1], Alex Stuart-Kelly[2], Sarah King[3], Ruth Murrel-Lagnado[2], Lewis Taylor[2], Andrew Penn[2]

[1]Department of Clinical Neuroscience, Brighton and Sussex Medical School, Falmer, United Kingdom, [2]School of Life Sciences, University of Sussex, Falmer, United Kingdom, [3]School of Psychology, University of Sussex, Falmer, United Kingdom

Introduction: Apolipoprotein E4 (*APOE4),* the major genetic risk factor for Alzheimer's Disease (AD), yet increasing evidence suggest *APOE4* may detrimentally alter neurophysiology independent of classical AD hallmarks(1). Whilst hippocampal synaptic dysregulation caused by *APOE4* is well-studied, the impact of *APOE4* on intrinsic neuronal membrane properties is poorly studied.

Aims/Objectives: This study then looks to functionally characterise the impact of Apolipoprotein E genotype (*APOE*) on intrinsic neuronal excitability.

Methods: *APOE*-targeted replacement(2) mice were housed in 12/hr light/dark cycles with *ad libitum* water and food. Organotypic hippocampal slices were prepared as previously described(3) before patch-clamp electrophysiology was performed at DIV21. A current-step protocol from -200 pA to +400 pA allowed visualisation and analysis of intrinsic membrane properties(4). Modulation of the NMDAR was made separately with the following drugs (in μM): 20 ketamine, 10 memantine hydrocholride, 5 D-APV, 5 GNE-9278. Analysis of the relationship between *APOE* genotype and drug condition was inferred through multilevel linear modelling and bootstrap resampling (10,000 resamples). Post-hoc ANOVA permutation testing then analysed the interaction term. 12 animals per genotype were included, with a minimum of four slices per animal being produced. Only one recording per cell was then included in the analysis.

Results: Depolarizing current injection into CA1 neurons of *APOE3* slice cultures caused neurons to fire at frequencies up to 11.00 Hz (95% *CI* [9.31, 12.31]). However, in *APOE4* neurons, the firing rate was -2.94 Hz (95% *CI* [-5.06, -0.78], p = .007) lower. While acute application of ketamine had little effect in *APOE3* neurons (+0.08 Hz, 95% *CI* [-2.94, +2.72], *p* = .95), ketamine increased firing rates more in *APOE4* (than in *APOE3*) neurons by +3.53 Hz (95% *CI* [+0.15, +7.18], *p* = .043). Similarly to ketamine, acute application of memantine had little effect in *APOE3* neurons (+0.71 Hz, 95% *CI* [-0.98, +2.65], *p* = .44) and increased firing rates more in *APOE4* (than in *APOE3*) neurons by +4.27 Hz (95% *CI* [+1.00, +7.24], *p* = .021). A two-way ANOVA permutation test confirmed a significant interaction: the effect of the drugs (ketamine or memantine) on maximum firing rate depended on the *APOE* genotype (*p* = .023). To then confirm whether these described effects were mediated by the NMDAR a more specific NMDAR antagonist was applied, D-APV. While acute application of D-APV had little effect in *APOE3* neurons (+1.88 Hz, 95% *CI* [-1.16, 5.29], *p* =.216), D-APV increased firing rates more in *APOE4* (than in *APOE3*) neurons by +8.15 Hz (95% *CI* [3.35, 12.87], *p* = < .001). Further confirming the involvement of the NMDAR, acute application of the positive allosteric modulator, GNE-9278 significantly decreased firing rates in *APOE3* neurons (-

5.51 Hz, 95% *CI* [-8.06, -2.66], p = < .001) and decreased firing rates more in *APOE3* (than in *APOE4*) neurons by -5.89 Hz (95% *CI* [-1.16, -10.56], p = .016).

Conclusion: Not only does APOE4 perturb action potential firing, but the rescue of this phenotype is also dependent on the NMDAR hinting at a conserved pathway that could act as a future therapeutic target.

1. Steele and Stuart OG and AC, Minkley L, Shaw K, Bonnar O, Anderle S, Penn AC, et al. A multi-hit hypothesis for an APOE4-dependent pathophysiological state. Eur J Neurosci [Internet]. 2022 [cited 2022 May 31];n/a(n/a). Available from: https://onlinelibrary.wiley.com/doi/abs/10.1111/ejn.15685 2. Sullivan PM, Mezdour H, Aratani Y, Knouff C, Najib J, Reddick RL, et al. Targeted Replacement of the Mouse Apolipoprotein E Gene with the Common Human APOE3 Allele Enhances Diet-induced Hypercholesterolemia and Atherosclerosis. J Biol Chem. 1997 Jul 18;272(29):17972–80. 3. Elmasri M, Lotti JS, Aziz W, Steele OG, Karachaliou E, Sakimura K, et al. Synaptic Dysfunction by Mutations in GRIN2B: Influence of Triheteromeric NMDA Receptors on Gain-of-Function and Loss-of-Function Mutant Classification. Brain Sci. 2022 Jun 15;12(6):789. 4. Telezhkin V, Schnell C, Yarova P, Yung S, Cope E, Hughes A, et al. Forced cell cycle exit and modulation of GABAA, CREB, and GSK3β signaling promote functional maturation of induced pluripotent stem cell-derived neurons. Am J Physiol-Cell Physiol. 2015 Dec 30;310(7):C520–41.

C59

Assessment of olfactory response to social and non-social cues in valproic acid induced rat model of autism

Süeda Tunçak[2], Sevgi Ece Koç[2], Ceren Oy[3], Şule Mergen[4], Gökhan Göktalay[4], Zehra Minbay[3], Bülent Gören[2]

[1]Bursa Uludağ University, Bursa, Turkey, [2]Department of Physiology, Faculty of Medicine, Bursa Uludağ University, Bursa, Turkey, [3]Department of Histology and Embryology, Faculty of Medicine, Bursa Uludağ University, Bursa, Turkey, [4]Department of Pharmacology, Faculty of Medicine, Bursa Uludağ University, Bursa, Turkey

Autism Spectrum Disorders (ASD), are characterized with impairments in communication, lack of interest in social interactions and repetitive behaviours. Prenatal valproic acid (VPA) exposure, is used for modelling ASD like symptoms in rodents (1). Olfactory bonding with mother is crucial for a healthy social development and this is often tested with olfactory discrimination test (2). However, this test contains social cues only and therefore lacks the ability to distinguish whether observed differences occur due to social impairments or olfactory problems. This study aims to investigate olfactory response to social and non-social cues in prenatal VPA exposed rats.

Pregnant Wistar Albino rats received either 400mg/kg VPA (n_{Mother}: 3; $n_{Pup: 8}$) or saline (n_{Mother}: 3; n_{Pup}: 8) on embryonic day 12.5 *intraperitoneally*. Female pups were tested for olfactory discrimination (OD) on postnatal day 9 (P9), anxiety on P30 and olfaction without social cues on P40. OD test was performed for 3 minutes in plexiglass container with clean bedding on one side and bedding from mother cage on the other. Latency to reach either bedding was measured and rats were immediately returned to mothers. Anxiety was measured in open field. Total distance moved, velocity and frequency to entre border and centre zones were measured. Olfaction without social cues was tested for 5 minutes in a hole-board apparatus that consisted 16 holes with 2cm diameter. Rats were habituated to hole-board for 3 days prior testing to reduce stress. Food was removed from cages 8 hours prior testing. The test included a strawberry milk jar as a non-social olfactory cue under one of the centre holes. Latency of head digging into any holes was measured. Statistical analysis was performed with Student's-t test on Sigma-Plot. The study was approved by Bursa Uludağ University's ethics committee (numbered: 2023-13/02).

Prenatal exposure to VPA impaired OD of mother/clean bedding. Latency to reach mother bedding was significantly increased in VPA group ($p<0.022$) whereas latency to reach any bedding showed no statistical difference between groups. In open field, VPA group showed decreased velocity ($P<0.003$) and frequency to entre both border ($p<0.001$) and centre zones ($p=0.002$). Control group had increased distance moved ($p<0.001$) and spent more time in centre areas compared to VPA group. In olfactory hole-board test, VPA group showed increased latency to dig their head into strawberry milk ($p=0.003$) whereas there was no significant difference between groups for latency of head digging into holes.

Olfaction is crucial in rodent survival. Inability to discriminate mother bedding from clean bedding suggests impairments in social communication. Results of open field test suggest increased anxiety in VPA group as expected from literature. For that reason, rats were habituated to hole-

board. Insignificant difference in latency of head-digging shows that anxiety was eliminated. Within these results, this study suggests an impaired response to olfactory cues, whether social or non-social. This new set of information should be taken into account especially when sociability is assessed in models of ASD as inability to discriminate novel conspecific may occur merely as a result of a problem in olfaction.

(1) Schneider T, & Przewłocki R. (2005). Neuropsychopharmacology, 30(1), 80-89. (2) Favre MR et al. (2013). Frontiers in behavioral neuroscience, 7, 88.